Integration of miRNA and mRNA expression with DNA copy number of Ewing sarcoma cell lines

Ilari Scheinin

Amsterdam April 26, 2011

Master's thesis

UNIVERSITY OF HELSINKI
Department of Biosciences

to my dear friend Laura,
who opened my eyes

HELSINGIN YLIOPISTO — HELSINGFORS UNIVERSITET — UNIVERSITY OF HELSINKI

Tiedekunta — Fakultet — Faculty	Laitos — Institution — Department
Faculty of Biological and Environmental Sciences	Department of Biosciences

Tekijä — Författare — Author
Ilari Scheinin

Työn nimi — Arbetets titel — Title

Integration of miRNA and mRNA expression with DNA copy number of Ewing sarcoma cell lines

Oppiaine — Läroämne — Subject
Biotechnology, specialization track of Bioinformatics and Systems Biology

Työn laji — Arbetets art — Level	Aika — Datum — Month and year	Sivumäärä — Sidoantal — Number of pages
Master's thesis	April 26, 2011	64 pages (77 with appendices)

Tiivistelmä — Referat — Abstract

Ewingin sarkooma on aggressiivinen ja erilaistumaton luu- ja pehmytkudossyöpä. Se vaivaa pääasiassa lapsia, nuoria ja nuoria aikuisia, ja on hieman yleisempi miehillä. Sen tunnusmerkki on kromosomien 11 ja 22 välillä tapahtuva uudelleenjärjestäytyminen, jonka tuloksena on EWSR1-FLI1 fuusiogeenin tuottama transkriptiofaktori.

Tämän tutkielman tarkotuksena on tunnistaa Ewingin sarkoomalle tärkeitä kohdegeeniehdokkaita käyttäen kolmea erityyppistä mikrosiruaineistoa. Array comparative genomic hybridization -teknologialla mitataan DNA:n kopiolukua, ja sen analysointi mahdollistaa yleisten kromosomipoikkeavuuksien tunnistamisen. mRNA- and miRNA-siruja käytetään proteiineja tuottavien ja miRNA-geenien ilmentymisen mittaamiseen, ja niiden tulokset yhdistetään kopiolukuaineistoon. Kromosomipoikkavuudet tyypillisesti sisältävät myös sivullisia geenejä varsinaisten syöpä- ja kasvurajoitegeenien lisäksi, ja yhdistäminen ilmentymisaineistoon mahdollistaa varsinaisten kohdegeenien tunnistamisen. Myös miRNA:iden ja niiden ennustettujen kohde-mRNA:iden välinen korrelaatio mitataan määrittämään transkription jälkeisen säätelyn vaikutusta mRNA:iden tasoille.

Yleisimmät kopiolukumonistumat tunnistettiin kromosomeista 8, 1q ja X. Häviämät olivat yleisimpiä raidassa 9p21.3, jonka kohdalla havaitiin myös katkoskohtien rikastuma muuhun genomiin verrattuna. Kopiolukumuutoksilla 9p21.3:ssa havaittiin olevan tilastollisesti merkitsevä vaikutus MTAP:n ilmentymiseen, mutta ei CDKN2A:n, joka on tunnettu kasvurajoitegeeni samassa kohtaa genomia. MTAP:n ilmentyminen oli myös alhaisempaa Ewing sarkooma -solulinjoissa kuin mesenkymaalisissa kantasoluissa. Kohonnutta ilmentymistä kopiolukumuutoksista johtuen ja verrokkinäytteen suhteen havaitiin geeneissä DCAF7, ENO2, MTCP1 ja STK40.

miRNA-geenien ilmentymistä verrattiin Ewingin sarkooma -solulinjojen ja mesenkymaalisten kantasolujen välillä. 21:n miRNA:n ilmentymisen havaitiin olevan koholla ja 32:n alhaisempi kuin vertailunäytteissä. Alhaisempi ilmentyminen havaitiin myös miR-145:n kohdalla, kuten on aikaisemminkin havaittu Ewingin sarkooman kohdalla. Fuusiogeeni EWSR1-FLI1 vaimentaa miR-145:n ilmentymistä, jonka yksi kohdegeeni taas on FLI1, synnyttäen näin vastavuoroisesti vaimentavan palautesilmukan.

Sen lisäksi että STK40:n ilmentyminen oli Ewing sarkooma -solulinjoissa koholla mesenkymaalisiin kantasoluihin nähden, ja että monistumien havaittiin nostaneen STK40:n ilmentymistä, sen havaittiin myös olevan kohdegeeni neljälle miRNA:lle, joiden ilmentyminen oli alentunut. SLCO5A1:n havaittiin olevan ainoa koholla oleva geeni usein monistuneella alueella kromosomissa 8. Alue oli monistunut yli 90 %:ssa solulinjoista, yleisyyden myös ollessa vierekkäisiä alueita korkeampi. Tämän lisäksi SLCO5A1 on kohdegeeni kolmelle miRNA:lle, joiden ilmentyminen oli alentunut mesenkymaalisiin kantasoluin verrattuna.

Avainsanat — Nyckelord — Keywords
Ewing sarcoma, microarray profiling, aCGH, mRNA, miRNA, copy number, bioinformatics

Säilytyspaikka — Förvaringsställe — Where deposited
Viikki Campus Library

Muita tietoja — övriga uppgifter — Additional information

HELSINGIN YLIOPISTO — HELSINGFORS UNIVERSITET — UNIVERSITY OF HELSINKI

Tiedekunta — Fakultet — Faculty	Laitos — Institution — Department
Faculty of Biological and Environmental Sciences	Department of Biosciences

Tekijä — Författare — Author
Ilari Scheinin

Työn nimi — Arbetets titel — Title

Integration of miRNA and mRNA expression with DNA copy number of Ewing sarcoma cell lines

Oppiaine — Läroämne — Subject
Biotechnology, specialization track of Bioinformatics and Systems Biology

Työn laji — Arbetets art — Level	Aika — Datum — Month and year	Sivumäärä — Sidoantal — Number of pages
Master's thesis	April 26, 2011	64 pages (77 with appendices)

Tiivistelmä — Referat — Abstract

Ewing sarcoma is an aggressive and poorly differentiated malignancy of bone and soft tissue. It primarily affects children, adolescents, and young adults, with a slight male predominance. It is characterized by a translocation between chromosomes 11 and 22 resulting in the EWSR1-FLI1 fusion transcription factor.

The aim of this study is to identify putative Ewing sarcoma target genes through an integrative analysis of three microarray data sets. Array comparative genomic hybridization is used to measure changes in DNA copy number, and analyzed to detect common chromosomal aberrations. mRNA and miRNA microarrays are used to measure expression of protein-coding and miRNA genes, and these results integrated with the copy number data. Chromosomal aberrations typically contain also bystanders in addition to the driving tumor suppressor and oncogenes, and integration with expression helps to identify the true targets. Correlation between expression of miRNAs and their predicted target mRNAs is also evaluated to assess the results of post-transcriptional miRNA regulation on mRNA levels.

The highest frequencies of copy number gains were identified in chromosome 8, 1q, and X. Losses were most frequent in 9p21.3, which also showed an enrichment of copy number breakpoints relative to the rest of the genome. Copy number losses in 9p21.3 were found have a statistically significant effect on the expression of MTAP, but not on CDKN2A, which is a known tumor-suppressor in the same locus. MTAP was also down-regulated in the Ewing sarcoma cell lines compared to mesenchymal stem cells. Genes exhibiting elevated expression in association with copy number gains and up-regulation compared to the reference samples included DCAF7, ENO2, MTCP1, and STK40.

Differentially expressed miRNAs were detected by comparing Ewing sarcoma cell lines against mesenchymal stem cells. 21 up-regulated and 32 down-regulated miRNAs were identified, including miR-145, which has been previously linked to Ewing sarcoma. The EWSR1-FLI1 fusion gene represses miR-145, which in turn targets FLI1 forming a mutually repressive feedback loop.

In addition higher expression linked to copy number gains and compared to mesenchymal stem cells, STK40 was also found to be a target of four different miRNAs that were all down-regulated in Ewing sarcoma cell lines compared to the reference samples. SLCO5A1 was identified as the only up-regulated gene within a frequently gained region in chromosome 8. This region was gained in over 90 % of the cell lines, and also with a higher frequency than the neighboring regions. In addition, SLCO5A1 was found to be a target of three miRNAs that were down-regulated compared to the mesenchymal stem cells.

Avainsanat — Nyckelord — Keywords
Ewing sarcoma, microarray profiling, aCGH, mRNA, miRNA, copy number, bioinformatics

Säilytyspaikka — Förvaringsställe — Where deposited
Viikki Campus Library

Muita tietoja — övriga uppgifter — Additional information

Contents

List of Figures

List of Tables

Abbreviations

aCGH	array CGH
AMP	adenosine monophosphate
BAC	bacterial artificial chromosome/clone
cAMP	cyclic AMP
CanGEM	Cancer GEnome Mine database
cDNA	complementary DNA
CGH	comparative genomic hybridization
CNV	copy number variation
CV	coefficient of variation = standard deviation / mean
DNA	deoxyribonucleic acid
ETS	E-twenty six / E26 transformation specific transcription factor family
FISH	fluorescent in situ hybridization
FET	FUS, EWSR1, TAF15
FLI1	Friend leukemia virus integration 1 transcription factor
GEO	Gene Expression Omnibus database
hMSC	human MSC
LOH	loss of heterozygosity
MAPK	mitogen-activated protein kinase
miRNA	micro RNA
mMSC	murine MSC
MPC	mesenchymal progenitor cell
MSC	mesenchymal stem cell
MSS	mesomelia-synostoses syndrome
NF-κB	nuclear factor kappa-light-chain-enhancer of activated B cells
RNA	ribonucleic acid
RNAi	RNA interference
SCID	severe combined immunodeficiency
siRNA	small interfering RNA
SRBCT	small round blue cell tumor
UDP	uniparental disomy
UTR	untranslated region

1 Introduction

1.1 Cancer in general

Cancer is a heterogeneous group of complex diseases that share certain characteristics: (1) ability of evade apoptosis, (2) limitless replicative potential, (3) sustained angiogenesis, (4) self-sufficiency in growth signals, (5) insensitivity to anti-growth signals, and (6) tissue invasion and metastasis (Hanahan and Weinberg 2000). There are various mechanisms through which a cancer cell can acquire these capabilities: point mutations in DNA sequence, larger chromosomal aberrations, or epigenetic changes. The alterations can affect protein-coding genes directly, or through miRNA genes, which in turn act as post-transcriptional regulators of many mRNAs controlling their translation into protein. Cancerous changes can be acquired through errors in normal homeostasis of somatic cells, or also be inherited thus elevating the risk of developing cancer in one's lifetime.

The number of changes, or "hits", required to develop cancer has been a question of interest. Nordling (1953) proposed six, based on the observation that the frequency of cancer in industrialized nations seemed to increase according to the sixth power of age. In 1971, Alfred Knudson performed statistical analysis of 48 retinoblastoma cases (Knudson 1971), and his model was able to explain the patterns of unilateral (only in one eye) and bilateral (both eyes) tumors by a requirement of two hits, first of which can be either inherited or acquired.

1.2 Ewing sarcoma

1.2.1 Clinical characteristics

Ewing sarcoma is an aggressive tumor of bone and soft tissue. It is poorly differentiated and has an unknown histogenesis. It was first described in 1921 by James Ewing, who referred to it as "diffuse endothelioma of bone" (Ewing 1921). After osteosarcoma, it is the second most common bone sarcoma in children and young adults (Ries et al. 1999). Symptoms usually include pair and/or mass, and imaging reveals a destructive/invasive lesion. After the development of molecular diagnostics, many cases of previously non-classified sarcomas have been diagnosed as Ewing sarcoma.

The highest peak of incidence is between ages 10 to 20. Patients are rarely older than 40 years (Pieper et al. 2008), although isolated cases in geriatric patients have been reported (Cheung et al. 2001). Median age at diagnosis is 14-15 years, and the annual incidence is around 3 cases per million children under 19 years of age. There is a slight male predominance with a male to female ratio of 1.2–1.9 to 1 (Cotterill et al. 2000; Esiashvili et al. 2008). In Finland, the annual number of new Ewing sarcoma cases ranges between five and eight (Joensuu et al. 2007).

There is a racial component in susceptibility to Ewing sarcoma, and Caucasians have a higher risk compared to people with African or Asian origin (Fraumeni and Glass 1970; Li et al. 1980; Parkin et al. 1993). In United States, the elevated probability of white children to develop Ewing sarcoma has been estimated to be 6–9 fold compared to African Americans (Ries et al. 1999; Jawad et al. 2009). Caucasians also show a higher frequency of bone tumors, lower frequency of soft tissue malignancies, and have a better overall survival (Worch et al. 2010). Other

common bone tumors, such as osteosarcoma, show relatively equal racial distributions.

Primary tumors occur most frequently (over 50 %) in the long bones of lower and upper extremities, or axially in pelvis, chest wall or spine (Cotterill et al. 2000). In the extremities, the location is more often in the mid section of the bone (diaphysis) than in the ends (epiphysis). In addition to bones, Ewing sarcoma can also affect soft tissue, such as kidneys, uterus, or skin. Despite these spatial tendencies, any bone or extra-skeletal tissue may be affected. Primary tumors in bone are more frequent in children and adolescents, while soft tissue is increasingly affected in adults.

At the time of diagnosis, about 25 % of patients have clinically evident metastases (Cotterill et al. 2000; Esiashvili et al. 2008). They occur most frequently in lung, bone, or bone marrow through hematogenous spread. However, 20–30 % of patients diagnosed with a localized tumor actually have micrometastases, which are undetectable by current routine procedures (Pfleiderer et al. 1995; West et al. 1997).

Other tumor types closely related to Ewing sarcoma include periperipheral primitive neuroectodermal tumor (PNET), peripheral neuroepithelioma, and Askin's tumor. PNET shows neural differentiation, and Askin's tumor is localized in the chest wall. All of these tumors are treated in similar fashion on the basis of their clinical presentation (e.g. metastasized or localized) rather than their histological subtype. This group of cancers is sometimes referred to as Ewing sarcoma family of tumors (ESFT), Ewing sarcoma/PNET, or simply Ewing sarcoma, which is the term used throughout this thesis.

Histologically Ewing sarcoma belongs to small round blue cell tumors

(SRBCTs), which also include desmoplastic small round cell tumor, hepatoblastoma, neuroblastoma, medulloblastoma, retinoblastoma, rhabdomyosarcoma, small-cell lymphoma, and Wilm's tumor. These tumors are more typically observed in children than adults, and are all poorly differentiated (Lessnick et al. 2009). The best known immunohistochemical hallmark of Ewing sarcoma is the cell surface antigen CD99, which is expressed in over 90 % of the cases (Kovar et al. 1990; Fellinger et al. 1991; Perlman et al. 1994). However, it does not exclusively distinguish Ewing sarcoma from other SRBCTs, or from other solid tumors, as heterogeneous positivity for CD99 is detected in a variety of tumors, including chondrosarcomas, lymphomas, neuroblatomas, osteoblastomas and sarcomas, rhabdomyosarcomas, and synovial sarcomas (Fellinger et al. 1991; Scotlandi et al. 1996; Lucas et al. 2001). CD99 is a 32 kD glycoprotein coded by the MIC2 gene, and is normally expressed in T cells (Gelin et al. 1989) and B cells (Dworzak et al. 1999). Other immunohistochemical markers that are variably expressed in Ewing sarcoma include FLI1 (Folpe et al. 2000), vimentin (Lucas et al. 2001), and cytokeratin (Collini et al. 2001),

Advances in multidisciplinary treatments have increased survival of Ewing sarcoma patients significantly. According to the US-based Surveillance, Epidemiology, and End Results (SEER) Program, 5-year survival has increased from 44 % to 68 % for localized disease after the 1970s. About 25 % of patients are diagnosed with metastases, and their 5-year survival has increased from 16 % to 39 % (Esiashvili et al. 2008). Compared to bone and bone marrow, pulmonary metastases have a slighly more faborable outcome. Long-term survival is about 50 % for localized and $<$20 % for disseminated disease (Paulussen et al. 2008). More than 30 % of patients relapse, which is often fatal. The time from initial diagnosis to first recurrence is a good predictor for survival in these cases. A recurrence within the first 2 years corresponded with only 7 % 5-year survival, whereas later incidents had a more favorable outcome at 30 % (Leavey et al. 2008). Overall, the absence of metastases at

the time of diagnosis (Terrier et al. 1996), small tumor volume (<200 ml) (Paulussen et al. 2001), good response to chemotherapy (Picci et al. 1997; Wunder et al. 1998), primary tumor site other than pelvis (Craft et al. 1997), and young age (Grier et al. 2003; Paulussen et al. 2008; Granowetter et al. 2009) have been shown to correlate with better clinical outcome.

Depending on the location and extent of the tumor, local treatment of Ewing sarcoma can consist of surgery, radiation therapy, or both. Systemic therapy was introduced in the 1970s and given to patients before and after surgery as neoadjuvant and adjuvant chemotherapy. The aim is to eliminate tumor cells and micrometastases throughout the body. Chemotherapy typically consists of a combination of different chemotherapeutic agents, e.g., doxorubicin, cyclophosphamide, ifosfamide, etoposide, and vincristine. (Thacker et al. 2005). While aggressive treatment does improve outcome, it can have serious side effects. These can include e.g. bacterial infections, pain, malnutrition, stomatitis, hair loss, nausea, and vomiting. It also elevates the risk of developing secondary malignancies, such as leukemias and solid tumors like radiation-induced osteosarcomas (Bacci et al. 2005; Navid et al. 2008). Identifying low-risk cases to avoid unnecessary treatment would therefore be beneficial for these patients.

1.2.2 Common translocations

A hallmark of Ewing sarcoma is a gene fusion between members of the FET and ETS gene families, most commonly between EWSR1 and FLI1. The FET family consists of FUS (fused in sarcoma; also known as TLS, translocated in liposarcoma), EWSR1 (Ewing sarcoma breakpoint region 1) and TAF15 (TATA-binding protein-associated factor 15). These proteins are expressed ubiquitously in cell cycle through all tissues,

are predominantly nuclear, and have roles in transcription and RNA processing and splicing. They contain an RNA-binding motif and interact with the RNA polymerase II (Tan and Manley 2009). ETS (E-twenty six or E26 transformation specific) is a gene family consisting of roughly 30 tissue-specific transcription factors. They contain a highly conserved helix-turn-helix DNA-binding motif, and comprise of both transcriptional activators and inhibitors (Sharrocks 2001).

The first observations of non-random translocations between chromosomes 11 and 22 in Ewing sarcoma were made in the 1980s (Aurias et al. 1984; Turc-Carel et al. 1984, 1988). The exact partners involved in this gene fusion were identified as EWSR1 (Ewing sarcoma breakpoint region 1) and FLI1 (Friend leukemia virus integration 1) roughly a decade later (Delattre et al. 1992). This was the first fusion gene to be characterized at the molecular level in sarcomas. The EWSR1 gene is located in 22q12.2 and supplies the fusion gene with a strong promoter containing a transactivation domain, while FLI1 (11q24.3) provides a DNA binding domain giving target specificity for transcriptional activation and repression (May et al. 1993a). The fusion gene functions as a transcription factor and enables Ewing sarcoma tumorigenesis (May et al. 1993b).

The most common fusion between EWSR1-FLI1 is known as type 1, and joins EWSR1 exons 1–7 with FLI1 exons 6–9. It is not transcribed as actively and has been shown to be associated with better survival than other EWSR1-FLI1 variants (de Alava et al. 1998). The second most common fusion is type 2, which also includes exon 5 of FLI1. At least 18 different types of in-frame fusions between EWSR1 and FLI1 are known. In some cases the fusion is out of frame, but restored through splicing.

In addition to FLI1, EWSR1 has also been shown to fuse with other

members of the ETS gene family. These include ERG (Zucman et al. 1993), ETV1 (Jeon et al. 1995), ETV4 (Kaneko et al. 1996), FEV (Peter et al. 1997), and ZNF278 (Mastrangelo et al. 2000). Alternatively, fusions involving the FUS gene have also been described, including FUS-ERG (Shing et al. 2003) and FUS-FEV (Ng et al. 2007). All fusion genes function as transcription factors, and despite structural differences, all seem to similarly induce cellular transformation and accelerate tumorigenesis without significant differences in clinical phenotypes (Ginsberg et al. 1999; Thompson et al. 1999). However, the rarity of the infrequent fusions make it difficult to obtain adequate sample sizes for reliable comparative studies. Table 1.1 lists the known Ewing sarcoma translocations.

Table 1.1: Translocations in Ewing sarcoma

translocation	gene fusion	prevalence	reference
t(11;22)(q24;q12)	EWSR1-FLI1	80–90%	Delattre et al. (1992)
t(21;22)(q22;q12)	EWSR1-ERG	5–10%	Zucman et al. (1993)
t(7;22)(p22;q12)	EWSR1-ETV1	rare	Jeon et al. (1995)
t(17;22)(q12;q12)	EWSR1-ETV4	rare	Kaneko et al. (1996)
t(2;22)(q33;q12)	EWSR1-FEV	rare	Peter et al. (1997)
t(1;22)(p36;q12)	EWSR1-ZNF278	rare	Mastrangelo et al. (2000)
t(16;21)(p11;q22)	FUS-ERG	rare	Shing et al. (2003)
t(2;16)(q35;p11)	FUS-FEV	rare	Ng et al. (2007)

The genomic sequence of EWSR1 provides a possible explanation for racial differences in susceptibility to Ewing sarcoma. Alu polymorphisms provide sites for recombination, and intron 6 of EWSR1 is rich in Alu elements. The size of this region is reduced by over 50 % in people of African origin compared to Caucasians (Zucman-Rossi et al. 1997).

The EWSR1-FLI1 fusion protein acts as a transcription factor with both up and down-regulated target genes. Specific to the up-regulated ones, GGAA microsatellite repeats have been shown to be binding targets. At least 4–5 repeats are required, and presence of more than nine has been shown to lead to increased target expression (Gangwal et al. 2008; Guillon et al. 2009). Polymorphisms in the GGAA

microsatellite loci could be another factor in susceptibility between individuals from different ethnic groups (Gangwal and Lessnick 2008). The ability to bind GGAA repeats is shared between many ETS gene family members, but the capability to activate their transcription seems to be specific only to fusion products (Gangwal et al. 2010).

Genes induced by the fusion product mainly belong to cell cycle regulation, proliferation, and response to DNA damage, while repressed ones are associated with differentiation and cell communication (Kauer et al. 2009). One critical up-regulated target is NR0B1 (nuclear receptor subfamily 0, group B, member 1), which has been shown to be required for optimal transformation (Kinsey et al. 2006). NR0B1 is a co-repressor protein that directly interacts with EWSR1-Fli1 to regulate transcription, and this protein-protein interaction is crucial for development of Ewing sarcoma, as mutations in NR0B1 disrupting the interaction directly block oncogenic transformation (Kinsey et al. 2009). Other targets found to be required for optimal transformation are NKX2-2 (NK2 homeobox 2) (Smith et al. 2006), and EZH2 (enhancer of zeste homolog 2) (Richter et al. 2009). Ewing sarcoma is dependent on IGF-1 (insulin-like growth factor-1) for tumor growth and survival, and this gene is also one of the up-regulated targets of the EWSR1-FLI1 fusion (Cironi et al. 2008). One direct down-regulated target is TGF-βR2 (transforming growth factor-beta receptor type II) (Hahm et al. 1999; Im et al. 2000).

Being the hallmark of Ewing sarcoma, these fusion genes are an interesting focus for targeted therapies. These fusions lead to abnormal DNA and protein sequences, that can only be found in the tumor cells and not elsewhere in the body. Knocking out expression of the EWSR1-FLI1 fusion gene using antisense oligonucleotides has been shown to dramatically inhibit tumor growth both in cell lines and mouse models (Kovar et al. 1996; Tanaka et al. 1997; Hu-Lieskovan et al. 2005).

The result is a decrease in cell proliferation and increased apoptosis. However, therapeutic applications are yet to reach clinical use. The fusion protein has proven to be difficult to study *in vitro*, because of poor solubility, difficulties in biochemical purification, and presence of unstructured regions. This has lead Uren and Toretsky (2005) to describe the EWSR-FLI1 fusion as "the perfect target without a therapeutic agent".

1.2.3 Other genomic alterations

In addition to the characteristic gene fusions, secondary genetic changes are detected in about 80 % of Ewing sarcomas at the time of diagnosis (Zielenska et al. 2001; Roberts et al. 2008). The most common copy number aberrations are gains of 1q, 8 and 12, and losses of 9p21.3 and 16q. Most of these changes have been associated with unfavorable clinical outcome, including the gain of 1q (Hattinger et al. 2002), deletion of 1p36 (Hattinger et al. 1999), loss of 9p21.3 (Huang et al. 2005), and loss of 16q (Hattinger et al. 2002). An unbalanced translocation between chromosomes 1 and 16 has been observed in about 10 % of cases, resulting in a derivate chromosome 16, and subsequent gain of 1q and loss of 16q. It has been associated with poor survival (Douglass et al. 1990; Hattinger et al. 2002).

Adverse effects on prognosis have also been described for an increase in the overall number of copy number aberrations (Sandberg and Bridge 2000; Zielenska et al. 2001), and for mutations in TP53, especially when combined with a deletion of the CDKN2A (cyclin-dependent kinase inhibitor 2A) gene (de Alava et al. 2000; Huang et al. 2005). Even though mutations affecting the tumor suppressor gene TP53 at 17p31.1 are one of the most common genetic alterations in sporadic cancers (Nigro et al. 1989), they are relatively rare in Ewing sarcoma (Patiño-García and

Sierrasesúmaga 1997; Tsuchiya et al. 2000; López-Guerrero et al. 2001; Huang et al. 2005).

1.2.4 Cell of origin

The exact cell type where Ewing sarcoma originates from has been under debate. Among proposed alternatives are endothelial, hematopoietic and neuronal cells. One of the challenges in identifying the cell of origin is the relative toxicity of the EWSR1-FLI1 fusion gene for a variety of cell types. Recent studies have suggested that the most probable origin is mesenchymal stem cells (MSC), also known as mesenchymal progenitor cells (MPC). These multipotent cells are capable of differentiating along a variety of lineages and have the capacity for self renewal. MSCs can differentiate along osteogenic, lipogenic, or adipogenic lineages, and the potential differentiated cell types include osteoblasts, chondrocytes, adipocytes, myocytes, neurons, hepatocytes, and pancreatic islet cells.

By using a retroviral expression vector, Riggi et al. (2005) introduced the EWSR1-FLI1 fusion gene into murine MPCs and were able to induce Ewing sarcoma-like tumors in SCID (severe combined immunodeficiency) mice. In addition to demonstrating the potential of MPCs to be the originating cell type of Ewing sarcoma, this also suggests that at least under immunocompromised conditions, the EWSR1-FLI1 fusion might be sufficient for tumor formation. Similar results were also obtained by Castillero-Trejo et al. (2005). In a further study, Riggi et al. (2008) introduced the EWSR1-FLI1 fusion gene into human MSCs, which resulted in a gene expression signature strikingly similar to that of Ewing sarcoma. However, these cells failed to induce tumors in a mouse xenograft model, suggesting that other transforming steps are also required. Another indication in this direction is

the observation that introduction of the EWSR1-FLI1 fusion gene into mouse bone marrow compartment resulted in leukemia, not Ewing sarcoma-like tumors (Torchia et al. 2007).

Kauer et al. (2009) studied five Ewing sarcoma cell lines with EWSR1-FLI1 expression silenced using RNA interference (RNAi) and compared the mRNA expression signatures against a collection of 80 normal tissues (Su et al. 2004). The highest correlation was observed with fetal lung fibroblasts, suggesting mesenchymal origin of Ewing sarcoma. An analogous approach was used by Potikyan et al. (2008), who made a similar comparison against the Celsius database (Day et al. 2007). This study identified IMR-90, a fetal fibroblast cell line, as a close match in terms of Affymetrix expression signatures. Also a third investigation using RNAi showed that the expression profiles of three EWSR1-FLI1-silenced Ewing sarcoma cell lines converge towards that of MSCs (Tirode et al. 2007). Furthermore, when treated with the appropriate conditions, these cells were able to differentiate along adipogenic, chondrogenic and osteocytic lineages, suggesting restoration of a MSC-like phenotype.

Although there is evidence suggesting mesenchymal stem cells to be the originating cell type of Ewing sarcomas, some uncertainty still remains. For example, the observation of Ewing sarcoma-like tumors upon introduction of the EWSR1-FLI1 fusion into murine MPCs (Riggi et al. 2005) has been questioned by Kovar and Bernard (2006). The interpretation of these tumors being similar to Ewing sarcoma was based on the presence of CD99 on the cell surface. Among humans, this antigen is a diagnostic hallmark of Ewing sarcoma, being present on more than 90% of the cases. A CD99 orthologue has been described in mice (Bixel et al. 2004), but bears similarities to the human gene mostly in its transmembrane region (Park et al. 2005). The antibody used to detect CD99 was O13 (Signet Laboratories,

Dedham, MA), which binds to the DGEN motif between residues 49 and 64 of human CD99 (Banting et al. 1989), a motif completely lacking from the murine gene. It therefore remains open whether the detected signal is derived from other proteins. The authors also point out that even after knocking down expression of EWSR1-FLI1, CD99 expression remains high in Ewing sarcoma cells. A precursor already expressing CD99 could therefore be expected, which is not the case for the mouse MPCs and the O13 antibody.

Even as uncertainty remains about the histogenesis of Ewing sarcoma, multiple pieces of evidence point towards mesenchymal stem cells as the cell of origin, and they are currently considered as the most probable alternative among the scientific community.

1.3 Microarray technology

1.3.1 Comparative genomic hybridization and DNA copy number

Each DNA locus of a diploid species, such as humans, is usually present in a normal copy number of two. One allele being inherited from the mother, and the other from the father. However, cancers frequently exhibit copy number aberrations. Portions of the genome can show homozygous (both copies) or heterozygous (one copy) deletions, gains of one or more copies, or higher-level amplifications. The field of cytogenetics has traditionally measured these copy number changes through comparative genomic hybridization (CGH). In this technology, tumor and reference DNAs are labeled with different fluorescent dyes, and hybridized to metaphase chromosomes fixed on a glass slide. The two samples compete with each other to hybridize to DNA sequences present on the glass, and the amount of fluorescent signal therefore

represents the relative abundance of DNA from specific loci. The main drawback of conventional CGH is its low resolution, as aberrations smaller than 5-10 Mb cannot be detected (Forozan et al. 1997).

The advent of array comparative genomic hybridization (aCGH) replaced the metaphase spreads with DNA sequences attached to a solid medium (Kallioniemi et al. 1992), and allowed more accurate detection of copy number aberrations (Pinkel et al. 1998). For these arrays, various sources of DNA have been used: BACs (bacterial artificial chromosomes/clones), cDNA (complementary DNA), and oligonucleotides (Ylstra et al. 2006). BAC arrays (Solinas-Toldo et al. 1997) produce clear results, but their resolution is limited to $\sim$ 1 Mb, because of the large size of the clones. cDNA probes have noisier signals, but increased resolution, and perhaps more importantly, allow mRNA expression measurements using the same array platform (Pollack et al. 1999). The latest development is the use of oligonucleotides, which can be either spotted on the array or synthesized *in situ* (Brennan et al. 2004; Carvalho et al. 2004). As the technology has matured, the number of oligonucleotide probes on the array has increased from tens of thousands to hundreds of thousands and even millions.

The majority of aCGH array platforms are two-channel arrays, such as those manufactured by Agilent Technologies (Santa Clara, CA, USA). DNA from test and reference samples are labeled with different fluorescent dyes and hybridized to the array. Additionally, single nucleotide polymorphism (SNP) microarrays, which were initially designed for genotyping purposes, are now also adopted for copy number analysis (Bignell et al. 2004; Zhao et al. 2005). While Agilent arrays use 60-mer oligonucleotides, SNP arrays have shorter 25-mer probes. SNP arrays have lower sensitivity and specificity, but their main advantage is that they enable the study of copy number neutral loss of heterozygosity (LOH) due to uniparental

disomy (UPD) (Cowell and Lo 2009; Tuna et al. 2009). They can also provide better detection of copy number aberrations in gene-poor areas (Greshock et al. 2007).

In addition to cancer, aCGH arrays are used to study congenital disorders, and also copy number variations (CNVs) in healthy populations. Both small and large-scale CNVs are widespread and common, and present an important source of genetic variation in the human genome (Sebat et al. 2004; Tuzun et al. 2005; Redon et al. 2006). They can contribute to disease susceptibility and might have a role in cancer etiology (Zhang et al. 2009; Shlien and Malkin 2010).

While different approaches to analysis of aCGH microarray data exist, they generally involve the following phases, either as separate steps or fused together: (1) Segmentation divides the normalized $\log_2$ ratios into non-overlapping segments, that most likely share a common copy number. (2) Calling assigns discrete copy numbers to the segments. While some algorithms are able to distinguish homozygous and heterozygous deletions from each other, and also gains and higher-level amplifications, others divide the data simply into gains, losses, and normal copy number. (3) An optional, but often performed step is also to identify regions with aberrations that are shared across different samples. At the moment there is no clear consensus in the aCGH community regarding which stage of data should be used for more downstream analysis, such as integration with expression. But compared to normalized or segmented $\log_2$ ratios, use of calls does have the benefit of a clear biological meaning (van Wieringen et al. 2007). In this study, segmentation was performed using DNAcopy (Venkatraman and Olshen 2007) and calling with CGHcall (van de Wiel et al. 2007), which fits the segmented values into a probabilistic model to obtain the discrete copy number calls. Along these calls, the algorithm also returns the probabilities with which the calls were made. While going from continuous $\log_2$ ratios to discrete, hard calls loses information and hence lowers the statistical

power, the call probabilities (or "soft calls") retain much of this information. Using them for downstream analysis steps can therefore yield improved results compared to the hard calls (van Wieringen and van de Wiel 2009), while still maintaining the added interpretability of gains and losses compared to continuous $\log_2$ ratios.

1.3.2 mRNA expression arrays and transcription

While DNA copy number aberrations are frequent in cancer, the purpose of DNA is to carry on hereditary information to offspring. In order to alter the functioning of the cell, the copy number change has to induce a change transcription levels. Measuring mRNA expression is the most common application of microarray technology. Just like aCGH microarrays, expression arrays can be prepared either by printing pre-produced DNA probes to a solid surface (spotted cDNA and oligonucleotide arrays) (Hughes et al. 2001), or by chemically synthesizing DNA probes on a solid surface using photolithography (Pease et al. 1994). The most common microarray technology for expression studies is the Affymetrix (Santa Clara, CA, USA) GeneChip® array platform, which uses the latter manufacturing process. These are single-channel arrays, but also two-color variants do exist for expression studies. While microarrays have been criticized for low reproducibility, the primary cause of variation has been shown to be biological differences and human factors, rather than the technology itself (Irizarry et al. 2005).

1.3.3 miRNA expression arrays and post-transcriptional regulation

Lately RNA expression arrays have also been designed to target miRNAs (micro RNAs). miRNAs are small $\sim$ 22 base pair RNA molecules that act as post-transcriptional regulators. Through their complementary sequence, they bind to

mRNAs molecules, usually resulting in degradation and/or blockage of translation, although up-regulation has also been described (Vasudevan et al. 2007). The most popular microarray platform is Agilent miRNA arrays, which contain 60-mer oligonucleotide probes and use a single-channel design.

2 Materials and Methods

2.1 Materials

2.1.1 Ewing sarcoma cell lines

A total of 22 different Ewing sarcoma cell lines were used in this study. All 22 were used for miRNA profiling, and a smaller subset of 11 cell lines also for aCGH and mRNA microarrays. Table 2.1 provides a summary of the cell lines and types of microarray data available. The raw array data is available in the CanGEM database (Scheinin et al. 2008) using accessions CG-SER-283 (miRNA), CG-SER-17 (aCGH), and CG-SER-266 (mRNA). However, the data sets are currently password-protected as manuscripts are still under review.

Table 2.1: Ewing sarcoma cell lines
For some cell lines, patient sex and type of gene fusion are not known.

cell line	sex	gene fusion	aCGH	mRNA	miRNA
6647	female	EWSR1-FLI1 type 2	X	X	X
H1474-P2					X
H825					X
IOR/BER		EWSR1-ERG			X
IOR/BRZ	male	EWSR1-FLI1 type 1	X	X	X
IOR/CAR	male	EWSR1-FLI1 type 1	X	X	X
IOR/CLB	female	EWSR1-FLI1 type 1	X	X	X
IOR/NGR	male	EWSR1-FLI1 type 1	X	X	X
IOR/RCH	female	EWSR1-FLI1 type 2	X	X	X
LAP35	female	EWSR1-FLI1 type 2	X	X	X
LT-68					X
MM-83		EWSR1-FLI1 type 1			X
RD-ES	male	EWSR1-FLI1 type 2	X	X	X
RM82		EWSR1-ERG			X
SK-ES-1	male	EWSR1-FLI1 type 2	X	X	X
SK-N-MC	female	EWSR1-FLI1 type 1	X	X	X
STA-ET2.1					X
STA-ET2.2					X
TC-71	male	EWSR1-FLI1 type 1	X	X	X
TC83-AH					X
VH-64		EWSR1-FLI1 type 2			X
WE68		EWSR1-FLI1 type 1			X

2.1.2 Reference samples

For aCGH, blood samples were obtained from Blood Service, Red Cross, Finland to be used as a normal reference. For sex-matched hybridizations, separate male and female references were used and they consisted of pooled blood samples from four individuals.

Two mesenchymal stem cells specimens were used as the normal reference for miRNA screening, and the microarrays were performed in our own laboratory along with the Ewing sarcoma cell line samples.

For the mRNA expression set, no reference data was available. Gene Expression Omnibus (GEO) database (Barrett et al. 2009) was queried for mesenchymal stem cell data measured with the same Affymetrix U133A Plus 2.0 microarray platform as the Ewing sarcoma cell lines. Series GSE7888 (Tanabe et al. 2008), which consists of 23 hMSC specimens derived from bone marrow, was downloaded and used as a reference.

2.2 Methods

As this thesis is focused on the downstream bioinformatic analyses and not on the generation of the microarray data, steps from DNA/RNA extraction to image analysis of the scanned arrays are not described. aCGH profiling was performed using the Human Genome CGH 44B oligo microarrays (Agilent Technologies, Santa Clara, CA, USA) as described by Savola et al. (2007). For mRNA expression, Affymetrix Human Genome U133 Plus 2.0 oligonucleotide arrays (Affymetrix, Santa Clara, CA, USA) were used as previously described for Ewing sarcoma patient

samples (Savola et al. 2009). Agilent miRNA V3 microarays were used to measure miRNA expression.

The data analysis was performed with Chipster (Kallio et al. Submitted, `http://chipster.csc.fi/`), which is a microarray analysis software developed by CSC (Espoo, Finland). Chipster provides a user-friendly graphical user interface for running tools written using the R statistical programming language (R Development Core Team 2009). Most of the functionality is provided with packages from the Bioconductor project (Gentleman et al. 2004). For aCGH analysis methods, the functionality was not previously available in Chipster, but has been implemented as a part ot this thesis work. Unless stated otherwise, all algorithms were run with default parameters, and p-values adjusted using the Benjamini-Hochberg method (Benjamini and Hochberg 1995).

2.2.1 Identifying gains and losses from aCGH data

For the aCGH data set, *normexp* background-correction was performed with an offset of 50, which has been shown to perform well with two-color arrays (Ritchie et al. 2007), and normalization was carried out using loess (Smyth and Speed 2003). A wavy pattern that is typically observed with aCGH profiles (Marioni et al. 2007) was removed using the NoWaves package (van de Wiel et al. 2009) and a calibration data set measured with the same array platform from clinical genetics samples (Siggberg et al. 2010). Log_2 ratios were then segmented with DNAcopy (Venkatraman and Olshen 2007) and called using CGHcall (van de Wiel et al. 2007) to identify gains and losses.

Common aberrations shared between samples were identified using CGHregions (van de Wiel and van Wieringen 2007), which compresses regions of adjacent array

elements into single data points when they are shared between almost all of the samples.

Loss and gain frequencies were calculated for each region, and converted from absolute to relative frequencies as follows: For each region, the mean loss (gain) frequency of the two adjacent regions was subtracted from the frequency of losses (gains) for this region. For the very first (last) region of every chromosome, only the frequency of the next (previous) one was used.

For each region, the percent overlap with reported copy number variations (CNVs) from the Database of Genomic Variants (Zhang et al. 2006) was also calculated.

To be able to inspect aberration frequencies of individual genes, the aCGH data was also converted from probe to gene-based as previously described (Scheinin et al. 2008). Briefly, the full list of human genes was downloaded from Ensembl 59 database (Flicek et al. 2011). For each gene, it was first checked whether there were probes on the array that overlap with the position of the gene. If yes, these probe(s) were used to derive the copy number call for this particular gene. If no, the last probe preceding and first one tailing the gene were used. If more than 50 % of the probes in question showed an aberration, that particular call was chosen for the gene. Otherwise the copy number of the gene was called as a normal.

2.2.2 Detecting differentially expressed mRNAs

The Affymetrix GeneChip® data of 11 Ewing cell lines and 23 mesenchymal stem cell reference samples (GSE7888) were normalized using the gcRMA algorithm (Wu et al. 2004).

Differentially expressed probe sets were identified with an empirical Bayes method (Smyth 2004) with a p-value cutoff of 0.05 and fold-change of at least two-fold.

As gcRMA normalization is performed across-arrays for the entire data set, and there can be a technological differences between the cell line data generated in our own laboratory and the data set downloaded from GEO, the 11 Ewing sarcoma cell lines were also normalized separately without the reference samples from GSE7888. This separately normalized data set was used for integrative analyses with the aCGH miRNA data sets. Before integration, 75% of probe sets with the lowest coefficient of variation ($CV = \textit{standard deviation} \,/\, \textit{mean}$) were filtered out.

2.2.3 Detecting differentially expressed miRNAs

Different ways of preprocessing Agilent miRNA have been compared by López-Romero et al. (2010), and the approach resulting in the lowest variability between biological replicates was used here. Briefly, background-correction was not performed, replicate probes were averaged by taking the median, $\log_2$ transformed intensities were normalized using quantile normalization, and finally, the RMA algorithm (Irizarry et al. 2003) was used to summarize multiple probes that hybridize to the same miRNA into a single expression value. As most of the miRNAs are not expected to be differentially expressed, 75% with the lowest coefficient of variation were filtered out.

Differentially expressed miRNAs were identified using an empirical Bayes method (Smyth 2004). The p-value threshold was set to 0.05 and a two-fold change was also required.

2.2.4 Identifying copy-number-induced expression changes

The effect of copy number changes on (miRNA or mRNA) expression was evaluated with the intCNGEan algorithm (van Wieringen and van de Wiel 2009). First, only those samples were selected that had both types of microarray data available. Then the two data sets were matched so that for each expression probe (or probe set), the closest aCGH probe was selected to represent its DNA copy number. Next, for each probe a choice was made on whether to perform a two-group test between "loss vs. no-loss (normal or gain)" or "no-gain (loss or normal) vs. gain". The choice was based on whether more losses or gains were observed for that particular aCGH probe. Finally, a permutation-based non-parametric test was used to evaluate the statistical significance of expression changes between the two groups.

2.2.5 Evaluating effect of miRNA expression on mRNA levels

To evaluate effects of miRNA expression on mRNA levels, predicted miRNA target genes were downloaded from PicTar (Krek et al. 2005) and TargetScan databases (Lewis et al. 2005). An intersection was taken between the two lists to only accept predictions present in both. Filtered miRNA and mRNA data sets were then paired with the target predictions and Kendall correlation coefficients and p-values calculated between each miRNA-target pair.

3 Results

A saved session for the Chipster analysis software can be downloaded from the following URL: `http://ilari.scheinin.fi/progradu.cs`

3.1 Copy number aberrations

After preprocessing, the aCGH data was segmented and called to identify copy number aberrations. Overall, more gains than losses were detected, with the most frequent gains located in chromosomes 8, 1q and X, and most frequent losses in 9p, 16q and 17p. Copy number profiles of individual samples are shown in Figure A.1 on page 67.

After calling, the dimensionality of the data was reduced by identifying common regions. As the exact breakpoints around driving cancer genes vary slightly from one sample to another, a loss of 1% of information was allowed to focus on biologically relevant results. This yielded a total of 284 regions. The most frequent losses and gains (over 50 % of the samples) are listed in Table 3.1, and all regions are listed in Table A.1 on page 74.

As copy number aberrations generally cover bystander genes in addition to the cancerous ones, gain and loss frequencies were also transformed from absolute to relative frequencies by subtracting from each region's frequency the mean frequency of the two adjacent regions. This allows better identification of regions containing the true driving genes from ones that show relatively high aberration frequencies based on their proximity to a region with a driving gene. Table 3.4 on page 35 lists regions with the highest relative aberration frequencies (at least 10 %),

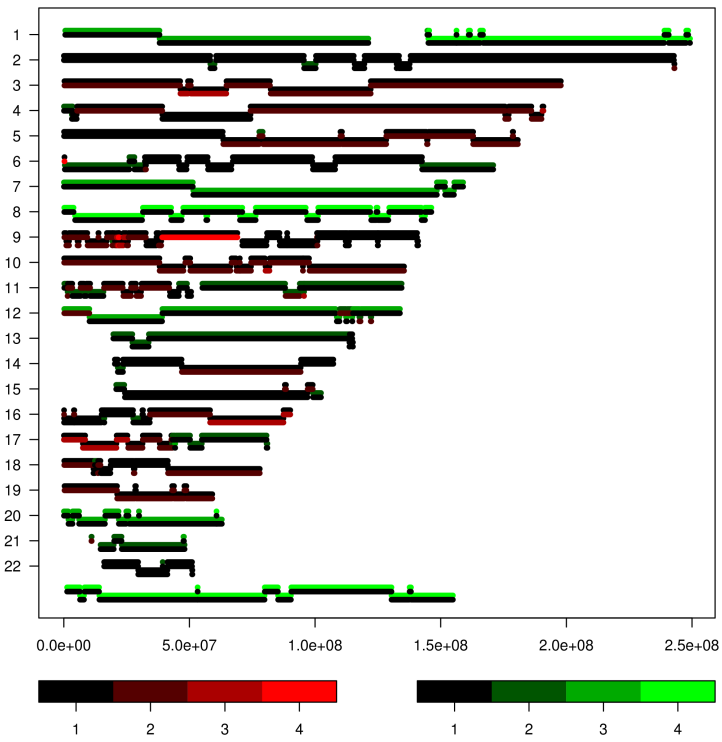

(a) regions

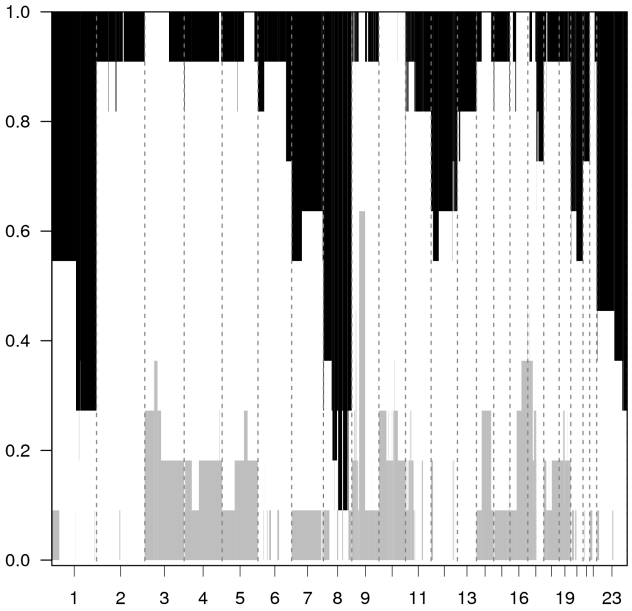

(b) frequencies

Figure 3.1: Copy number regions
(a) Each chromosome is shown as a horizontal line, and breakpoints are marked with small vertical bumps. The frequencies of gains and losses are shown with different shades of green and red, respectively. The abundance of breakpoints in 9p is evident and is focused around 9p21.3.
(b) Frequencies of losses are shown in gray (values from the scale on the left) and gains in black (values "1 - left scale"), with the data ordered by genomic position along the x-axis.

Table 3.1: Most common copy number aberrations by absolute frequencies
List of regions with absolute loss/gain frequencies of at least 50 %. The three columns marked as "aCGH probes" show the starting base pair position of the first microarray probe, the end position of the last probe, and the total number of microarray probes within the region. The percentage overlap with reported CNVs from the Database of Genomic Variants is listed in the "CNV %" column. Relative frequencies are obtained from absolute frequencies by subtracting from the region's frequency the mean frequency of the two adjacent regions.

			aCGH probes				absolute % of		relative % of	
	chr	cytobands	start	end	num	CNV %	losses	gains	losses	gains
59	6	p25.3	259 528	293 492	2	100	81.8	0	81.8	0
112	9	p21.3	21 978 346	22 008 225	4	100	63.6	0	9.1	0
121	9	p11.1-q21.11	39 140 222	69 073 065	5	39.4	63.6	0	50.0	0
111	9	p21.3	21 805 270	21 968 098	5	83.1	54.5	9.1	0	4.6
113	9	p21.3	22 008 596	22 009 028	2	100	54.5	0	0	0

(a) losses

			aCGH probes				absolute % of		relative % of	
	chr	cytobands	start	end	num	CNV %	losses	gains	losses	gains
83	8	q12.1	56 682 642	57 129 002	12	71.7	0	90.9	0	9.1
85	8	q13.2-q13.3	70 106 133	70 744 066	8	18.8	0	90.9	0	13.7
88	8	q21.11-q22.1	76 402 380	96 269 295	204	33.1	0	90.9	0	18.2
90	8	q22.2-q24.12	101 251 572	121 937 154	225	20.7	0	90.9	0	18.2
93	8	q24.13-q24.21	124 997 293	129 147 781	48	10.4	0	90.9	0	13.7
7	1	q22	156 264 255	156 307 404	3	0	0	81.8	0	9.1
9	1	q23.3	161 133 330	161 677 035	24	63	0	81.8	0	9.1
82	8	q11.1-q12.1	47 536 057	56 652 072	70	33.5	0	81.8	0	0
84	8	q12.1-q13.2	57 229 343	69 867 282	148	21.7	0	81.8	0	0
92	8	q24.13	124 403 872	124 857 149	9	0	0	81.8	0	0
6	1	q21.1-q22	145 440 247	156 254 642	315	57.2	0	72.7	0	0
8	1	q22-q23.3	156 316 721	161 123 686	143	4.2	0	72.7	0	0
10	1	q23.3-q24.1	161 697 689	165 664 592	63	39.6	0	72.7	0	0
12	1	q24.1-q43	166 921 615	238 888 928	1217	26.7	0	72.7	0	4.6
13	1	q43	239 011 002	240 724 580	15	37.5	9.1	72.7	9.1	0
14	1	q43-q44	240 755 779	247 605 063	105	32.8	0	72.7	0	0
15	1	q44	247 695 693	248 480 808	17	100	9.1	72.7	9.1	0
16	1	q44	249 104 603	249 212 667	7	80.4	0	72.7	0	0
78	8	p23.3-p23.2	191 530	3 889 590	36	54.1	9.1	72.7	0	9.1
81	8	p11.21-q11.1	42 729 970	46 943 014	12	22.9	0	72.7	0	0
86	8	q13.3	70 890 166	71 024 682	3	10.5	0	72.7	0	0
87	8	q13.3-q21.11	71 126 134	76 351 498	64	17.5	9.1	72.7	9.1	0
89	8	q22.1-q22.2	96 846 254	101 164 771	66	28.1	9.1	72.7	9.1	0
91	8	q24.12-q24.13	122 329 490	124 357 012	23	9.3	0	72.7	0	0
94	8	q24.21-q24.3	129 505 388	142 270 534	106	20.1	9.1	72.7	9.1	0
95	8	q24.3	142 367 717	143 742 450	14	52.4	0	72.7	0	0
96	8	q24.3	143 744 897	146 280 019	85	74.6	9.1	72.7	9.1	0
282	X	q26.2-q26.3	130 419 292	137 430 408	98	22.4	0	72.7	0	9.1
284	X	q27.1-q28	138 231 171	154 841 454	236	31.6	0	72.7	0	9.1
5	1	q21.1	145 413 388	145 416 395	2	100	0	63.6	0	0
11	1	q24.1	165 696 716	166 826 147	17	21.9	0	63.6	0	0
79	8	p23.2-p12	4 494 837	31 158 464	366	50.8	9.1	63.6	4.6	0
80	8	p12-p11.21	31 488 003	42 704 918	141	15.5	0	63.6	0	0
274	X	p22.31	6 457 403	8 032 119	16	82.8	9.1	63.6	0	9.1
281	X	q21.31-q26.2	90 530 805	130 407 536	462	31.1	0	63.6	0	0
283	X	q26.3-q27.1	137 628 563	138 145 138	9	1.3	0	63.6	0	0
4	1	q21.1	145 076 147	145 194 112	4	100	9.1	54.5	4.6	0
259	20	q13.33	60 791 724	60 814 359	2	100	0	54.5	0	9.0
273	X	p22.33-p22.31	1 314 894	6 385 370	36	67.2	9.1	54.5	0	0
275	X	p22.31-p22.2	8 266 181	14 039 227	77	21.2	9.1	54.5	4.6	0
276	X	p22.2-p11.22	14 167 254	53 221 664	494	35	0	54.5	0	0
277	X	p11.22	53 240 164	53 283 765	2	100	9.1	54.5	9.1	0
278	X	p11.22-q21.1	53 325 084	79 884 773	293	40.4	0	54.5	0	0
279	X	q21.1-q21.2	79 975 0	85 198 467	52	15	9.1	54.5	9.1	0
280	X	q21.2-q21.31	85 282 468	90 374 528	36	31.4	0	54.5	0	0

(b) gains

together with the number of differentially expressed mRNAs and miRNAs within these regions.

The probe-based aCGH data was also converted to gene-based to be able to assess aberration frequencies of individual genes. The full list of 49 733 genes from Ensembl version 59 (Flicek et al. 2011) can be found from the saved Chipster session.

3.2 Differentially expressed mRNAs

As no Affymetrix expression measurements of mesenchymal stem cells were available from our own laboratory, an external and previously published data set was used. Series GSE7888 (Tanabe et al. 2008) was retrieved from the Gene Expression Omnibus database (Barrett et al. 2009). After normalizing the 11 Ewing sarcoma cell lines together with the 23 reference samples, a total of 14 903 differentially expressed probe sets (corresponding to 8 366 genes) were detected. Instead of choosing more stringent cutoffs for p-values (0.05) and fold change (at least two-fold) to obtain a more manageable list of differentially expressed mRNAs, these more tolerant values were chosen because external reference samples were used. As this results in increased technical bias between the two data sets, use of strict criteria could miss the more interesting biological differences while returning only technical ones. For this reason, the long list of differentially expressed mRNAs was selected to not to be used on its own, but instead to be integrated with DNA copy number results from the aCGH data set and as predicted targets of miRNAs.

3.3 Differentially expressed miRNAs

miRNAs differentially expressed in the 22 Ewing sarcoma cell lines compared to the two reference samples were detected with empirical Bayes. Selecting miRNAs with a p-value smaller than 0.05 and an at least two-fold change in expression resulted in 32 down-regulated and 21 up-regulated miRNAs, which are listed in Table 3.2.

3.4 Effect of DNA copy number on miRNA expression

To evaluate the effect of changes in DNA copy number to miRNA expression, an integrated analysis was performed for the Agilent aCGH and miRNA expression data sets. Figure 3.2 shows heatmaps of the data sets after each expression probe has been paired with the closest aCGH probe to represent its copy number, and individual samples are shown in Figure A.2 on page 70.

After probe matching, a permutation-based non-parametric test was performed to measure the significance of copy-number-induced expression changes. After multiple testing correction, all p-values were larger than 0.05. The two smallest ones were for miR-206 (p-value 0.114) and miR-25 (0.133), and their expression is plotted in Figure 3.3.

In addition to the systematic testing for copy-number-induced expression changes, the list of differentially expressed miRNAs was also annotated with aberration frequencies for the miRNA loci. Down-regulated miRNAs that also show elevated frequencies of losses include miR-31 and miR-31b (45.5%), and miR-22, miR-140-5p and miR-140-3p (36.4 %). Up-regulation and frequent gains can be seen with miR-20b and miR-30b (72.7 %), and miR-106b, miR-93, miR-25 and

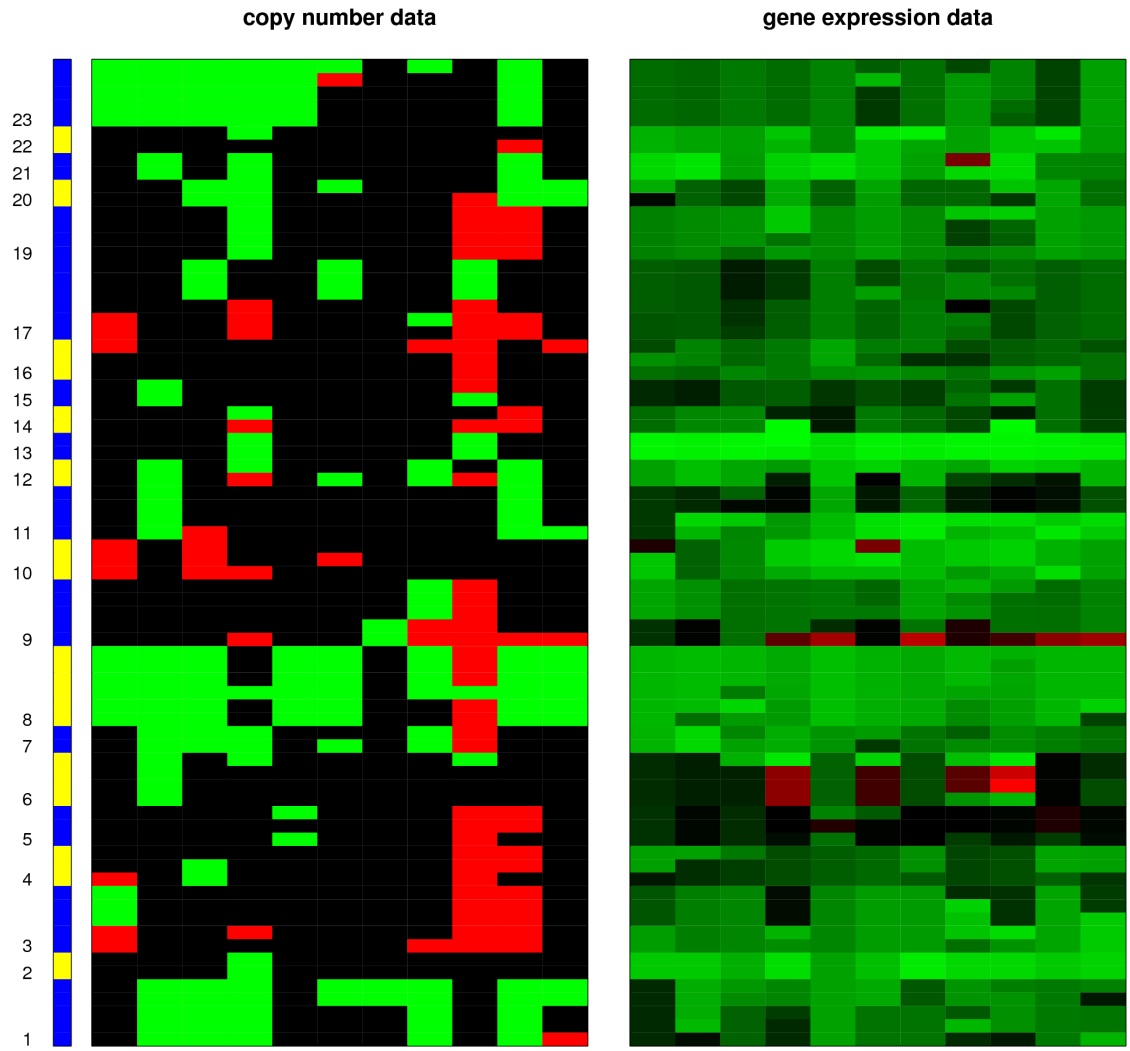

Figure 3.2: aCGH and miRNA heatmaps
Copy number data is shown on the left and miRNA expression on the right. Chromosomes are ordered along the y-axis and samples are shown in the same order for both data sets. Green depicts gains and up-regulation, while losses and down-regulation are shown in red.

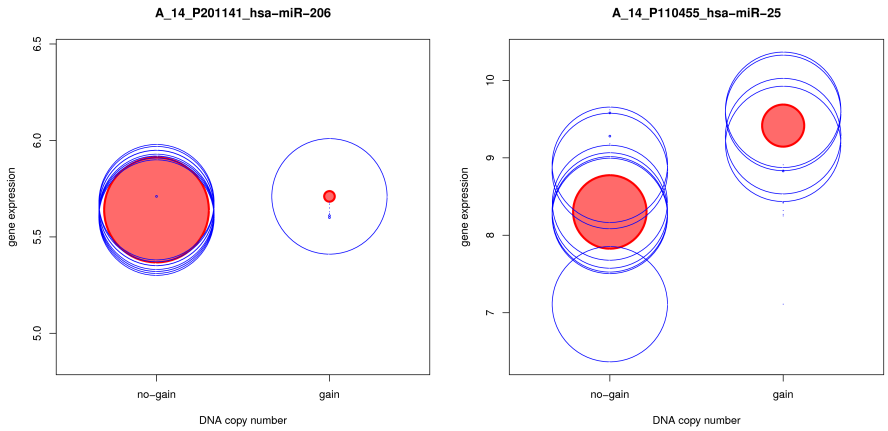

(a) miR-206 **(b)** miR-25

Figure 3.3: Differential miRNA expression induced by copy number aberrations
For each miRNA, the samples were split into two groups based the observed pattern of copy number aberrations. The comparison was either "loss vs. no-loss (normal or gain)" or "no-gain (loss or normal) vs. gain" and the grouping is labeled on the x-axis. The center of each circle marks the expression level of the miRNA for an individual sample, and the radius represents the probability of the corresponding copy number call. Probabilities of 0% shrink the circles into dots. The red circles mark the mean expression (height) and probability (radius).

miR-331-3p (36.4 %). The entire list of differentially expressed miRNAs together with aberration frequencies is shown in Table 3.2.

3.5 Effect of DNA copy number on mRNA expression

The effect of DNA copy number changes on mRNA expression was tested in a similar fashion as for the miRNA data set.Figure 3.4 shows heatmaps of the data sets after each expression probe set has been paired with the closest aCGH probe, and individual samples are shown in Figure A.3 on page 73.

After probe matching, a permutation test identified a total of 11 probe sets with copy-number-induced changes in expression. They represented 10 different genes, with two distinct probe sets covering the MTAP gene. For three genes (EZH1,

Table 3.2: Differentially expressed miRNAs and their aberration frequencies
The miRNAs without chromosome and cytoband information are present in more than one location in the genome.

miRNA	chr	cytoband	p-value	fold-change	absolute losses	% of gains
hsa-miR-100	11	q24.1	<0.001	4.5	0	18.2
hsa-miR-21	17	q23.1	<0.001	4.37	0	27.3
hsa-miR-125b			<0.001	3.61		
hsa-miR-145	5	q32	<0.001	3.37	18.2	0
hsa-miR-22	17	p13.3	<0.001	3.29	36.4	0
hsa-miR-886-3p			0.001	3.19		
hsa-let-7i	12	q14.1	0.003	2.89	0	36.4
hsa-miR-193a-3p	17	q11.2	<0.001	2.37	18.2	0
hsa-miR-23b	9	q22.32	<0.001	2.37	9.1	9.1
hsa-miR-27b	9	q22.32	<0.001	2.24	9.1	9.1
hsa-miR-365			<0.001	2.12		
hsa-miR-27a	19	p13.13	0.022	2.10	18.2	9.1
hsa-miR-30a	6	q13	<0.001	2.07	0	9.1
hsa-miR-143	5	q32	<0.001	2.03	18.2	0
hsa-miR-31	9	p21.3	<0.001	2.01	45.5	9.1
hsa-miR-140-5p	16	q22.1	<0.001	1.91	36.4	0
hsa-miR-23a	19	p13.13	0.016	1.84	18.2	9.1
hsa-miR-137	1	p21.3	<0.001	1.67	0	45.5
hsa-miR-376c	14	q32.31	0.011	1.61	9.1	9.1
hsa-miR-31*	9	p21.3	<0.001	1.50	45.5	9.1
hsa-miR-21*	17	q23.1	<0.001	1.49	0	27.3
hsa-miR-221	X	p11.3	0.005	1.47	0	54.5
hsa-miR-193b	16	p13.12	<0.001	1.40	9.1	0
hsa-miR-199a-5p			0.045	1.31		
hsa-miR-140-3p	16	q22.1	<0.001	1.30	36.4	0
hsa-miR-376a			0.044	1.25		
hsa-miR-222	X	p11.3	<0.001	1.25	0	54.5
hsa-miR-377	14	q32.31	0.005	1.25	9.1	9.1
hsa-miR-136	14	q32.2	<0.001	1.25	9.1	9.1
hsa-miR-152	17	q21.32	<0.001	1.23	0	27.3
hsa-miR-193a-5p	17	q11.2	<0.001	1.21	18.2	0
hsa-miR-127-3p	14	q32.2	0.002	1.20	9.1	9.1

(a) down-regulated miRNAs

miRNA	chr	cytoband	p-value	fold-change	absolute losses	% of gains
hsa-miR-20a	13	q31.3	<0.001	-3.11	0	18.2
hsa-miR-17	13	q31.3	<0.001	-2.95	0	18.2
hsa-miR-19a	13	q31.3	<0.001	-2.55	0	18.2
hsa-miR-19b			<0.001	-2.43		
hsa-miR-106b	7	q22.1	<0.001	-2.25	9.1	36.4
hsa-miR-9*			0.027	-2.13		
hsa-miR-93	7	q22.1	<0.001	-2.06	9.1	36.4
hsa-miR-92a			<0.001	-2.01		
hsa-miR-20b	X	q26.2	<0.001	-1.98	0	72.7
hsa-miR-18a	13	q31.3	0.006	-1.92	0	18.2
hsa-miR-15b	3	q25.33	<0.001	-1.80	18.2	9.1
hsa-miR-25	7	q22.1	0.031	-1.37	9.1	36.4
hsa-miR-181b			0.039	-1.36		
hsa-miR-16			<0.001	-1.22		
hsa-miR-324-5p	17	p13.1	<0.001	-1.20	36.4	0
hsa-miR-128			0.027	-1.16		
hsa-miR-331-3p	12	q22	0.010	-1.15	0	36.4
hsa-miR-126	9	q34.3	0.002	-1.13	9.1	9.1
hsa-miR-320d			0.031	-1.09		
hsa-miR-30b	8	q24.22	0.010	-1.06	9.1	72.7
hsa-miR-1246			0.019	-1.01		

(b) up-regulated miRNAs

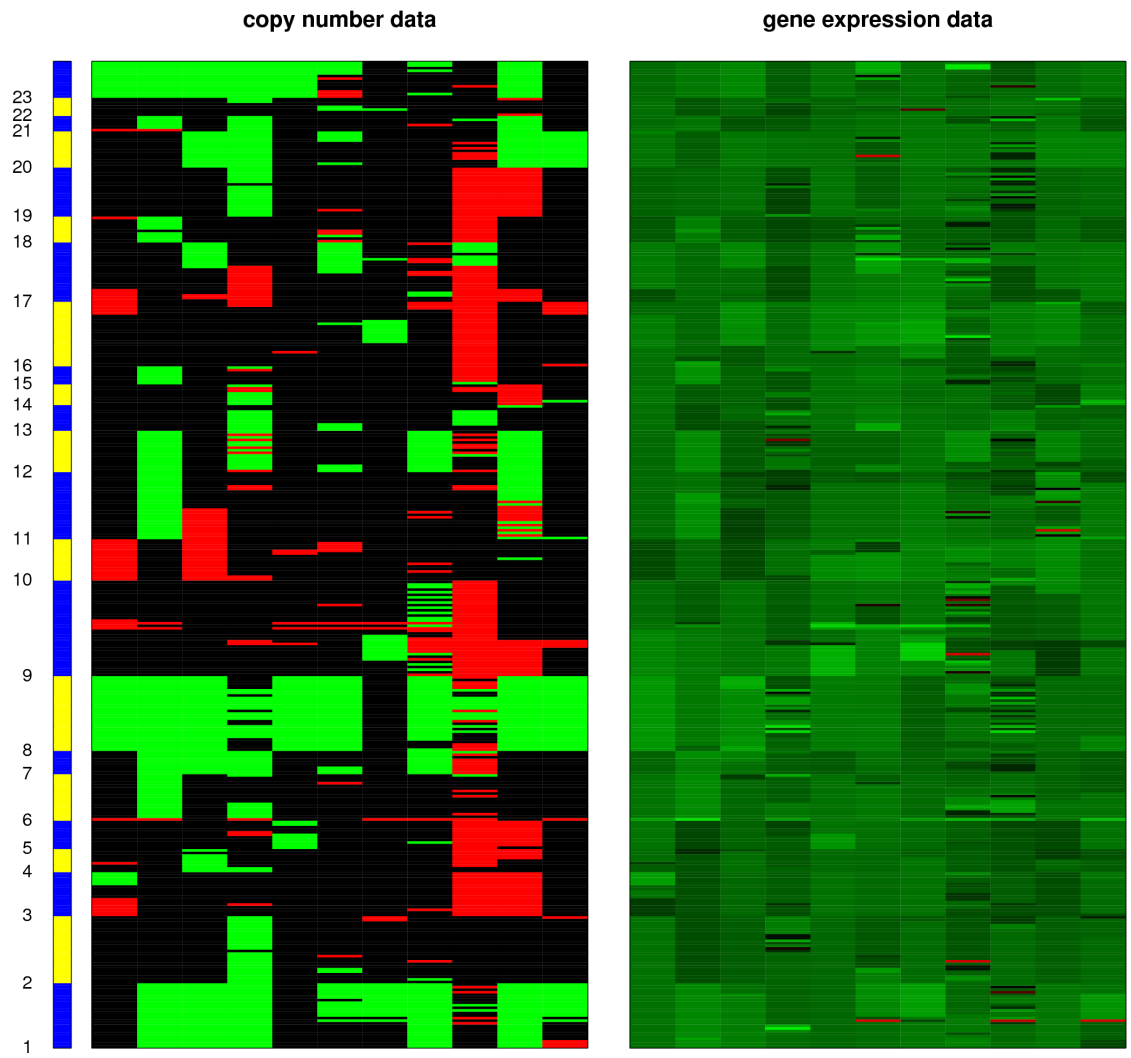

Figure 3.4: aCGH and mRNA heatmaps
Copy number data is shown on the left and mRNA expression on the right. Chromosomes are ordered along the y-axis and samples are shown in the same order for both data sets. Green depicts gains and up-regulation, while losses and down-regulation are shown in red.

Table 3.3: mRNAs with copy-number-induced expression changes
The table lists all mRNA expression probe sets whose expression has a statistically significant correlation with DNA copy number. P-values were all <0.001. Shown is also the fold-change between the Ewing sarcoma cell lines and the mesenchymal stem cell reference, and the aberration frequencies from the aCGH data.

probe set	gene	chr	cytoband	comparison	aCGH probe	fold-change	absolute % of losses	absolute % of gains
201313_at	ENO2	12	p13.31	gain	A_14_P121634	-1.39	18.2	36.4
204956_at	MTAP	9	p21.3	loss	A_14_P101143	1.40	54.5	9.1
212332_at	RBL2	16	q12.2	loss	A_14_P123561	-0.75	27.2	0
212930_at	ATP2B1	12	q21.33	gain	A_14_P131824	2.01	0	36.4
221745_at	DCAF7	17	q23.3	gain	A_14_P137769	-2.37	0	27.2
223852_s_at	STK40	1	p34.3	gain	A_14_P135095	-1.78	9.1	45.5
224521_s_at	CCDC77	12	p13.33	gain	A_14_P127808	-0.28	18.2	36.4
226371_at	JARID1A	12	p13.33	gain	A_14_P107722	-0.52	18.2	36.4
231984_at	MTAP	9	p21.3	loss	A_14_P101143	0.61	54.5	9.1
244790_at	MTCP1	X	q28	gain	A_14_P135923	-1.60	0	72.7
32259_at	EZH1	17	q21.2	loss	A_14_P119420	0.45	27.2	9.1

MTAP, and RBL2), the comparison performed was "loss vs. no-loss (normal or gain)" and for seven (ATP2B1, CCDC77, DCAF7, ENO2, JARID1A, MTCP1, and STK40) "no-gain (loss or normal) vs. gain". Table 3.3 lists all Affymetrix probe sets where the p-value for copy-number-induced changes in expression was smaller than 0.05. Also listed in this table is the fold-change between the 11 Ewing sarcoma cell lines compared to the 23 mesenchymal stem cells from GEO series GSE7888, and also the aberration frequencies observed in the aCGH data.

Of the genes showing significantly lower expression related to copy number losses, MTAP was also found to be down-regulated compared to the mesenchymal stem cells. Similarly, DCAF7, ENO2, MTCP1, and STK40 showed elevated expression in association to copy number gains together with up-regulation compared to the mesenchymal stem cells.

In search of the driving genes of frequent copy number aberrations, the regions with most frequent relative aberration frequencies were investigated for overlapping genes that were also found to be differentially expressed. Table 3.4 shows a list of regions with relative aberration frequencies of over 10 % annotated with the number of differentially expressed mRNAs and miRNAs. Only down-regulated ones

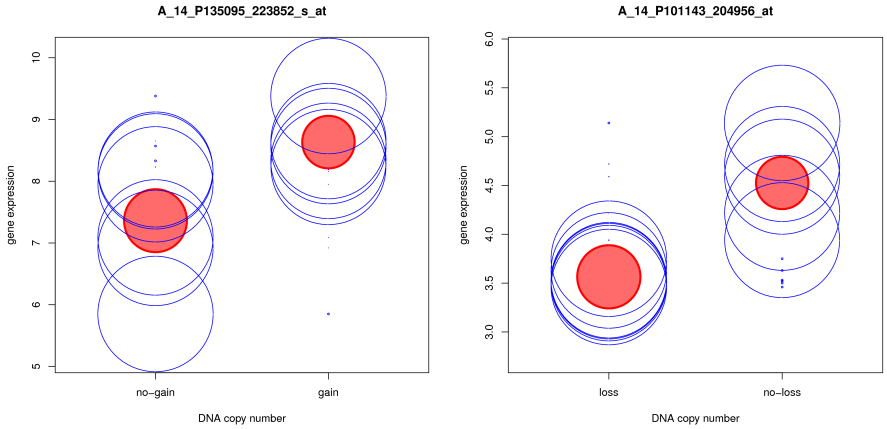

(a) STK40

(b) MTAP

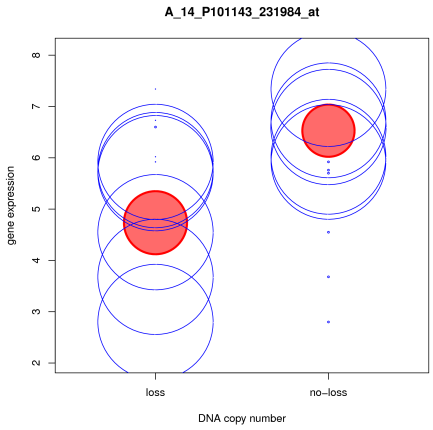

(c) MTAP

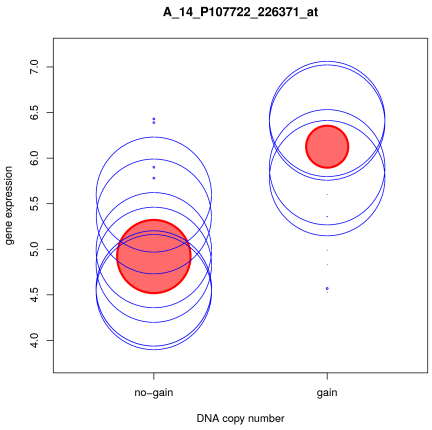

(d) JARID1A

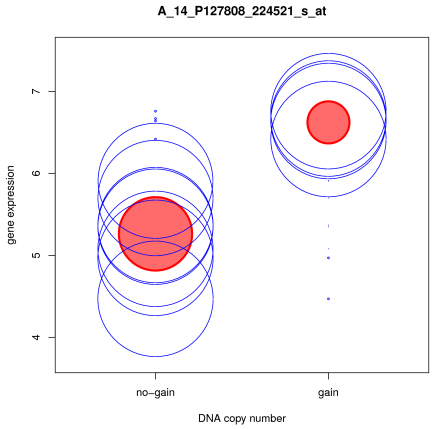

(e) CCDC77

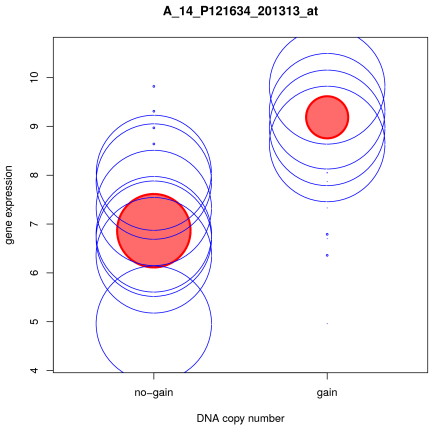

(f) ENO2

Figure 3.5: Differential mRNA expression induced by copy number aberrations
For each probe set, the samples were split into two groups based the observed pattern of copy number aberrations. The comparison was either "loss vs. no-loss (normal or gain)" or "no-gain (loss or normal) vs. gain" and the grouping is labeled on the x-axis. The center of each circle marks the expression level of the probe set for an individual sample, and the radius represents the probability of the corresponding copy number call. Probabilities of 0% shrink the circles into dots. The red circles mark the mean expression (height) and probability (radius).

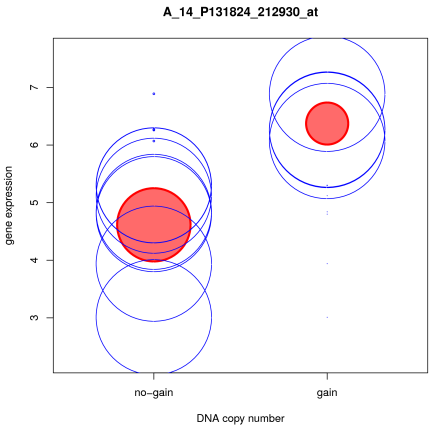

(g) ATP2B1

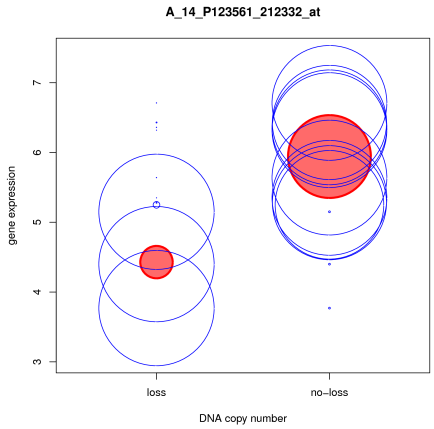

(h) RBL2

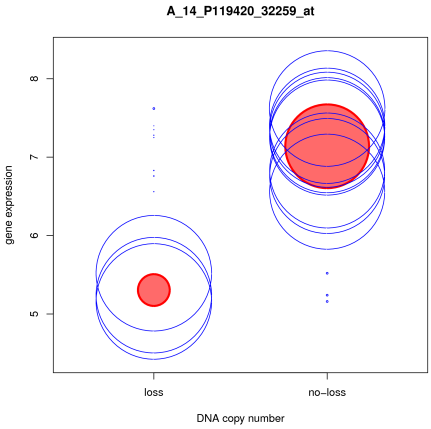

(i) EZH1

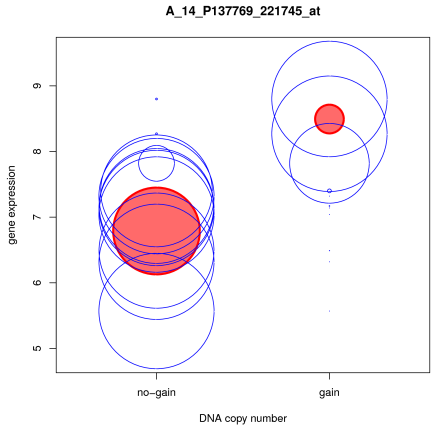

(j) DCAF7

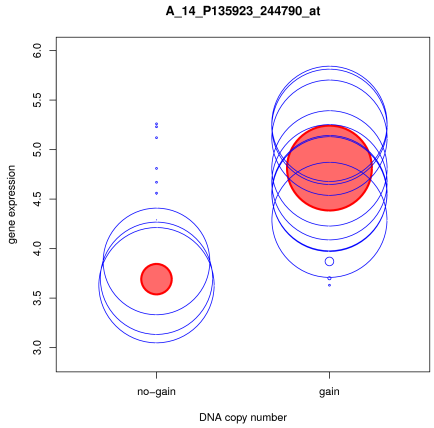

(k) MTCP1

Figure 3.5: Differential mRNA expression induced by copy number alterations (cont.)

Table 3.4: Most common copy number alterations by relative frequencies and differentially expressed genes
Regions with a relative frequency for copy number aberrations of over 10 % are annotated with the number of differentially expressed mRNAs and miRNAs.
(a) Regions with a high relative frequency of losses contain a total of 193 down-regulated mRNA probe sets representing 134 genes. Regions with a small number of putative targets include region 121 (KGFLP1 and CNTNAP3B), region 64 (HLA-DRB1, HLA-DRB5), region 168 (C11orf75, NOX4), and region 178 (SDSL).
(b) Regions with a high relative frequency of gains contain a total of 159 up-regulated mRNA probe sets representing 79 genes. Region 85 contains the SLCO5A1 gene, and region 175 genes ALKBH2, SSH1, UNG, and USP30.

			aCGH probes				absolute % of		relative % of		down-regulated	
	chr	cytobands	start	end	num	CNV %	losses	gains	losses	gains	mRNAs	miRNAs
59	6	p25.3	259 528	293 492	2	100	81.8	0	81.8	0	0	0
121	9	p11.1-q21.11	39 140 222	69 073 065	5	39.4	63.6	0	50.0	0	2	0
170	11	q21	95 591 751	95 621 376	2	0	36.4	18.2	36.4	0	0	0
46	4	q35.2	190 482 637	190 884 259	3	100	45.5	0	27.3	0	0	0
28	2	q37.3	242 930 819	243 041 363	3	100	18.2	9.1	18.2	0	0	0
64	6	p21.32	32 488 879	32 713 164	5	100	18.2	9.1	18.2	0	3	0
168	11	q14.2-q21	88 240 997	93 885 399	55	46.4	18.2	18.2	18.2	0	2	0
172	12	p13.33-p13.2	179 706	10 164 582	244	38.4	18.2	36.4	18.2	0	38	0
176	12	q24.11-q24.12	109 857 930	112 280 894	69	3.1	18.2	27.3	18.2	0	13	0
181	12	q24.22-q24.23	117 619 855	118 104 214	14	11.1	18.2	27.3	18.2	0	0	0
183	12	q24.31	122 156 586	122 370 332	7	13	18.2	27.3	18.2	0	0	0
194	14	q21.2-q32.12	46 975 576	94 247 844	753	19.9	27.3	0	18.2	0	133	0
261	21	q11.1	10 991 392	11 096 085	3	100	18.2	18.2	18.2	0	0	0
178	12	q24.13-q24.21	112 890 753	114 634 078	40	4.3	18.2	27.3	13.7	0	2	0
242	19	p12-q11	21 242 399	28 272 555	49	51.9	27.3	9.1	13.7	0	0	0

(a) losses

			aCGH probes				absolute % of		relative % of		up-regulated	
	chr	cytobands	start	end	num	CNV %	losses	gains	losses	gains	mRNAs	miRNAs
72	6	q24.1-q27	142 597 923	170 892 301	368	38.5	0	27.3	0	18.2	56	0
88	8	q21.11-q22.1	76 402 380	96 269 295	204	33.1	0	90.9	0	18.2	40	0
90	8	q22.2-q24.12	101 251 572	121 937 154	225	20.7	0	90.9	0	18.2	43	0
269	22	q13.1	39 359 112	39 385 484	3	100	0	18.2	0	18.2	0	0
85	8	q13.2-q13.3	70 106 133	70 744 066	8	18.8	0	90.9	0	13.7	2	0
93	8	q24.13-q24.21	124 997 293	129 147 781	48	10.4	0	90.9	0	13.7	13	0
175	12	q23.3-q24.11	108 641 156	109 700 234	31	37.9	0	45.5	0	13.7	5	0

(b) gains

are shown for regions with frequent losses, and up-regulated for gains.

3.6 Effect of miRNA expression on mRNA levels

As the function of miRNAs is to bind to mRNA molecules blocking translation and causing degradation, the correlation between expression of miRNAs and mRNAs was evaluated. Combining the filtered data sets with target predictions from PicTar

(Krek et al. 2005) and TargetScan databases (Lewis et al. 2005) resulted in a total of 12 169 miRNA-mRNA pairs. After correcting for multiple testing, the lowest p-value was 0.167 observed with the pair of miR-22 and FBN2 (Kendall tau rank correlation coefficient $\tau = -0.891$). The rest of the p-values were all larger than 0.5.

In search of the putative driving oncogenes and tumor suppressors behind the frequent copy number aberrations, the lists of genes in the regions showing high relative aberration frequencies were intersected with miRNA-mRNA pairing data. Of the 134 down-regulated genes found in regions with over 10 % relative frequency of losses, five were found to be targets of at least three miRNAs that are up-regulated compared to the mesenchymal stem cells. These include BTBD7 (targeted by six up-regulated miRNAs), SMOC1 (6), FOXJ2 (4), FRMD6 (4), and SLC2A3 (3).

Similarly, of the 79 up-regulated genes in frequently gained (in terms of relative frequency) regions, three were targets of at least three down-regulated miRNAs: QKI (target of seven down-regulated miRNAs), PKIA (4), and SLCO5A1 (3).

Finally, when pairing miRNA-mRNA target pairing with those mRNA expression probe sets whose expression was found to have a statistically significant effect from DNA copy number changes, the STK40 was found to be a target of 4 down-regulated miRNAs: miR-21, miR-27a, let-7i, and miR-27b.

4 Discussion

An integrative analysis of microarray data from Ewing sarcoma cell lines has been performed. aCGH, miRNA, and mRNA data sets have been analyzed individually and also through integrative approaches. The most frequent copy number aberrations have been identified, as have differentially expressed miRNAs compared to mesenchymal stem cell specimens. For mRNA expression, no reference sample data was available from our own laboratory, so an external data set was used. Due to large differences, differentially expressed mRNAs were not identified per se, but instead this information was used to complement other approaches. Integrative analyses were performed to identify copy -number-induced miRNA and mRNA expression, and also to measure correlation between expression of miRNAs and their predicted target genes.

One factor significantly limiting the feasibility of genomics approach to the data analysis is the small sample size. miRNA measurements consisted of 22 Ewing sarcoma cell lines and two mesenchymal stem cell reference samples, but aCGH and mRNA data sets both contained only 11 cell lines. Increasing the sample size could dramatically improve the results of the analyses.

Analysis of the Agilent aCGH data set identified aberrations in DNA copy number, and all detected regions are listed in Table A.1 on page 74. Those showing gains or losses in more than 50 % of the samples have been listed in Table 3.1 on page 25. The most frequent losses were in 6p25.3 (81.8 %), three regions (111–113, frequencies between 63.6 % and 54.5 %) in 9p, and around the centromere of chromosome 9 (63.6 %). Because pericentromeric regions contain highly repetitive sequences, their mapping is more difficult and they are generally poorly targeted by aCGH microarrays (Horvath et al. 2000). Therefore copy number changes around

centromeres (and telomeres) should be evaluated with caution. The region in 6p25.3 is entirely within CNVs reported in the Database of Genomic Variants (Zhang et al. 2006), and contains no genes found to be down-regulated. It therefore more likely represents normal copy number variation in the human population than a cancerous aberration. Losses in 9p are known to be common in many cancers including Ewing sarcoma, and the loss of the CDKN2A gene has been linked with poor survival (Huang et al. 2005). This gene has also been shown to be affected by microdeletions small enough to be missed using FISH (fluorescent *in situ* hybridization) (Savola et al. 2007). CDKN2A is located in the reverse strand of chromosome 9 and is contained within regions 111 (lost in 54.5 %) and 112 (63.6 %) in this analysis. The adjacent tumor suppressor gene CDKN2B is overlaps regions 112 and 113 (54.5 %).

The most frequent gains were in chromosome 8 (up to 90.9 %), 1q (81.8 %), X (72.7 %), and one isolated region in 20q13.33 (54.5 %). However, the last one is completely overlapping with reported CNVs, and contains no differentially expressed genes, so it is arising most likely simply because of normal copy number variation. Trisomy of chromome 8 and gains in 1q are both frequent in Ewing sarcoma, and although more rare, trisomy of X has also been reported (Patiño-García et al. 1999).

An interesting observation is also the relatively large number of distinct regions (40) in chromosome 9. Dividing the number of regions with the base pair length covered by the probes on the Agilent 44K microarray (from the start of first probe to the end of the last probe in the same chromosome) results in 0.28 regions per megabase of genomic sequence. The mean value across all chromosomes is 0.11 regions / Mb. Other breakpoint-rich chromosomes are 17 (0.20 regions / Mb) and 20 (0.19), while chromosomes 3 and 2 show relatively few distinct regions (0.04 and 0.05, respectively). In chromosome 9, the breakpoints are concentrated especially on the 9p21.3 cytogenetic band, which is split into 10 different regions (1.75 regions / Mb).

The observed copy number changes in this cytoband are mostly losses with the frequency varying between 18.2 % and 63.6 %.

As copy number aberrations around driving genes typically cover areas much larger than just the target gene, aberration frequencies were also converted to relative frequencies by subtracting from the frequency of each region the mean frequency of its neighbors. This identifies regions that have higher aberration frequencies than their surrounding areas. Table 3.4 on page 35 lists regions with highest relative aberration frequencies. Interestingly, while in general more gains than losses were observed, there are 15 regions of losses and 7 regions of gains with frequencies higher than 10 %. Losses therefore appear to be smaller and their boundaries more precisely located than for gains. This could be a result of differences between functional consequences of gains of oncogenes vs. losses of tumor-suppressors.

Identified by both high absolute and relative loss frequencies are regions 59 (6p25.3) and 121 (9p11.1–q21.11). The first one contains no differentially expressed genes, and is likely only a CNV, while the later one contains the centromere, which makes the finding suspicious. The two down-regulated genes in this region are KGFLP1 (keratinocyte growth factor-like protein 1) and CNTNAP3B (contactin associated protein-like 3B). Regions with high absolute and relative frequency of gains include regions 85 (8q13.2–q13.3), 88 (8q21.11–q22.1), 90 (8q22.2–q24.12), and 93 (8q24.13–q24.21). Region 85 only contains one up-regulated gene (SLCO5A1, solute carrier organic anion transporter family member 5A1), while the other three contain a total of 96 up-regulated Affymetrix probe sets.

Differentially expressed probe sets were identified by comparing our Ewing sarcoma cell line data with an external reference data set downloaded from the GEO database. GSE7888 consists of 23 mesenchymal stem cell samples. As the reference

data comes from a different laboratory, and is likely to contain bias in addition to the real biological differences, the list of differentially expressed mRNAs was only used in conjunction with the aCGH or miRNA data sets.

Integration of aCGH and expression data helps to identify the driving targets behind copy number aberrations, and the effect of copy number on mRNA expression was tested using a genomics approach. A permutation-based non-parametric test was used to identify Affymetrix probe sets whose expression had been significantly altered by copy number changes. Of the resulting 10 genes, MTAP was lost in 54.5 % of the samples and also down-regulated compared to the mesenchymal reference samples. Four genes were associated with gains and up-regulation: DCAF7, ENO2, MTCP1, and STK40.

MTAP (methylthioadenosine phosphorylase) is located in 9p21.3 and overlaps with the CDKN2A gene. Deletions in this locus are common in a wide variety of cancers, but they are often attributed solely to CDKN2A while the loss of MTAP is regarded as a byproduct. However, it has been shown that mice with a null MTAP allele develop T-cell lymphomas demonstrating that MTAP has in independent tumor suppressor function unrelated to CDKN2A (Kadariya et al. 2009). Also, while the aberration patterns for these two genes are identical in our data, the expression of CDKN2A was not found to be altered by copy number in a statistically significant level, although it was slightly lower among cell lines exhibiting a loss. Losses of MTAP have been previously described in Ewing sarcoma, but only in the context of combined deletion of MTAP and CDKN2A (Brownhill et al. 2007).

DCAF7 (DDB1 and CUL4 associated factor 7) has been shown to activate stem cell-related gene expression leading to an increase in cancer stem cells in luminal B breast cancer (Sircoulomb et al. 2011). It has also been shown to partic-

ipate in craniofacial development of the zebrafish and is required for the formation of the equivalent of the upper jaw, the palatoquadrate (Nissen et al. 2006). ENO2 (enolase 2) is a hypoxia-induced gene, which has been linked to multiple cancers, including prostatic small-cell neuroendocrine carcinoma (Clegg et al. 2003), gastric cancer (Arao et al. 2006), and renal cell carcinoma (Teng et al. 2011). MTCP1 (mature T-cell proliferation 1) was identified in 1993 as the first candidate gene potentially involved in the leukemogenic process of mature T cell proliferations (Stern et al. 1993). It has also been shown to modify T-cell homeostasis before leukemogenesis in transgenic mice (Joiner et al. 2007).

STK40 (serine/threonine kinase 40), which is also known as SHIK (SINK-homologous serine/threonine-protein kinase), has been shown to inhibit TNF-triggered (tumor necrosis factor) NF-κB activation, and also to inhibit p53-mediated transcription in a dose-dependent manner (Huang et al. 2003). No effect on p53 proteins levels were observed, but its activity is known to be controlled through various different mechanisms including regulation of transcription or translation, alterations in protein half-life, post-translational phosphorylation or acetylation, redox modulations, and alterations in its intracellular localization. STK40 has also been shown to activate the MAPK (mitogen-activated protein kinase) pathway and induce differentiation in mouse embryonic stem cells (Li et al. 2010). Hofmann et al. (2010) showed that POU3F1 (POU class 3 homeobox 1) was needed for efficient up-regulation of STK40. POU3F1 (also known as Oct-6) is a member of the octamer transcription factor family and functions mainly in developmental processes, and also acts as a co-activator of innate immune responses. POU3F1 is found to be up-regulated in the Ewing sarcoma cell lines with no losses and a gain in 45.5 % of the samples.

The miRNA comparison of 22 Ewing sarcoma cell lines against two mesenchymal stem cell reference samples identified a total of 53 differentially expressed

miRNAs. 32 were down-regulated in the cell lines compared to the reference, and 21 were up-regulated. The most frequent losses among the down-regulated miRNAs were miR-31 and miR-31* in 9p21.3 (lost in 45.5 %), miR-140-3p and miR-140-5p in 16q22.1 (36.4 %), and miR-22 in 17p13.3 (36.4 %). Most frequent gains are for miR-30b in 8q24.22 (72.7 %); miR-20b in Xq26.2 (72.7 %); miR-25, miR-93 and miR-106b in 7q22.1 (36.4 %); and miR-331-3p in 12q22 (36.4 %). However, the permutation-based non-parametric testing failed to identify statistical significance in copy-number-induced expression changes of miRNAs. This could mean that other mechanisms than copy number are more important in miRNA regulation. Also, our small sample size of 11 cell lines for the integration analyses might be a limiting factor.

Additional experiments are needed to identify the most important miRNAs and their functional roles in Ewing sarcoma. The only one described so far is miR-145, which is located in 5q32 (Riggi et al. 2010). The EWSR1-FLI1 fusion gene suppresses expression of miR-145, which is found to be down-regulated in this study with 18.2 % losses and no gains. FLI1 is one of the targets of miR-145, so they form a mutually repressive feedback loop (Zhang et al. 2011).

As the biological function of miRNAs is post-transcriptional gene regulation, this relationship was assessed by measuring the correlation between expression of miRNAs and their predicted target mRNAs. However, this approach failed to identify pairs with statistically significant correlation. The lowest p-value was 0.167 between miR-22 and FBN2 (fibrillin 2). However, compared to the mesenchymal stem cells, both miR-22 and FBN2 are down-regulated in the Ewing sarcoma cell lines, which makes the relevance of the observed correlation questionable.

As miRNAs can lead to lowered protein expression either by causing

degradation of the mRNA molecules or by simply blocking translation, these alternatives can have different outcomes when measuring such correlations. If only translation is blocked but the mRNA molecule is not degraded, it can still bind to the microarray. The exact mechanism depends on the complementarity of the miRNA and mRNA sequences. Perfect complementarity leads into mRNA degradation, while incomplete complementarity silences the gene by blocking protein translation. However, microarray experiments have shown that miRNA expression does lead to large-scale reductions of mRNA and not only protein levels (Lim et al. 2005).

Interestingly, even though miRNAs act to down-regulate their target mRNAs, almost half of the pairs tested (5 730 out of 12 169) had a positive correlation coefficient. One possible explanation is that this is a result of other regulatory mechanisms overriding the effect of miRNAs. For example, the effect of increased expression induced by a gain in copy number could be larger in magnitude than can be compensated with increased expression of a miRNA. Even though miRNA-mRNA pairs with negative correlation are the ones agreeing with our understanding of miRNA regulation, pairs with positive correlation could provide an interesting approach to identify processes that have in a way escaped the regulatory control of the cell.

Our limited sample size probably has to be increased in order to find significant correlations between miRNA and mRNA target gene expression. In an attempt to integrate miRNA-mRNA target predictions with the copy number data, those mRNAs that were found to be differentially expressed and targeted by multiple differentially expressed miRNAs were identified. The list of down-regulated mRNAs targeted by at least three up-regulated miRNAs was intersected with the list of 134 genes found in regions with over 10 % relative frequency of losses. This identified five genes that show both deletions and down-regulation through multi-

ple miRNAs: BTBD7 (targeted by six up-regulated miRNAs), SMOC1 (6), FOXJ2 (4), FRMD6 (4), and SLC2A3 (3). BTBD7 (BTB (POZ) domain containing 7) promotes epithelial tissue remodeling and formation of branched organs (Onodera et al. 2010). SMOC1 (SPARC related modular calcium binding 1) inhibits bone morphogenetic protein signaling downstream of receptor binding and is essential for post-gastrulation development in xenopus (Thomas et al. 2009). FOXJ2 (forkhead box J2) is a transcription factor, whose over-expression has been shown to be lethal (Martín-de Lara et al. 2008). FRMD6 (FERM domain containing 6) links cytoskeleton with the plasma membrane, and its localization to plasma membrane is induced by EGF (epidermal growth factor), which is found to be up-regulated in the Ewing sarcoma cell lines. SLC2A3 (solute carrier family 2 member 3) is glucose transporter, and rather than being down-regulated like here, its over-expression has been linked with various carcinomas and melanoma, with a possible role in angiogenesis (Ayala et al. 2010; Tsukioka et al. 2007; Parente et al. 2008).

The list of up-regulated mRNAs that are targeted by at least three down-regulated miRNAs was similarly intersected with the list of 79 genes found in areas of frequent copy number gain (relative frequency more than 10 %). Three genes were identified: QKI (target of seven down-regulated miRNAs), PKIA (4), and SLCO5A1 (3). QKI (quaking homolog) is expressed in neural progenitors, but their expression is down-regulated during neuronal differentiation (Hardy 1998). PKIA (cAMP-dependent protein kinase inhibitor alpha) is an inhibitor of PKA (protein kinase A), which is responsible for most of the of functions regulated by cAMP (cyclic AMP). Its role in disorders is not well described (Van Patten et al. 1987). SLCO5A1 (solute carrier organic anion transporter family member 5A1) belongs to the family of organic anion transporters, which transport a variety of amphipathic organic molecules via an anion exchange mechanism. In the Ewing cell lines it is up-regulated, but its only reported link to disease phenotypes is an observation

of copy number loss. The locus encompassing SLCO5A1 and SULF1 is found to be deleted in Mesomelia-synostoses syndrome (MSS), which is a rare autosomal-dominant disorder characterized by mesomelic limb shortening, acral synostoses, and multiple congenital malformations (Isidor et al. 2010).

The lists of differentially expressed mRNAs targeted by multiple differentially expressed miRNAs were also intersected with the ten genes showing copy-number-induced expression changes in the permutation-based statistical test. This identified STK40 as a target of four down-regulated miRNAs in addition to being gained in 45.4 % of the samples, showing statistically significant increase in expression due to a change in copy number, and being up-regulated in Ewing sarcoma cell lines compared to the mesenchymal stem cell reference data set.

Among the known targets of the EWSR1-FLI1 fusion gene expected patterns were observed. Genes known to be required for optimal transformation showed up-regulation in comparison to the mesenchymal stem cells, and also contained an elevated frequency of gains. NROB1 had a gain in 54.5 % of samples, and NKX2-2, EZH2 and IGF-1 in 36.4 %. All these genes were found to be up-regulated compared to mesenchymal stem cells, and none had any copy number losses. On the other hand, TGF-βR2 was down-regulated with 27.3 % losses and no gains.

The most interesting putative novel target genes arising from this analysis are the ones with copy-number-induced expression changes. MTAP is found to be down-regulated in the Ewing sarcoma cell lines compared to mesenchymal stem cell reference, and also to exhibit frequent losses that lower its expression. Therefore, it is possible that MTAP might have a distinct tumor-suppressor function separate from the CDKN2A gene in the same locus. Putative oncogenes include DCAF7, ENO2, MTCP1, and STK40, which are all linked with higher expression in association with

copy number gains, and also up-regulation compared to mesenchymal stem cells. Additionally, STK40 is also targeted by four down-regulated miRNAs. Another gene exhibiting potential perturbations both from copy number and miRNAs is SLCO5A1. It is a target of three down-regulated miRNAs, is up-regulated compared to the reference samples, and is located in a region with an absolute and relative gain frequency of 90.9 % and 13.7 %, respectively.

Future plans regarding the putative target genes include analyses of published, external Ewing sarcoma microarray data sets to verify these findings. Also further validation with immunohistochemistry and/or functional assays is being considered.

As our understanding of crucial molecular events in the Ewing sarcoma transformation develops, future improvements in therapy can hopefully one day put an end to it being a taker of lives of children and young adults in their prime.

Acknowledgements

I would like to thank my supervisor, professor Sakari Knuutila, for guidance and financial support. I would also like to thank the people who performed the microarray experiments producing the data analyzed in this thesis: Neda Mosakhani for miRNA, Suvi Savola for aCGH, and Filippo Nardi for the mRNA data set. Personnel of the Laboratory of Cytomolecular Genetics is also thanked for a pleasant working environment.

For this thesis project I also visited Instituto Ortopedico Rizzoli in Bologna, Italy. I would like to thank Piero Picci and Katia Scotlandi for this opportunity and Fumihiko Nakatani and Andrea Grilli for providing clinical data and other information regarding the cell lines used in this work.

References

Arao T., Yanagihara K., Takigahira M., Takeda M., Koizumi F., Shiratori Y., and Nishio K. ZD6474 inhibits tumor growth and intraperitoneal dissemination in a highly metastatic orthotopic gastric cancer model. *Int J Cancer*, 118(2):483–9, 2006. 41

Aurias A., Rimbaut C., Buffe D., Zucker J. M., and Mazabraud A. Translocation involving chromosome 22 in Ewing's sarcoma. A cytogenetic study of four fresh tumors. *Cancer Genet Cytogenet*, 12(1):21–5, 1984. 6

Ayala F. R. R., Rocha R. M., Carvalho K. C., Carvalho A. L., da Cunha I. W., Lourenço S. V., and Soares F. A. GLUT1 and GLUT3 as potential prognostic markers for Oral Squamous Cell Carcinoma. *Molecules*, 15(4):2374–87, 2010. 44

Bacci G., Longhi A., Barbieri E., Ferrari S., Mercuri M., Briccoli A., Versari M., Pignotti E., and Picci P. Second malignancy in 597 patients with Ewing sarcoma of bone treated at a single institution with adjuvant and neoadjuvant chemotherapy between 1972 and 1999. *J Pediatr Hematol Oncol*, 27(10):517–20, 2005. 5

Banting G. S., Pym B., Darling S. M., and Goodfellow P. N. The MIC2 gene product: epitope mapping and structural prediction analysis define an integral membrane protein. *Mol Immunol*, 26(2):181–8, 1989. 12

Barrett T., Troup D. B., Wilhite S. E., Ledoux P., Rudnev D., Evangelista C., Kim I. F., Soboleva A., Tomashevsky M., Marshall K. A., Phillippy K. H., Sherman P. M., Muertter R. N., and Edgar R. NCBI GEO: archive for high-throughput functional genomic data. *Nucleic Acids Res*, 37(Database issue):D885–90, 2009. 18, 26

Benjamini Y. and Hochberg Y. Controlling the false discovery rate: a practical and powerful approach to multiple testing. *J Roy Stat Soc Ser B*, 57(1):289–300, 1995. 19

Bignell G. R., Huang J., Greshock J., Watt S., Butler A., West S., Grigorova M., Jones K. W., Wei W., Stratton M. R., Futreal P. A., Weber B., Shapero M. H., and Wooster R. High-resolution analysis of DNA copy number using oligonucleotide microarrays. *Genome Res*, 14(2):287–95, 2004. 13

Bixel G., Kloep S., Butz S., Petri B., Engelhardt B., and Vestweber D. Mouse CD99 participates in T-cell recruitment into inflamed skin. *Blood*, 104(10):3205–13, 2004. 11

Brennan C., Zhang Y., Leo C., Feng B., Cauwels C., Aguirre A. J., Kim M., Protopopov A., and Chin L. High-resolution global profiling of genomic alterations with long oligonucleotide microarray. *Cancer Res*, 64(14):4744–8, 2004. 13

Brownhill S. C., Taylor C., and Burchill S. A. Chromosome 9p21 gene copy number and prognostic significance of p16 in ESFT. *Br J Cancer*, 96(12):1914–23, 2007. 40

Carvalho B., Ouwerkerk E., Meijer G. A., and Ylstra B. High resolution microarray comparative genomic hybridisation analysis using spotted oligonucleotides. *J Clin Pathol*, 57(6):644–6, 2004. 13

Castillero-Trejo Y., Eliazer S., Xiang L., Richardson J. A., and Ilaria Jr R. L. Expression of the EWS/FLI-1 oncogene in murine primary bone-derived cells results in EWS/FLI-1-dependent, Ewing sarcoma-like tumors. *Cancer Res*, 65 (19):8698–705, 2005. 10

Cheung C. C., Kandel R. A., Bell R. S., Mathews R. E., and Ghazarian D. M. Extraskeletal Ewing sarcoma in a 77-year-old woman. *Arch Pathol Lab Med*, 125 (10):1358–60, 2001. 2

Cironi L., Riggi N., Provero P., Wolf N., Suvà M.-L., Suvà D., Kindler V., and Stamenkovic I. IGF1 is a common target gene of Ewing's sarcoma fusion proteins in mesenchymal progenitor cells. *PLoS One*, 3(7):e2634, 2008. 8

Clegg N., Ferguson C., True L. D., Arnold H., Moorman A., Quinn J. E., Vessella R. L., and Nelson P. S. Molecular characterization of prostatic small-cell neuroendocrine carcinoma. *Prostate*, 55(1):55–64, 2003. 41

Collini P., Sampietro G., Bertulli R., Casali P. G., Luksch R., Mezzelani A., Sozzi G., and Pilotti S. Cytokeratin immunoreactivity in 41 cases of ES/PNET confirmed by molecular diagnostic studies. *Am J Surg Pathol*, 25(2):273–4, 2001. 4

Cotterill S. J., Ahrens S., Paulussen M., Jürgens H. F., Voûte P. A., Gadner H., and Craft A. W. Prognostic factors in Ewing's tumor of bone: analysis of 975 patients from the European Intergroup Cooperative Ewing's Sarcoma Study Group. *J Clin Oncol*, 18(17):3108–14, 2000. 2, 3

Cowell J. K. and Lo K. C. Application of oligonucleotides arrays for coincident comparative genomic hybridization, ploidy status and loss of heterozygosity studies in human cancers. *Methods Mol Biol*, 556:47–65, 2009. 14

Craft A. W., Cotterill S. J., Bullimore J. A., and Pearson D. Long-term results from the first UKCCSG Ewing's Tumour Study (ET-1). United Kingdom Children's Cancer Study Group (UKCCSG) and the Medical Research Council Bone Sarcoma Working Party. *Eur J Cancer*, 33(7):1061–9, 1997. 5

Day A., Carlson M. R. J., Dong J., O'Connor B. D., and Nelson S. F. Celsius: a community resource for Affymetrix microarray data. *Genome Biol*, 8(6):R112, 2007. 11

de Alava E., Kawai A., Healey J. H., Fligman I., Meyers P. A., Huvos A. G., Gerald W. L., Jhanwar S. C., Argani P., Antonescu C. R., Pardo-Mindan F. J., Ginsberg J., Womer R., Lawlor E. R., Wunder J., Andrulis I., Sorensen P. H., Barr F. G., and Ladanyi M. EWS-FLI1 fusion transcript structure is an independent determinant of prognosis in Ewing's sarcoma. *J Clin Oncol*, 16(4):1248–55, 1998. 6

de Alava E., Antonescu C. R., Panizo A., Leung D., Meyers P. A., Huvos A. G., Pardo-Mindán F. J., Healey J. H., and Ladanyi M. Prognostic impact of P53 status in Ewing sarcoma. *Cancer*, 89(4):783–92, 2000. 9

Delattre O., Zucman J., Plougastel B., Desmaze C., Melot T., Peter M., Kovar H., Joubert I., de Jong P., and Rouleau G. Gene fusion with an ETS DNA-binding domain caused by chromosome translocation in human tumours. *Nature*, 359 (6391):162–5, 1992. 6, 7

Douglass E. C., Rowe S. T., Valentine M., Parham D., Meyer W. H., and Thompson E. I. A second nonrandom translocation, der(16)t(1;16)(q21;q13), in Ewing sarcoma and peripheral neuroectodermal tumor. *Cytogenet Cell Genet*, 53(2-3):87–90, 1990. 9

Dworzak M. N., Fritsch G., Fleischer C., Printz D., Fröschl G., Buchinger P., Mann G., and Gadner H. CD99 (MIC2) expression in paediatric B-lineage leukaemia/lymphoma reflects maturation-associated patterns of normal B-lymphopoiesis. *Br J Haematol*, 105(3):690–5, 1999. 4

Esiashvili N., Goodman M., and Marcus Jr R. B. Changes in incidence and survival of Ewing sarcoma patients over the past 3 decades: Surveillance Epidemiology and End Results data. *J Pediatr Hematol Oncol*, 30(6):425–30, 2008. 2, 3, 4

Ewing J. Diffuse endothelioma of bone. *Proc N Y Pathol Soc*, 21:17–24, 1921. 2

Fellinger E. J., Garin-Chesa P., Triche T. J., Huvos A. G., and Rettig W. J. Immunohistochemical analysis of Ewing's sarcoma cell surface antigen p30/32MIC2. *Am J Pathol*, 139(2):317–25, 1991. 4

Flicek P., Amode M. R., Barrell D., Beal K., Brent S., Chen Y., Clapham P., Coates G., Fairley S., Fitzgerald S., Gordon L., Hendrix M., Hourlier T., Johnson N., Kähäri A., Keefe D., Keenan S., Kinsella R., Kokocinski F., Kulesha E., Larsson P., Longden I., McLaren W., Overduin B., Pritchard B., Riat H. S., Rios D., Ritchie G. R. S., Ruffier M., Schuster M., Sobral D., Spudich G., Tang Y. A., Trevanion S., Vandrovcova J., Vilella A. J., White S., Wilder S. P., Zadissa A., Zamora J., Aken B. L., Birney E., Cunningham F., Dunham I., Durbin R., Fernández-Suarez X. M., Herrero J., Hubbard T. J. P., Parker A., Proctor G., Vogel J., and Searle S. M. J. Ensembl 2011. *Nucleic Acids Res*, 39(Database issue):D800–6, 2011. 20, 26

Folpe A. L., Hill C. E., Parham D. M., O'Shea P. A., and Weiss S. W. Immunohistochemical detection of FLI-1 protein expression: a study of 132 round cell tumors with emphasis on CD99-positive mimics of Ewing's sarcoma/primitive neuroectodermal tumor. *Am J Surg Pathol*, 24(12):1657–62, 2000. 4

Forozan F., Karhu R., Kononen J., Kallioniemi A., and Kallioniemi O. P. Genome screening by comparative genomic hybridization. *Trends Genet*, 13(10):405–9, 1997. 13

Fraumeni Jr J. F. and Glass A. G. Rarity of Ewing's sarcoma among U.S. Negro children. *Lancet*, 1(7642):366–7, 1970. 2

Gangwal K. and Lessnick S. L. Microsatellites are EWS/FLI response elements: genomic "junk" is EWS/FLI's treasure. *Cell Cycle*, 7(20):3127–32, 2008. 8

Gangwal K., Sankar S., Hollenhorst P. C., Kinsey M., Haroldsen S. C., Shah A. A., Boucher K. M., Watkins W. S., Jorde L. B., Graves B. J., and Lessnick S. L. Microsatellites as EWS/FLI response elements in Ewing's sarcoma. *Proc Natl Acad Sci U S A*, 105(29):10149–54, 2008. 7

Gangwal K., Close D., Enriquez C. A., Hill C. P., and Lessnick S. L. Emergent properties of EWS/FLI regulation via GGAA microsatellites in Ewing's sarcoma. *Genes Cancer*, 1(2):177–187, 2010. 8

Gelin C., Aubrit F., Phalipon A., Raynal B., Cole S., Kaczorek M., and Bernard A. The E2 antigen, a 32 kd glycoprotein involved in T-cell adhesion processes, is the MIC2 gene product. *EMBO J*, 8(11):3253–9, 1989. 4

Gentleman R. C., Carey V. J., Bates D. M., Bolstad B., Dettling M., Dudoit S., Ellis B., Gautier L., Ge Y., Gentry J., Hornik K., Hothorn T., Huber W., Iacus S., Irizarry R., Leisch F., Li C., Maechler M., Rossini A. J., Sawitzki G., Smith C., Smyth G., Tierney L., Yang J. Y. H., and Zhang J. Bioconductor: open software development for computational biology and bioinformatics. *Genome Biol*, 5(10): R80, 2004. 19

Ginsberg J. P., de Alava E., Ladanyi M., Wexler L. H., Kovar H., Paulussen M., Zoubek A., Dockhorn-Dworniczak B., Juergens H., Wunder J. S., Andrulis I. L., Malik R., Sorensen P. H., Womer R. B., and Barr F. G. EWS-FLI1 and EWS-ERG gene fusions are associated with similar clinical phenotypes in Ewing's sarcoma. *J Clin Oncol*, 17(6):1809–14, 1999. 7

Granowetter L., Womer R., Devidas M., Krailo M., Wang C., Bernstein M., Marina N., Leavey P., Gebhardt M., Healey J., Shamberger R. C., Goorin A., Miser J., Meyer J., Arndt C. A. S., Sailer S., Marcus K., Perlman E., Dickman P., and Grier H. E. Dose-intensified compared with standard chemotherapy for nonmetastatic Ewing sarcoma family of tumors: a Children's Oncology Group Study. *J Clin Oncol*, 27(15):2536–41, 2009. 5

Greshock J., Feng B., Nogueira C., Ivanova E., Perna I., Nathanson K., Protopopov A., Weber B. L., and Chin L. A comparison of DNA copy number profiling platforms. *Cancer Res*, 67(21):10173–80, 2007. 14

Grier H. E., Krailo M. D., Tarbell N. J., Link M. P., Fryer C. J. H., Pritchard D. J., Gebhardt M. C., Dickman P. S., Perlman E. J., Meyers P. A., Donaldson S. S., Moore S., Rausen A. R., Vietti T. J., and Miser J. S. Addition of ifosfamide and etoposide to standard chemotherapy for Ewing's sarcoma and primitive neuroectodermal tumor of bone. *N Engl J Med*, 348(8):694–701, 2003. 5

Guillon N., Tirode F., Boeva V., Zynovyev A., Barillot E., and Delattre O. The oncogenic EWS-FLI1 protein binds in vivo GGAA microsatellite sequences with potential transcriptional activation function. *PLoS One*, 4(3):e4932, 2009. 7

Hahm K. B., Cho K., Lee C., Im Y. H., Chang J., Choi S. G., Sorensen P. H., Thiele C. J., and Kim S. J. Repression of the gene encoding the TGF-beta type II receptor is a major target of the EWS-FLI1 oncoprotein. *Nat Genet*, 23(2): 222–7, 1999. 8

Hanahan D. and Weinberg R. A. The hallmarks of cancer. *Cell*, 100(1):57–70, 2000. 1

Hardy R. J. QKI expression is regulated during neuron-glial cell fate decisions. *J Neurosci Res*, 54(1):46–57, 1998. 44

Hattinger C. M., Rumpler S., Strehl S., Ambros I. M., Zoubek A., Pötschger U., Gadner H., and Ambros P. F. Prognostic impact of deletions at 1p36 and numerical aberrations in Ewing tumors. *Genes Chromosomes Cancer*, 24(3):243–54, 1999. 9

Hattinger C. M., Pötschger U., Tarkkanen M., Squire J., Zielenska M., Kiuru-Kuhlefelt S., Kager L., Thorner P., Knuutila S., Niggli F. K., Ambros P. F., Gadner H., and Betts D. R. Prognostic impact of chromosomal aberrations in Ewing tumours. *Br J Cancer*, 86(11):1763–9, 2002. 9

Hofmann E., Reichart U., Gausterer C., Guelly C., Meijer D., Müller M., and Strobl B. Octamer-binding factor 6 (Oct-6/Pou3f1) is induced by interferon and contributes to dsRNA-mediated transcriptional responses. *BMC Cell Biol*, 11:61, 2010. 41

Horvath J. E., Schwartz S., and Eichler E. E. The mosaic structure of human pericentromeric DNA: a strategy for characterizing complex regions of the human genome. *Genome Res*, 10(6):839–52, 2000. 37

Hu-Lieskovan S., Heidel J. D., Bartlett D. W., Davis M. E., and Triche T. J. Sequence-specific knockdown of EWS-FLI1 by targeted, nonviral delivery of small interfering RNA inhibits tumor growth in a murine model of metastatic Ewing's sarcoma. *Cancer Res*, 65(19):8984–92, 2005. 8

Huang H.-Y., Illei P. B., Zhao Z., Mazumdar M., Huvos A. G., Healey J. H., Wexler L. H., Gorlick R., Meyers P., and Ladanyi M. Ewing sarcomas with p53 mutation or p16/p14ARF homozygous deletion: a highly lethal subset associated with poor chemoresponse. *J Clin Oncol*, 23(3):548–58, 2005. 9, 10, 38

Huang J., Teng L., Liu T., Li L., Chen D., Li F., Xu L.-G., Zhai Z., and Shu H.-B. Identification of a novel serine/threonine kinase that inhibits TNF-induced NF-κB activation and p53-induced transcription. *Biochem Biophys Res Commun*, 309 (4):774–8, 2003. 41

Hughes T. R., Mao M., Jones A. R., Burchard J., Marton M. J., Shannon K. W., Lefkowitz S. M., Ziman M., Schelter J. M., Meyer M. R., Kobayashi S., Davis C., Dai H., He Y. D., Stephaniants S. B., Cavet G., Walker W. L., West A., Coffey E., Shoemaker D. D., Stoughton R., Blanchard A. P., Friend S. H., and Linsley P. S. Expression profiling using microarrays fabricated by an ink-jet oligonucleotide synthesizer. *Nat Biotechnol*, 19(4):342–7, 2001. 15

Im Y. H., Kim H. T., Lee C., Poulin D., Welford S., Sorensen P. H., Denny C. T., and Kim S. J. EWS-FLI1, EWS-ERG, and EWS-ETV1 oncoproteins of Ewing tumor family all suppress transcription of transforming growth factor beta type ii receptor gene. *Cancer Res*, 60(6):1536–40, 2000. 8

Irizarry R. A., Bolstad B. M., Collin F., Cope L. M., Hobbs B., and Speed T. P. Summaries of Affymetrix GeneChip probe level data. *Nucleic Acids Res*, 31(4): e15, 2003. 21

Irizarry R. A., Warren D., Spencer F., Kim I. F., Biswal S., Frank B. C., Gabrielson E., Garcia J. G. N., Geoghegan J., Germino G., Griffin C., Hilmer S. C., Hoffman E., Jedlicka A. E., Kawasaki E., Martínez-Murillo F., Morsberger L., Lee H., Petersen D., Quackenbush J., Scott A., Wilson M., Yang Y., Ye S. Q., and Yu W. Multiple-laboratory comparison of microarray platforms. *Nat Methods*, 2(5):345–50, 2005. 15

Isidor B., Pichon O., Redon R., Day-Salvatore D., Hamel A., Siwicka K. A., Bitner-Glindzicz M., Heymann D., Kjellén L., Kraus C., Leroy J. G., Mortier G. R., Rauch A., Verloes A., David A., and Le Caignec C. Mesomelia-synostoses syndrome results from deletion of SULF1 and SLCO5A1 genes at 8q13. *Am J Hum Genet*, 87(1):95–100, 2010. 45

Jawad M. U., Cheung M. C., Min E. S., Schneiderbauer M. M., Koniaris L. G., and Scully S. P. Ewing sarcoma demonstrates racial disparities in incidence-related and sex-related differences in outcome: an analysis of 1631 cases from the SEER database, 1973-2005. *Cancer*, 115(15):3526–36, 2009. 2

Jeon I. S., Davis J. N., Braun B. S., Sublett J. E., Roussel M. F., Denny C. T., and Shapiro D. N. A variant Ewing's sarcoma translocation (7;22) fuses the EWS gene to the ETS gene ETV1. *Oncogene*, 10(6):1229–34, 1995. 7

Joensuu H., Robers P. J., Lyly T., and Tenhunen M. *Syöpätaudit*. Duodecim, 2007. 2

Joiner M., Le Toriellec E., Despouy G., and Stern M. H. The MTCP1 oncogene modifies T-cell homeostasis before leukemogenesis in transgenic mice. *Leukemia*, 21(2):362–6, 2007. 41

Kadariya Y., Yin B., Tang B., Shinton S. A., Quinlivan E. P., Hua X., Klein-Szanto A., Al-Saleem T. I., Bassing C. H., Hardy R. R., and Kruger W. D. Mice heterozygous for germ-line mutations in methylthioadenosine phosphorylase (MTAP) die prematurely of T-cell lymphoma. *Cancer Res*, 69(14):5961–9, 2009. 40

Kallioniemi A., Kallioniemi O. P., Sudar D., Rutovitz D., Gray J. W., Waldman F., and Pinkel D. Comparative genomic hybridization for molecular cytogenetic analysis of solid tumors. *Science*, 258(5083):818–821, 1992. 13

Kaneko Y., Yoshida K., Handa M., Toyoda Y., Nishihira H., Tanaka Y., Sasaki Y., Ishida S., Higashino F., and Fujinaga K. Fusion of an ETS-family gene, EIAF, to EWS by t(17;22)(q12;q12) chromosome translocation in an undifferentiated sarcoma of infancy. *Genes Chromosomes Cancer*, 15(2):115–21, 1996. 7

Kauer M., Ban J., Kofler R., Walker B., Davis S., Meltzer P., and Kovar H. A molecular function map of Ewing's sarcoma. *PLoS One*, 4(4):e5415, 2009. 8, 11

Kinsey M., Smith R., and Lessnick S. L. NR0B1 is required for the oncogenic phenotype mediated by EWS/FLI in Ewing's sarcoma. *Mol Cancer Res*, 4(11): 851–9, 2006. 8

Kinsey M., Smith R., Iyer A. K., McCabe E. R. B., and Lessnick S. L. EWS/FLI and its downstream target NR0B1 interact directly to modulate transcription and oncogenesis in Ewing's sarcoma. *Cancer Res*, 69(23):9047–55, 2009. 8

Knudson Jr A. G. Mutation and cancer: statistical study of retinoblastoma. *Proc Natl Acad Sci U S A*, 68(4):820–3, 1971. 1

Kovar H. and Bernard A. CD99-positive "Ewing's sarcoma" from mouse-bone marrow-derived mesenchymal progenitor cells? *Cancer Res*, 66(19):9786; author reply 9786, 2006. 11

Kovar H., Dworzak M., Strehl S., Schnell E., Ambros I. M., Ambros P. F., and Gadner H. Overexpression of the pseudoautosomal gene MIC2 in Ewing's sarcoma and peripheral primitive neuroectodermal tumor. *Oncogene*, 5(7):1067–70, 1990. 4

Kovar H., Aryee D. N., Jug G., Henöckl C., Schemper M., Delattre O., Thomas G., and Gadner H. EWS/FLI-1 antagonists induce growth inhibition of ewing tumor cells in vitro. *Cell Growth Differ*, 7(4):429–37, 1996. 8

Krek A., Grün D., Poy M. N., Wolf R., Rosenberg L., Epstein E. J., MacMenamin P., da Piedade I., Gunsalus K. C., Stoffel M., and Rajewsky N. Combinatorial microRNA target predictions. *Nat Genet*, 37(5):495–500, 2005. 22, 36

Leavey P. J., Mascarenhas L., Marina N., Chen Z., Krailo M., Miser J., Brown K., Tarbell N., Bernstein M. L., Granowetter L., Gebhardt M., Grier H. E., and Children's Oncology Group . Prognostic factors for patients with Ewing sarcoma (EWS) at first recurrence following multi-modality therapy: a report from the Children's Oncology Group. *Pediatr Blood Cancer*, 51(3):334–8, 2008. 4

Lessnick S. L., Dei Tos A. P., Sorensen P. H. B., Dileo P., Baker L. H., Ferrari S., and Hall K. S. Small round cell sarcomas. *Semin Oncol*, 36(4):338–46, 2009. 4

Lewis B. P., Burge C. B., and Bartel D. P. Conserved seed pairing, often flanked by adenosines, indicates that thousands of human genes are microRNA targets. *Cell*, 120(1):15–20, 2005. 22, 36

Li F. P., Tu J. T., Liu F. S., and Shiang E. L. Rarity of Ewing's sarcoma in China. *Lancet*, 1(8180):1255, 1980. 2

Li L., Sun L., Gao F., Jiang J., Yang Y., Li C., Gu J., Wei Z., Yang A., Lu R., Ma Y., Tang F., Kwon S. W., Zhao Y., Li J., and Jin Y. Stk40 links the pluripotency factor Oct4 to the Erk/MAPK pathway and controls extraembryonic endoderm differentiation. *Proc Natl Acad Sci U S A*, 107(4):1402–7, 2010. 41

Lim L. P., Lau N. C., Garrett-Engele P., Grimson A., Schelter J. M., Castle J., Bartel D. P., Linsley P. S., and Johnson J. M. Microarray analysis shows that some microRNAs downregulate large numbers of target mRNAs. *Nature*, 433 (7027):769–73, 2005. 43

López-Guerrero J. A., Pellín A., Noguera R., Carda C., and Llombart-Bosch A. Molecular analysis of the 9p21 locus and p53 genes in Ewing family tumors. *Lab Invest*, 81(6):803–14, 2001. 10

López-Romero P., González M. A., Callejas S., Dopazo A., and Irizarry R. A. Processing of Agilent microRNA array data. *BMC Res Notes*, 3:18, 2010. 21

Lucas D. R., Bentley G., Dan M. E., Tabaczka P., Poulik J. M., and Mott M. P. Ewing sarcoma vs lymphoblastic lymphoma. A comparative immunohistochemical study. *Am J Clin Pathol*, 115(1):11–7, 2001. 4

Marioni J. C., Thorne N. P., Valsesia A., Fitzgerald T., Redon R., Fiegler H., Andrews T. D., Stranger B. E., Lynch A. G., Dermitzakis E. T., Carter N. P., Tavaré S., and Hurles M. E. Breaking the waves: improved detection of copy number variation from microarray-based comparative genomic hybridization. *Genome Biol*, 8(10):R228, 2007. 19

Martín-de Lara F., Sánchez-Aparicio P., Arias de la Fuente C., and Rey-Campos J. Biological effects of FoxJ2 over-expression. *Transgenic Res*, 17(6):1131–41, 2008. 44

Mastrangelo T., Modena P., Tornielli S., Bullrich F., Testi M. A., Mezzelani A., Radice P., Azzarelli A., Pilotti S., Croce C. M., Pierotti M. A., and Sozzi G. A novel zinc finger gene is fused to EWS in small round cell tumor. *Oncogene*, 19 (33):3799–804, 2000. 7

May W. A., Gishizky M. L., Lessnick S. L., Lunsford L. B., Lewis B. C., Delattre O., Zucman J., Thomas G., and Denny C. T. Ewing sarcoma 11;22 translocation produces a chimeric transcription factor that requires the DNA-binding domain encoded by FLI1 for transformation. *Proc Natl Acad Sci U S A*, 90(12):5752–6, 1993a. 6

May W. A., Lessnick S. L., Braun B. S., Klemsz M., Lewis B. C., Lunsford L. B., Hromas R., and Denny C. T. The Ewing's sarcoma EWS/FLI-1 fusion gene encodes a more potent transcriptional activator and is a more powerful transforming gene than FLI-1. *Mol Cell Biol*, 13(12):7393–8, 1993b. 6

Navid F., Billups C., Liu T., Krasin M. J., and Rodriguez-Galindo C. Second cancers in patients with the Ewing sarcoma family of tumours. *Eur J Cancer*, 44 (7):983–91, 2008. 5

Ng T. L., O'Sullivan M. J., Pallen C. J., Hayes M., Clarkson P. W., Winstanley M., Sorensen P. H. B., Nielsen T. O., and Horsman D. E. Ewing sarcoma with novel translocation t(2;16) producing an in-frame fusion of FUS and FEV. *J Mol Diagn*, 9(4):459–63, 2007. 7

Nigro J. M., Baker S. J., Preisinger A. C., Jessup J. M., Hostetter R., Cleary K., Bigner S. H., Davidson N., Baylin S., and Devilee P. Mutations in the p53 gene occur in diverse human tumour types. *Nature*, 342(6250):705–8, 1989. 9

Nissen R. M., Amsterdam A., and Hopkins N. A zebrafish screen for craniofacial mutants identifies wdr68 as a highly conserved gene required for endothelin-1 expression. *BMC Dev Biol*, 6:28, 2006. 41

Nordling C. O. A new theory on cancer-inducing mechanism. *Br J Cancer*, 7(1): 68–72, 1953. 1

Onodera T., Sakai T., Hsu J. C.-f., Matsumoto K., Chiorini J. A., and Yamada K. M. Btbd7 regulates epithelial cell dynamics and branching morphogenesis. *Science*, 329(5991):562–5, 2010. 44

Parente P., Coli A., Massi G., Mangoni A., Fabrizi M. M., and Bigotti G. Immunohistochemical expression of the glucose transporters Glut-1 and Glut-3 in human malignant melanomas and benign melanocytic lesions. *J Exp Clin Cancer Res*, 27:34, 2008. 44

Park S. H., Shin Y. K., Suh Y. H., Park W. S., Ban Y. L., Choi H.-S., Park H. J., and Jung K. C. Rapid divergency of rodent CD99 orthologs: implications for the evolution of the pseudoautosomal region. *Gene*, 353(2):177–88, 2005. 11

Parkin D. M., Stiller C. A., and Nectoux J. International variations in the incidence of childhood bone tumours. *Int J Cancer*, 53(3):371–6, 1993. 2

Patiño-García A. and Sierrasesúmaga L. Analysis of the p16INK4 and TP53 tumor suppressor genes in bone sarcoma pediatric patients. *Cancer Genet Cytogenet*, 98 (1):50–5, 1997. 9

Patiño-García A., López de Mesa R., de Alava E., and Sierrasesúmaga L. Clinical and molecular features of Ewing sarcoma in a patient with triple-X syndrome. *Cancer Genet Cytogenet*, 113(2):188–90, 1999. 38

Paulussen M., Ahrens S., Dunst J., Winkelmann W., Exner G. U., Kotz R., Amann G., Dockhorn-Dworniczak B., Harms D., Müller-Weihrich S., Welte K., Kornhuber B., Janka-Schaub G., Göbel U., Treuner J., Voûte P. A., Zoubek A., Gadner H., and Jürgens H. Localized Ewing tumor of bone: final results of the Cooperative Ewing's Sarcoma Study CESS 86. *J Clin Oncol*, 19(6):1818–29, 2001. 5

Paulussen M., Craft A. W., Lewis I., Hackshaw A., Douglas C., Dunst J., Schuck A., Winkelmann W., Köhler G., Poremba C., Zoubek A., Ladenstein R., van den Berg H., Hunold A., Cassoni A., Spooner D., Grimer R., Whelan J., McTiernan A., Jürgens H., and European Intergroup Cooperative Ewing's Sarcoma Study-92 . Results of the EICESS-92 Study: two randomized trials of Ewing's sarcoma treatment–cyclophosphamide compared with ifosfamide in standard-risk patients and assessment of benefit of etoposide added to standard treatment in high-risk patients. *J Clin Oncol*, 26(27):4385–93, 2008. 4, 5

Pease A. C., Solas D., Sullivan E. J., Cronin M. T., Holmes C. P., and Fodor S. P. Light-generated oligonucleotide arrays for rapid DNA sequence analysis. *Proc Natl Acad Sci U S A*, 91(11):5022–6, 1994. 15

Perlman E. J., Dickman P. S., Askin F. B., Grier H. E., Miser J. S., and Link M. P. Ewing's sarcoma–routine diagnostic utilization of mic2 analysis: a pediatric oncology group/children's cancer group intergroup studyy. *Hum Pathol*, 25(3): 304–7, 1994. 4

Peter M., Couturier J., Pacquement H., Michon J., Thomas G., Magdelenat H., and Delattre O. A new member of the ETS family fused to EWS in Ewing tumors. *Oncogene*, 14(10):1159–64, 1997. 7

Pfleiderer C., Zoubek A., Gruber B., Kronberger M., Ambros P. F., Lion T., Fink F. M., Gadner H., and Kovar H. Detection of tumour cells in peripheral blood and bone marrow from ewing tumour patients by RT-PCR. *Int J Cancer*, 64(2): 135–9, 1995. 3

Picci P., Böhling T., Bacci G., Ferrari S., Sangiorgi L., Mercuri M., Ruggieri P., Manfrini M., Ferraro A., Casadei R., Benassi M. S., Mancini A. F., Rosito P., Cazzola A., Barbieri E., Tienghi A., Brach del Prever A., Comandone A., Bacchini P., and Bertoni F. Chemotherapy-induced tumor necrosis as a prognostic factor in localized Ewing's sarcoma of the extremities. *J Clin Oncol*, 15(4):1553–9, 1997. 5

Pieper S., Ranft A., Braun-Munzinger G., Jurgens H., Paulussen M., and Dirksen U. Ewing's tumors over the age of 40: a retrospective analysis of 47 patients treated according to the International Clinical Trials EICESS 92 and EURO-E.W.I.N.G. 99. *Onkologie*, 31(12):657–63, 2008. 2

Pinkel D., Segraves R., Sudar D., Clark S., Poole I., Kowbel D., Collins C., Kuo W. L., Chen C., Zhai Y., Dairkee S. H., Ljung B. M., Gray J. W., and Albertson D. G. High resolution analysis of DNA copy number variation using comparative genomic hybridization to microarrays. *Nat Genet*, 20(2):207–11, 1998. 13

Pollack J. R., Perou C. M., Alizadeh A. A., Eisen M. B., Pergamenschikov A., Williams C. F., Jeffrey S. S., Botstein D., and Brown P. O. Genome-wide analysis of DNA copy-number changes using cDNA microarrays. *Nat Genet*, 23(1):41–6, 1999. 13

Potikyan G., France K. A., Carlson M. R. J., Dong J., Nelson S. F., and Denny C. T. Genetically defined EWS/FLI1 model system suggests mesenchymal origin of Ewing's family tumors. *Lab Invest*, 88(12):1291–302, 2008. 11

R Development Core Team . *R: A Language and Environment for Statistical Computing*. R Foundation for Statistical Computing, Vienna, Austria, 2009. URL `http://www.R-project.org`. ISBN 3-900051-07-0. 19

Redon R., Ishikawa S., Fitch K. R., Feuk L., Perry G. H., Andrews T. D., Fiegler H., Shapero M. H., Carson A. R., Chen W., Cho E. K., Dallaire S., Freeman J. L., Gonzalez J. R., Gratacos M., Huang J., Kalaitzopoulos D., Komura D., MacDonald J. R., Marshall C. R., Mei R., Montgomery L., Nishimura K., Okamura K., Shen F., Somerville M. J., Tchinda J., Valsesia A., Woodwark C., Yang F., Zhang J., Zerjal T., Zhang J., Armengol L., Conrad D. F., Estivill X., Tyler-Smith C., Carter N. P., Aburatani H., Lee C., Jones K. W., Scherer S. W., and Hurles M. E. Global variation in copy number in the human genome. *Nature*, 444(7118):444–454, 2006. 14

Richter G. H. S., Plehm S., Fasan A., Rössler S., Unland R., Bennani-Baiti I. M., Hotfilder M., Löwel D., von Luettichau I., Mossbrugger I., Quintanilla-Martinez L., Kovar H., Staege M. S., Müller-Tidow C., and Burdach S. EZH2 is a mediator of EWS/FLI1 driven tumor growth and metastasis blocking endothelial and neuro-ectodermal differentiation. *Proc Natl Acad Sci U S A*, 106(13):5324–9, 2009. 8

Ries L. A. G., Smith M. A., Gurney J. G., Linet M., Tamra T., Young J. L., and Bunin (eds.) G. R. *Cancer Incidence and Survival among Children and*

Adolescents: United States SEER Program 1975-1995. National Cancer Institute, SEER Program. NIH Pub. No. 99-4649. Bethesda, MD, 1999. 2

Riggi N., Cironi L., Provero P., Suvà M.-L., Kaloulis K., Garcia-Echeverria C., Hoffmann F., Trumpp A., and Stamenkovic I. Development of Ewing's sarcoma from primary bone marrow-derived mesenchymal progenitor cells. *Cancer Res*, 65 (24):11459–68, 2005. 10, 11

Riggi N., Suvà M.-L., Suvà D., Cironi L., Provero P., Tercier S., Joseph J.-M., Stehle J.-C., Baumer K., Kindler V., and Stamenkovic I. EWS-FLI-1 expression triggers a Ewing's sarcoma initiation program in primary human mesenchymal stem cells. *Cancer Res*, 68(7):2176–85, 2008. 10

Riggi N., Suvà M.-L., De Vito C., Provero P., Stehle J.-C., Baumer K., Cironi L., Janiszewska M., Petricevic T., Suvà D., Tercier S., Joseph J.-M., Guillou L., and Stamenkovic I. EWS-FLI-1 modulates miRNA145 and SOX2 expression to initiate mesenchymal stem cell reprogramming toward ewing sarcoma cancer stem cells. *Genes Dev*, 24(9):916–32, 2010. 42

Ritchie M. E., Silver J., Oshlack A., Holmes M., Diyagama D., Holloway A., and Smyth G. K. A comparison of background correction methods for two-colour microarrays. *Bioinformatics*, 23(20):2700–7, 2007. 19

Roberts P., Burchill S. A., Brownhill S., Cullinane C. J., Johnston C., Griffiths M. J., McMullan D. J., Bown N. P., Morris S. P., and Lewis I. J. Ploidy and karyotype complexity are powerful prognostic indicators in the Ewing's sarcoma family of tumors: a study by the United Kingdom Cancer Cytogenetics and the Children's Cancer and Leukaemia Group. *Genes Chromosomes Cancer*, 47(3): 207–20, 2008. 9

Sandberg A. A. and Bridge J. A. Updates on cytogenetics and molecular genetics of bone and soft tissue tumors: Ewing sarcoma and peripheral primitive neuroectodermal tumors. *Cancer Genet Cytogenet*, 123(1):1–26, 2000. 9

Savola S., Nardi F., Scotlandi K., Picci P., and Knuutila S. Microdeletions in 9p21.3 induce false negative results in CDKN2A FISH analysis of Ewing sarcoma. *Cytogenet Genome Res*, 119(1-2):21–6, 2007. 18, 38

Savola S., Klami A., Tripathi A., Niini T., Serra M., Picci P., Kaski S., Zambelli D., Scotlandi K., and Knuutila S. Combined use of expression and CGH arrays pinpoints novel candidate genes in Ewing sarcoma family of tumors. *BMC Cancer*, 9:17, 2009. 19

Scheinin I., Myllykangas S., Borze I., Bohling T., Knuutila S., and Saharinen J. CanGEM: mining gene copy number changes in cancer. *Nucleic Acids Res*, 36 (Database issue):D830–D835, 2008. 17, 20

Scotlandi K., Serra M., Manara M. C., Benini S., Sarti M., Maurici D., Lollini P. L., Picci P., Bertoni F., and Baldini N. Immunostaining of the p30/32MIC2 antigen and molecular detection of EWS rearrangements for the diagnosis of Ewing's sarcoma and peripheral neuroectodermal tumor. *Hum Pathol*, 27(4):408–16, 1996. 4

Sebat J., Lakshmi B., Troge J., Alexander J., Young J., Lundin P., Maner S., Massa H., Walker M., Chi M., Navin N., Lucito R., Healy J., Hicks J., Ye K., Reiner A., Gilliam T. C., Trask B., Patterson N., Zetterberg A., and Wigler M. Large-scale copy number polymorphism in the human genome. *Science*, 305(5683):525–528, 2004. 14

Sharrocks A. D. The ETS-domain transcription factor family. *Nat Rev Mol Cell Biol*, 2(11):827–37, 2001. 6

Shing D. C., McMullan D. J., Roberts P., Smith K., Chin S.-F., Nicholson J., Tillman R. M., Ramani P., Cullinane C., and Coleman N. FUS/ERG gene fusions in Ewing's tumors. *Cancer Res*, 63(15):4568–76, 2003. 7

Shlien A. and Malkin D. Copy number variations and cancer susceptibility. *Curr Opin Oncol*, 22(1):55–63, 2010. 14

Siggberg L., Ala-Mello S., Jaakkola E., Kuusinen E., Schuit R., Kohlhase J., Böhm D., Ignatius J., and Knuutila S. Array CGH in molecular diagnosis of mental retardation - A study of 150 Finnish patients. *Am J Med Genet A*, 152A(6): 1398–410, 2010. 19

Sircoulomb F., Nicolas N., Ferrari A., Finetti P., Bekhouche I., Rousselet E., Lonigro A., Adélaïde J., Baudelet E., Esteyriès S., Wicinski J., Audebert S., Charafe-Jauffret E., Jacquemier J., Lopez M., Borg J.-P., Sotiriou C., Popovici C., Bertucci F., Birnbaum D., Chaffanet M., and Ginestier C. ZNF703 gene amplification at 8p12 specifies luminal B breast cancer. *EMBO Mol Med*, 3(3):153–66, 2011. 40

Smith R., Owen L. A., Trem D. J., Wong J. S., Whangbo J. S., Golub T. R., and Lessnick S. L. Expression profiling of EWS/FLI identifies NKX2.2 as a critical target gene in Ewing's sarcoma. *Cancer Cell*, 9(5):405–16, 2006. 8

Smyth G. K. Linear models and empirical Bayes methods for assessing differential expression in microarray experiments. *Stat Appl Genet Mol Biol*, 3:Article3, 2004. 21

Smyth G. K. and Speed T. Normalization of cDNA microarray data. *Methods*, 31 (4):265–273, 2003. 19

Solinas-Toldo S., Lampel S., Stilgenbauer S., Nickolenko J., Benner A., Döhner H., Cremer T., and Lichter P. Matrix-based comparative genomic hybridization: biochips to screen for genomic imbalances. *Genes Chromosomes Cancer*, 20(4): 399–407, 1997. 13

Stern M. H., Soulier J., Rosenzwajg M., Nakahara K., Canki-Klain N., Aurias A., Sigaux F., and Kirsch I. R. MTCP-1: a novel gene on the human chromosome Xq28 translocated to the T cell receptor alpha/delta locus in mature T cell proliferations. *Oncogene*, 8(9):2475–83, 1993. 41

Su A. I., Wiltshire T., Batalov S., Lapp H., Ching K. A., Block D., Zhang J., Soden R., Hayakawa M., Kreiman G., Cooke M. P., Walker J. R., and Hogenesch J. B. A gene atlas of the mouse and human protein-encoding transcriptomes. *Proc Natl Acad Sci U S A*, 101(16):6062–6067, 2004. 11

Tan A. Y. and Manley J. L. The TET family of proteins: functions and roles in disease. *J Mol Cell Biol*, 1(2):82–92, 2009. 6

Tanabe S., Sato Y., Suzuki T., Suzuki K., Nagao T., and Yamaguchi T. Gene expression profiling of human mesenchymal stem cells for identification of novel markers in early- and late-stage cell culture. *J Biochem*, 144(3):399–408, 2008. 18, 26

Tanaka K., Iwakuma T., Harimaya K., Sato H., and Iwamoto Y. EWS-Fli1 antisense oligodeoxynucleotide inhibits proliferation of human Ewing's sarcoma and primitive neuroectodermal tumor cells. *J Clin Invest*, 99(2):239–47, 1997. 8

Teng P.-N., Hood B. L., Sun M., Dhir R., and Conrads T. P. Differential proteomic analysis of renal cell carcinoma tissue interstitial fluid. *J Proteome Res*, 10(3): 1333–42, 2011. 41

Terrier P., Llombart-Bosch A., and Contesso G. Small round blue cell tumors in bone: prognostic factors correlated to Ewing's sarcoma and neuroectodermal tumors. *Semin Diagn Pathol*, 13(3):250–7, 1996. 5

Thacker M. M., Temple H. T., and Scully S. P. Current treatment for Ewing's sarcoma. *Expert Rev Anticancer Ther*, 5(2):319–31, 2005. 5

Thomas J. T., Canelos P., Luyten F. P., and Moos Jr M. Xenopus SMOC-1 inhibits bone morphogenetic protein signaling downstream of receptor binding and is essential for postgastrulation development in Xenopus. *J Biol Chem*, 284(28): 18994–9005, 2009. 44

Thompson A. D., Teitell M. A., Arvand A., and Denny C. T. Divergent Ewing's sarcoma EWS/ETS fusions confer a common tumorigenic phenotype on NIH3T3 cells. *Oncogene*, 18(40):5506–13, 1999. 7

Tirode F., Laud-Duval K., Prieur A., Delorme B., Charbord P., and Delattre O. Mesenchymal stem cell features of Ewing tumors. *Cancer Cell*, 11(5):421–9, 2007. 11

Torchia E. C., Boyd K., Rehg J. E., Qu C., and Baker S. J. EWS/FLI-1 induces rapid onset of myeloid/erythroid leukemia in mice. *Mol Cell Biol*, 27(22):7918–34, 2007. 11

Tsuchiya T., Sekine K., Hinohara S., Namiki T., Nobori T., and Kaneko Y. Analysis of the p16INK4, p14ARF, p15, TP53, and MDM2 genes and their prognostic implications in osteosarcoma and Ewing sarcoma. *Cancer Genet Cytogenet*, 120 (2):91–8, 2000. 10

Tsukioka M., Matsumoto Y., Noriyuki M., Yoshida C., Nobeyama H., Yoshida H., Yasui T., Sumi T., Honda K.-I., and Ishiko O. Expression of glucose transporters in epithelial ovarian carcinoma: correlation with clinical characteristics and tumor angiogenesis. *Oncol Rep*, 18(2):361–7, 2007. 44

Tuna M., Knuutila S., and Mills G. B. Uniparental disomy in cancer. *Trends Mol Med*, 15(3):120–8, 2009. 14

Turc-Carel C., Philip I., Berger M. P., Philip T., and Lenoir G. M. Chromosome study of Ewing's sarcoma (ES) cell lines. Consistency of a reciprocal translocation t(11;22)(q24;q12). *Cancer Genet Cytogenet*, 12(1):1–19, 1984. 6

Turc-Carel C., Aurias A., Mugneret F., Lizard S., Sidaner I., Volk C., Thiery J. P., Olschwang S., Philip I., and Berger M. P. Chromosomes in Ewing's sarcoma. I. An evaluation of 85 cases of remarkable consistency of t(11;22)(q24;q12). *Cancer Genet Cytogenet*, 32(2):229–38, 1988. 6

Tuzun E., Sharp A. J., Bailey J. A., Kaul R., Morrison V. A., Pertz L. M., Haugen E., Hayden H., Albertson D., Pinkel D., Olson M. V., and Eichler E. E. Fine-scale structural variation of the human genome. *Nat Genet*, 37(7):727–732, 2005. 14

Uren A. and Toretsky J. A. Ewing's sarcoma oncoprotein EWS-FLI1: the perfect target without a therapeutic agent. *Future Oncol*, 1(4):521–8, 2005. 9

van de Wiel M. A. and van Wieringen W. N. CGHregions: dimension reduction for array CGH data with minimal information loss. *Cancer Informatics*, 3:55–63, 2007. 19

van de Wiel M. A., Kim K. I., Vosse S. J., van Wieringen W. N., Wilting S. M., and Ylstra B. CGHcall: calling aberrations for array CGH tumor profiles. *Bioinformatics*, 23(7):892–894, 2007. 14, 19

van de Wiel M. A., Brosens R., Eilers P. H. C., Kumps C., Meijer G. A., Menten B., Sistermans E., Speleman F., Timmerman M. E., and Ylstra B. Smoothing waves in array CGH tumor profiles. *Bioinformatics*, 25(9):1099–1104, 2009. 19

Van Patten S. M., Heisermann G. J., Cheng H. C., and Walsh D. A. Tyrosine kinase catalyzed phosphorylation and inactivation of the inhibitor protein of the cAMP-dependent protein kinase. *J Biol Chem*, 262(7):3398–403, 1987. 44

van Wieringen W. N. and van de Wiel M. A. Nonparametric testing for DNA copy number induced differential mRNA gene expression. *Biometrics*, 65(1):19–29, 2009. 15, 22

van Wieringen W. N., van de Wiel M. A., and Ylstra B. Normalized, segmented or called aCGH data? *Cancer Inform*, 3:321–327, 2007. 14

Vasudevan S., Tong Y., and Steitz J. A. Switching from repression to activation: microRNAs can up-regulate translation. *Science*, 318(5858):1931–4, 2007. 16

Venkatraman E. S. and Olshen A. B. A faster circular binary segmentation algorithm for the analysis of array CGH data. *Bioinformatics*, 23(6):657–663, 2007. 14, 19

West D. C., Grier H. E., Swallow M. M., Demetri G. D., Granowetter L., and Sklar J. Detection of circulating tumor cells in patients with Ewing's sarcoma and peripheral primitive neuroectodermal tumor. *J Clin Oncol*, 15(2):583–8, 1997. 3

Worch J., Matthay K. K., Neuhaus J., Goldsby R., and DuBois S. G. Ethnic and racial differences in patients with Ewing sarcoma. *Cancer*, 116(4):983–8, 2010. 2

Wu Z., Irizarry R. A., Gentleman R., Murillo F. M., and Spencer F. A model based background adjustment for oligonucleotide expression arrays. *Johns Hopkins University, Dept. of Biostatistics Working Papers*, page Working Paper 1, 2004. 20

Wunder J. S., Paulian G., Huvos A. G., Heller G., Meyers P. A., and Healey J. H. The histological response to chemotherapy as a predictor of the oncological outcome of operative treatment of Ewing sarcoma. *J Bone Joint Surg Am*, 80(7):1020–33, 1998. 5

Ylstra B., van den Ijssel P., Carvalho B., Brakenhoff R. H., and Meijer G. A. BAC to the future! or oligonucleotides: a perspective for micro array comparative genomic hybridization (array CGH). *Nucleic Acids Res*, 34(2):445–450, 2006. 13

Zhang F., Gu W., Hurles M. E., and Lupski J. R. Copy number variation in human health, disease, and evolution. *Annu Rev Genomics Hum Genet*, 10:451–81, 2009. 14

Zhang J., Feuk L., Duggan G. E., Khaja R., and Scherer S. W. Development of bioinformatics resources for display and analysis of copy number and other structural variants in the human genome. *Cytogenet Genome Res*, 115(3-4):205–14, 2006. 20, 38

Zhang J., Guo H., Zhang H., Wang H., Qian G., Fan X., Hoffman A. R., Hu J.-F., and Ge S. Putative tumor suppressor miR-145 inhibits colon cancer cell growth by targeting oncogene Friend leukemia virus integration 1 gene. *Cancer*, 117(1): 86–95, 2011. 42

Zhao X., Weir B. A., LaFramboise T., Lin M., Beroukhim R., Garraway L., Beheshti J., Lee J. C., Naoki K., Richards W. G., Sugarbaker D., Chen F., Rubin M. A., Jänne P. A., Girard L., Minna J., Christiani D., Li C., Sellers W. R., and Meyerson M. Homozygous deletions and chromosome amplifications in human lung carcinomas revealed by single nucleotide polymorphism array analysis. *Cancer Res*, 65 (13):5561–70, 2005. 13

Zielenska M., Zhang Z. M., Ng K., Marrano P., Bayani J., Ramirez O. C., Sorensen P., Thorner P., Greenberg M., and Squire J. A. Acquisition of secondary structural chromosomal changes in pediatric Ewing sarcoma is a probable prognostic factor for tumor response and clinical outcome. *Cancer*, 91(11):2156–64, 2001. 9

Zucman J., Melot T., Desmaze C., Ghysdael J., Plougastel B., Peter M., Zucker J. M., Triche T. J., Sheer D., and Turc-Carel C. Combinatorial generation of variable fusion proteins in the Ewing family of tumours. *EMBO J*, 12(12):4481–7, 1993. 7

Zucman-Rossi J., Batzer M. A., Stoneking M., Delattre O., and Thomas G. Interethnic polymorphism of EWS intron 6: genome plasticity mediated by Alu retroposition and recombination. *Hum Genet*, 99(3):357–63, 1997. 7

Appendices

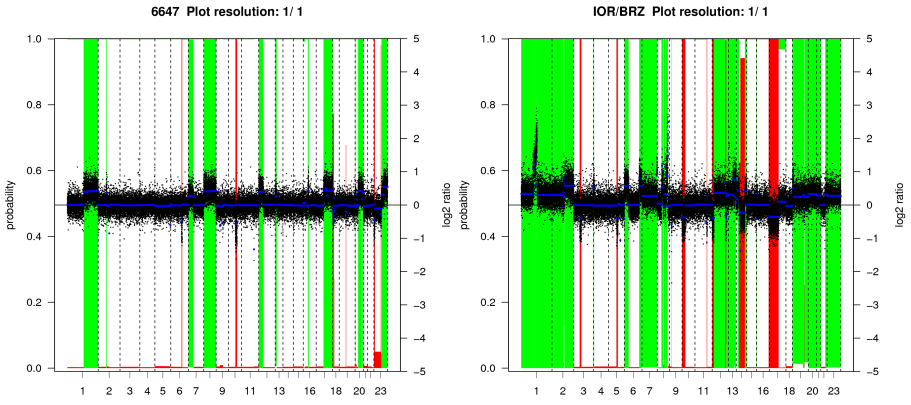

(a) 6647

(b) IOR/BRZ

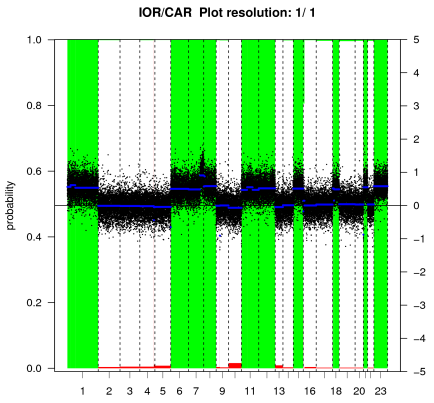

(c) IOR/CAR

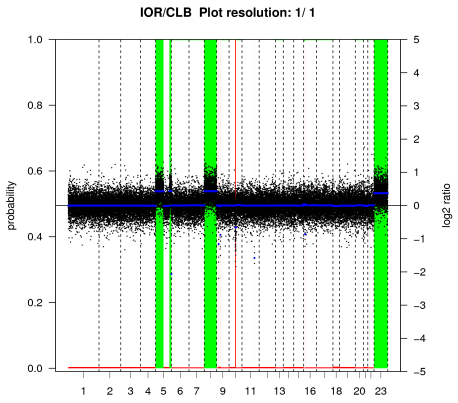

(d) IOR/CLB

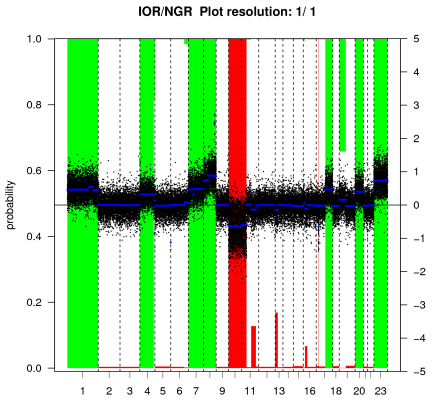

(e) IOR/NGR

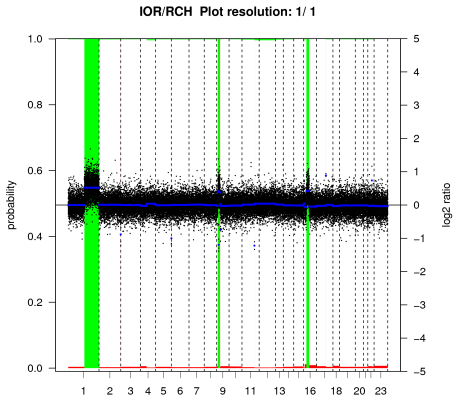

(f) IOR/RCH

Figure A.1: aCGH profiles of individual cell lines
For each sample, data is ordered by genomic position and chromosomes are marked on the x-axis. Normalized log ratios are shown as black dots and segmented values in blue, using the right-hand scale. The probabilities of losses are shown with red bars, and their values can be read from the scale on the left. Gain probabilities are shown in green, and their values are "1 - value on the left scale". When the probabilities exceed the 50% threshold (the center line), the segment is called as aberrated.

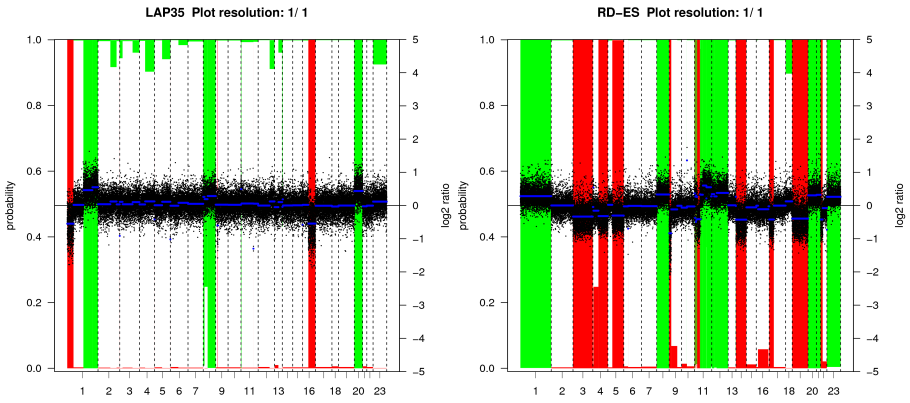

(g) LAP35

(h) RE-ES

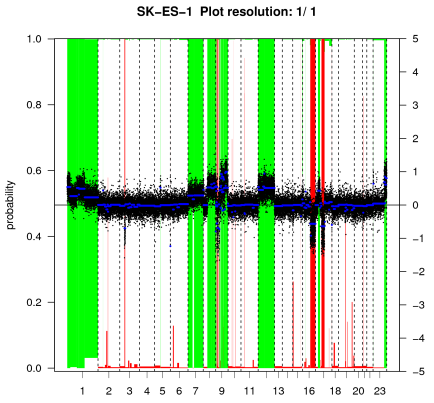

(i) SK-ES-1

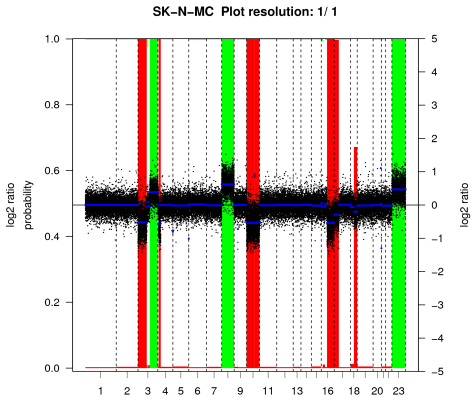

(j) SK-N-MC

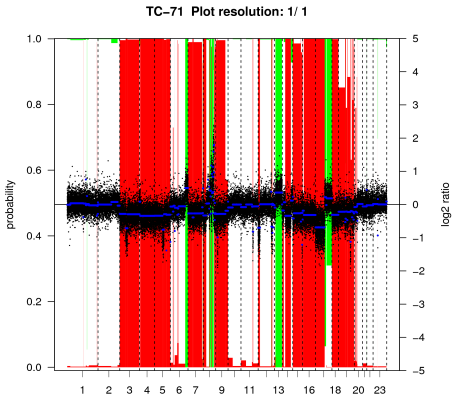

(k) TC-71

Figure A.1: aCGH profiles of individual cell lines (cont.)

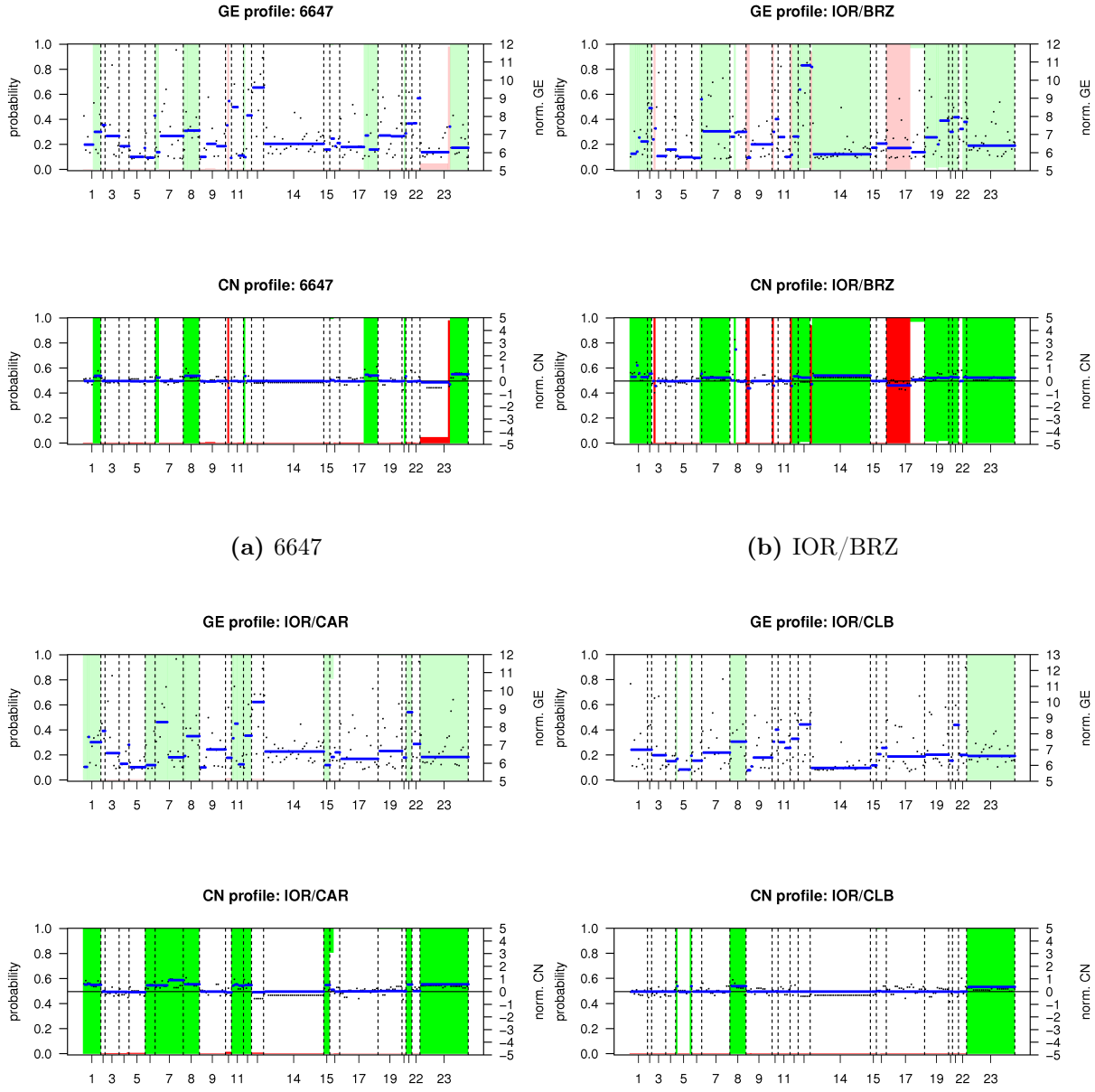

(a) 6647 **(b)** IOR/BRZ

(c) IOR/CAR **(d)** IOR/CLB

Figure A.2: aCGH and miRNA expression profiles of individual cell lines
The upper plots show miRNA expression with black dots, and mean values across regions in blue. Regions are determined by the copy number data, which is shown at the bottom. Please refer to Figure A.1 for details on the copy number profiles.

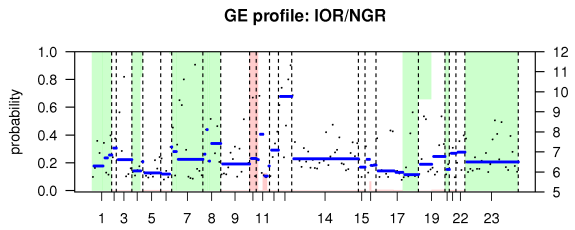

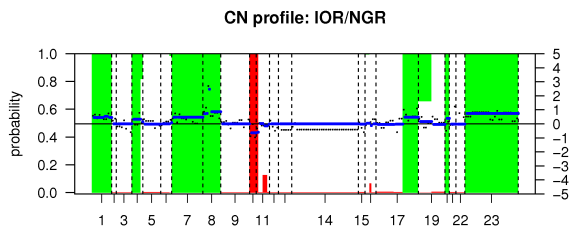

(e) IOR/NGR

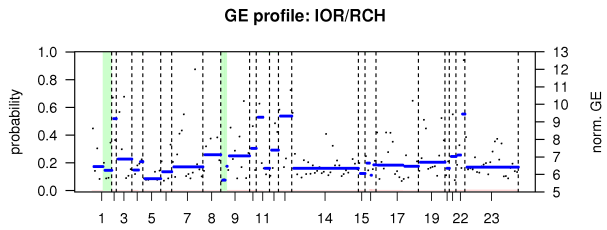

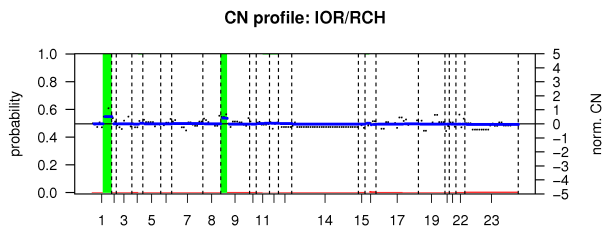

(f) IOR/RCH

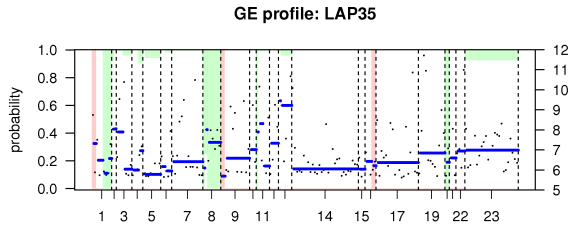

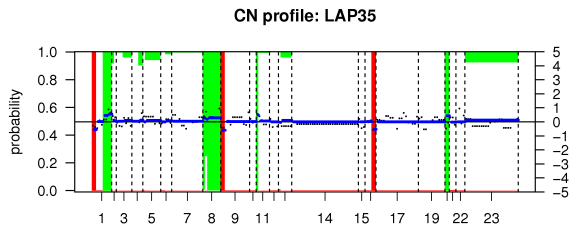

(g) LAP35

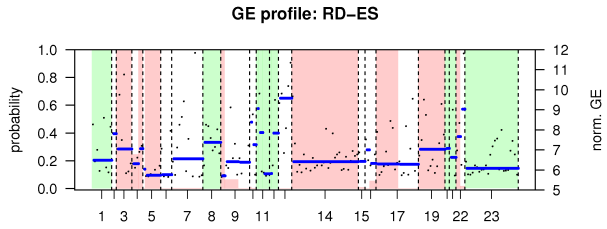

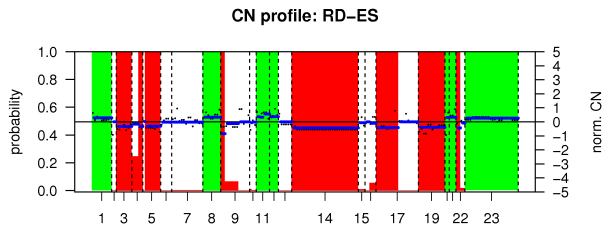

(h) RD-ES

Figure A.2: aCGH and miRNA expression profiles of individual cell lines (cont.)

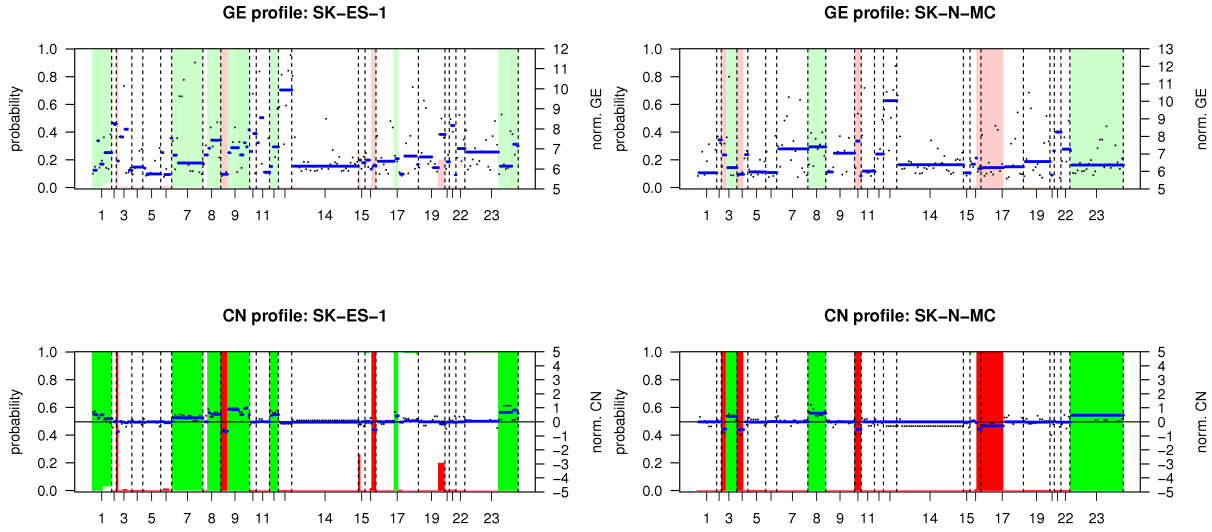

(i) SK-ES-1

(j) SK-N-MC

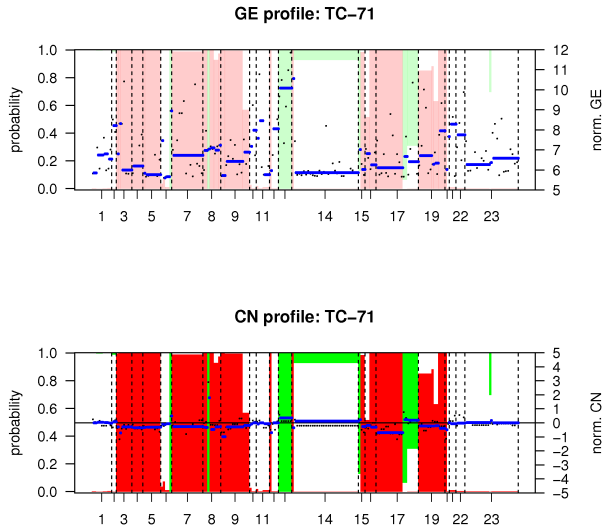

(k) TC-71

Figure A.2: aCGH and miRNA expression profiles of individual cell lines (cont.)

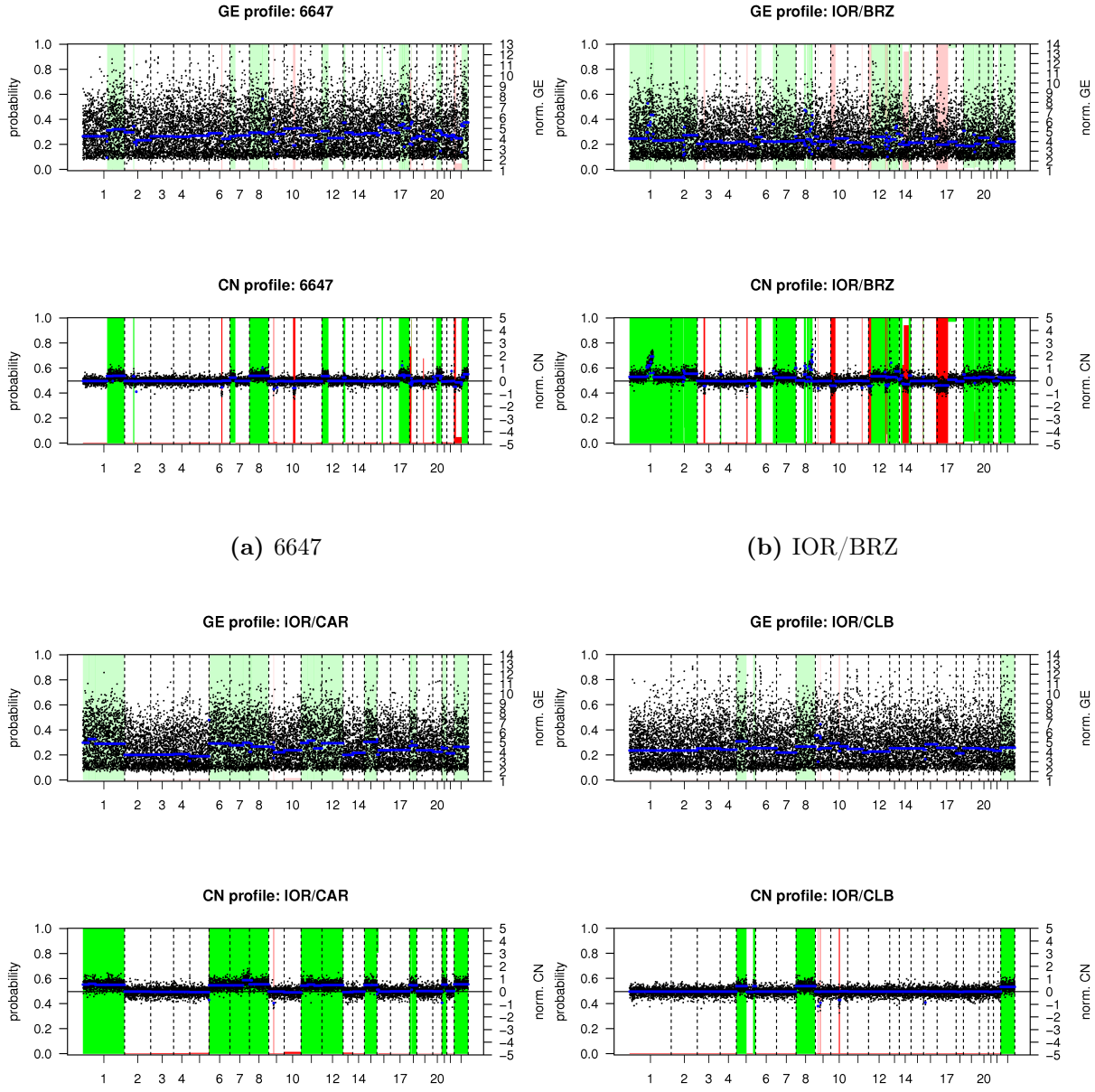

(a) 6647 **(b)** IOR/BRZ

(c) IOR/CAR **(d)** IOR/CLB

Figure A.3: aCGH and mRNA expression profiles of individual cell lines
The upper plots show mRNA probe set measurements with black dots, and mean expression across regions in blue. Regions are determined by the copy number data, which is shown in the bottom plots. Please refer to Figure A.1 for details on the copy number profiles.

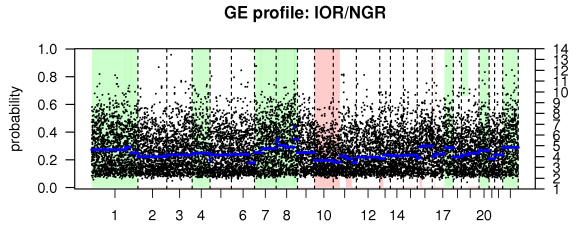

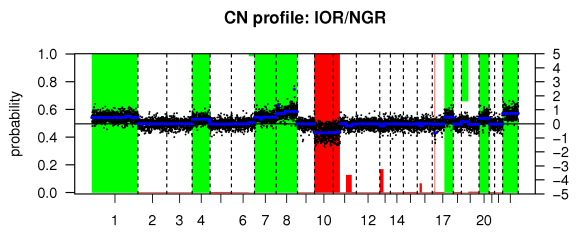

(e) IOR/NGR

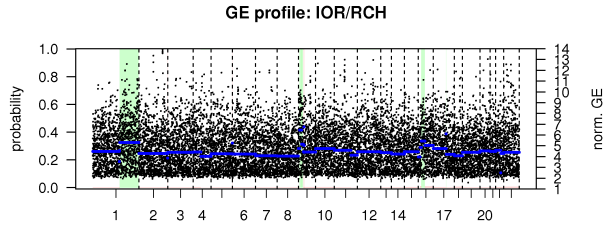

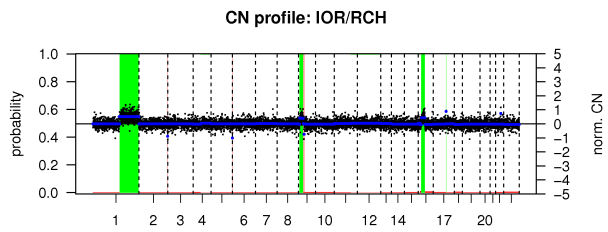

(f) IOR/RCH

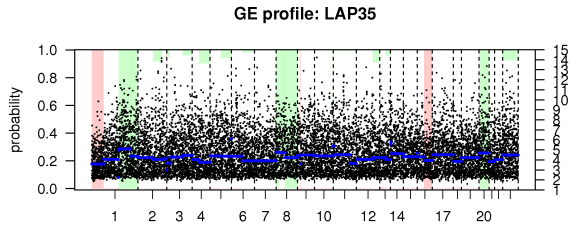

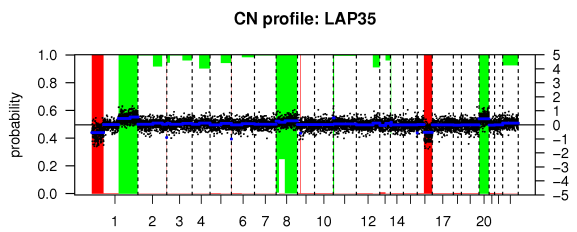

(g) LAP35

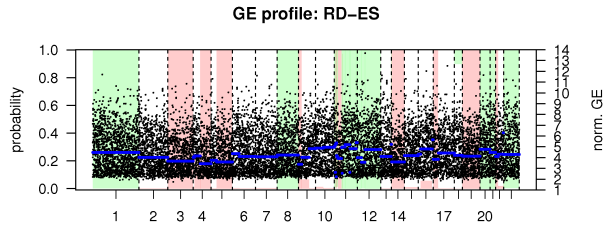

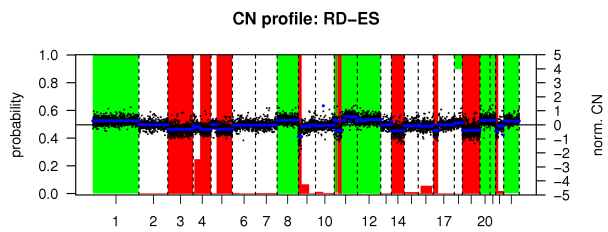

(h) RD-ES

Figure A.3: aCGH and mRNA expression profiles of individual cell lines (cont.)

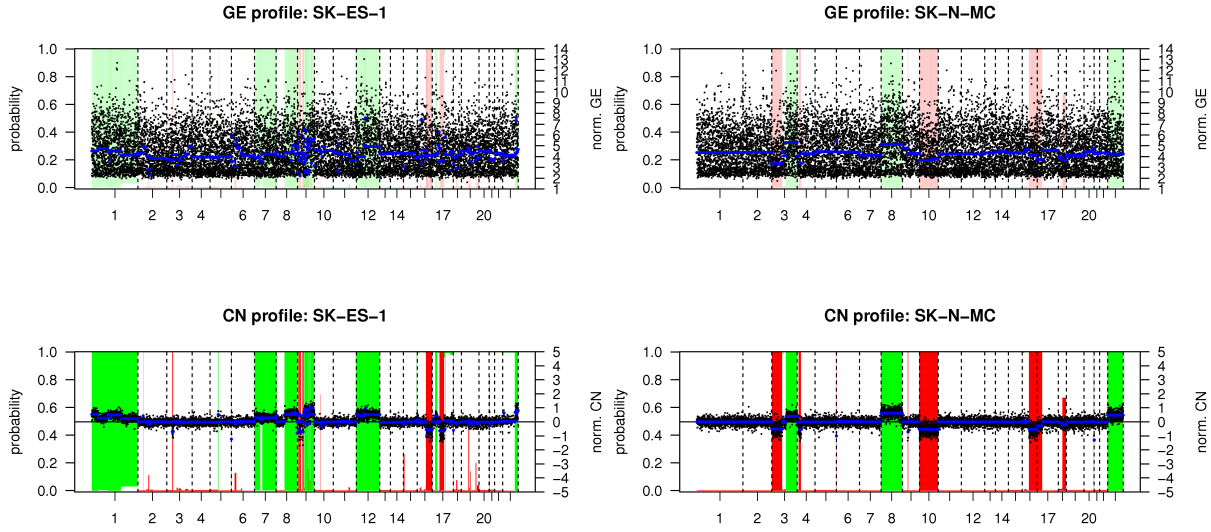

(i) SK-ES-1

(j) SK-N-MC

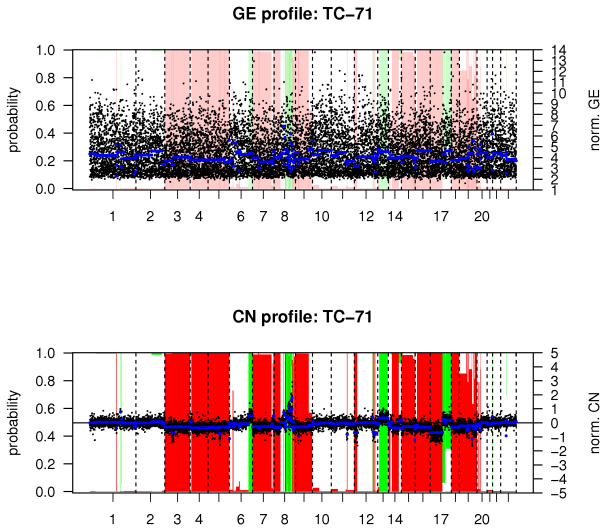

(k) TC-71

Figure A.3: aCGH and mRNA expression profiles of individual cell lines (cont.)

Table A.1: All copy number regions.
All regions detected from the aCGH data set are listed here and marked with a running number. Columns marked with "aCGH probes" show the starting base pair position of the first microarray probe, the ending position of the last probe, and the total number of probes within the region. CNV % is the percent overlap of the region with reported copy number variations from the Database of Genomic Variants. Relative % of gains and losses are obtained for each region from the absolute frequencies by subtracting the mean frequency of the two adjacent regions from the frequency of the region itself. The last two columns list the number of differentially expressed (up or down-regulated) Affymetrix probe sets and miRNAs.

			aCGH probes				absolute % of		relative % of		diff. expressed	
	chr	cytobands	start	end	num	CNV %	losses	gains	losses	gains	mRNAs	miRNAs
1	1	p36.33-p34.3	564 405	38 077 901	826	34.7	9.1	45.5	9.1	0	364	0
2	1	p34.3-p11.2	38 111 284	121 184 327	1302	26.1	0	45.5	0	0	510	1
3	1	q21.1	144 679 875	145 039 814	7	100	9.1	45.5	4.6	0	9	0
4	1	q21.1	145 076 147	145 194 112	4	100	9.1	54.5	4.6	0	3	0
5	1	q21.1	145 413 388	145 416 395	2	100	0	63.6	0	0	3	0
6	1	q21.1-q22	145 440 247	156 254 642	315	57.2	0	72.7	0	0	171	0
7	1	q22	156 264 255	156 307 404	3	0	0	81.8	0	9.1	1	0
8	1	q22-q23.3	156 316 721	161 123 686	143	4.2	0	72.7	0	0	41	0
9	1	q23.3	161 133 330	161 677 035	24	63	0	81.8	0	9.1	3	0
10	1	q23.3-q24.1	161 697 689	165 664 592	63	39.6	0	72.7	0	0	24	0
11	1	q24.1	165 696 716	166 826 147	17	21.9	0	63.6	0	0	4	0
12	1	q24.1-q43	166 921 615	238 888 928	1217	26.7	0	72.7	0	4.6	391	0
13	1	q43	239 011 002	240 724 580	15	37.5	9.1	72.7	9.1	0	5	0
14	1	q43-q44	240 755 779	247 605 063	105	32.8	0	72.7	0	0	45	0
15	1	q44	247 695 693	248 480 808	17	100	9.1	72.7	9.1	0	0	0
16	1	q44	249 104 603	249 212 667	7	80.4	0	72.7	0	0	2	0
17	2	p25.3-p16.1	39 193	58 276 025	670	37	0	9.1	0	0	241	0
18	2	p16.1	58 313 482	60 013 522	9	97.1	0	18.2	0	9.1	1	0
19	2	p16.1-q11.1	60 604 088	95 530 689	367	42.9	0	9.1	0	0	172	0
20	2	q11.1-q11.2	95 635 960	100 260 984	87	43.7	0	18.2	0	9.1	43	0
21	2	q11.2-q14.1	100 343 561	115 386 809	176	34.2	0	9.1	0	0	52	0
22	2	q14.1-q14.2	115 716 437	119 628 018	28	34.1	9.1	9.1	9.1	0	9	0
23	2	q14.2-q21.1	119 700 566	132 190 404	119	34	0	9.1	0	0	35	0
24	2	q21.1	132 488 017	132 493 761	2	100	9.1	9.1	9.1	0	0	0
25	2	q21.1-q21.2	132 493 872	133 402 608	6	84	0	9.1	0	4.6	0	0
26	2	q21.2-q22.1	133 419 863	137 637 948	52	22.2	0	0	0	0	12	0
27	2	q22.1-q37.3	137 993 436	242 815 971	1353	21	0	9.1	0	4.6	484	0
28	2	q37.3	242 930 819	243 041 363	3	100	18.2	9.1	18.2	0	1	0
29	3	p26.3-p21.31	249 727	46 303 825	630	28.4	27.3	0	0	0	186	0
30	3	p21.31	46 413 237	49 407 882	103	25	36.4	0	9.1	0	41	0
31	3	p21.31	49 421 684	50 539 265	56	42.2	27.3	0	0	0	21	0
32	3	p21.2-p14.1	50 601 246	64 666 993	234	18.4	36.4	0	9.1	0	60	0
33	3	p14.1-p12.1	64 730 243	82 045 784	138	30.3	27.3	0	0	0	56	0
34	3	p12.1-q21.1	82 326 665	122 133 734	403	18.2	18.2	0	0	0	124	0
35	3	q21.1-q29	122 160 926	197 803 819	1052	29.1	18.2	9.1	0	9.1	349	1
36	4	p16.3	72 447	3 144 567	75	61.4	0	18.2	0	0	40	0
37	4	p16.3	3 205 842	3 323 643	4	1.4	0	27.3	0	9.1	0	0
38	4	p16.3	3 336 757	3 519 926	7	72.7	0	18.2	0	0	2	0
39	4	p16.3-p16.2	3 585 660	5 141 701	20	49.9	9.1	9.1	0	0	5	0
40	4	p16.2-p14	5 287 958	39 161 046	285	33.9	18.2	9.1	9.1	0	79	0
41	4	p14-q13.3	39 219 586	74 301 973	356	23.2	9.1	9.1	0	0	94	0
42	4	q13.3-q34.1	74 318 110	175 595 546	1102	24	18.2	9.1	0	4.6	361	0
43	4	q34.1-q34.2	175 635 034	177 061 108	14	29.9	27.3	0	9.1	0	0	0
44	4	q34.2-q35.1	177 111 420	186 068 278	80	18.4	18.2	0	0	0	25	0
45	4	q35.1-q35.2	186 178 095	190 114 925	46	70.6	18.2	9.1	0	9.1	16	0
46	4	q35.2	190 482 637	190 884 259	3	100	45.5	0	27.3	0	0	0
47	5	p15.33-q12.3	95 243	63 256 989	583	26.1	9.1	9.1	0	0	183	0
48	5	q12.3-q14.1	63 462 871	77 755 097	183	31.9	18.2	9.1	4.6	0	98	0
49	5	q14.1	77 786 678	79 143 318	28	7.2	18.2	18.2	0	9.1	14	0
50	5	q14.1-q22.1	79 323 300	110 077 811	257	31.5	18.2	9.1	0	0	86	0
51	5	q22.1	110 092 392	110 712 614	6	26.2	27.3	9.1	4.6	4.6	1	0
52	5	q22.1-q23.3	110 782 376	128 316 183	187	23.9	27.3	0	4.6	0	55	0
53	5	q23.3-q31.3	128 337 712	144 298 833	313	19.7	18.2	0	0	0	132	0
54	5	q32	144 528 871	144 777 028	2	0	27.3	0	9.1	0	0	0
55	5	q32-q34	145 132 120	162 901 108	273	19.2	18.2	0	0	0	93	2
56	5	q34-q35.3	162 905 744	178 597 117	213	23.2	18.2	9.1	0	4.6	79	0
57	5	q35.3	178 640 943	178 830 409	4	90.4	27.3	9.1	9.1	0	0	0
58	5	q35.3	178 989 628	180 684 500	44	67.3	18.2	9.1	0	0	27	0
59	6	p25.3	259 528	293 492	2	100	81.8	0	81.8	0	0	0
60	6	p25.3-p22.2	407 463	26 056 162	334	17.2	0	18.2	0	9.1	111	0
61	6	p22.2-p22.1	26 095 217	28 097 800	68	29.5	9.1	18.2	9.1	0	15	0
62	6	p22.1-p21.32	28 097 826	32 189 229	162	46.9	0	18.2	0	4.6	95	0
63	6	p21.32	32 261 671	32 412 468	5	39.7	0	9.1	0	0	0	0
64	6	p21.32	32 488 879	32 713 164	5	100	18.2	9.1	18.2	0	3	0
65	6	p21.32-p21.1	32 728 845	45 822 194	332	20.1	0	9.1	0	0	133	0
66	6	p21.1-p12.3	45 879 434	48 853 380	43	36.6	9.1	9.1	9.1	0	6	0
67	6	p12.3-p11.2	49 149 033	57 246 988	104	14.9	0	9.1	0	0	36	0
68	6	p11.2-q12	57 393 140	66 705 014	37	39.2	9.1	9.1	9.1	0	4	0

Continued on the next page...

	chr	cytobands	aCGH probes start	aCGH probes end	num	CNV %	absolute % of losses	absolute % of gains	relative % of losses	relative % of gains	diff. expressed mRNAs	diff. expressed miRNAs
69	6	q12-q16.1	67 257 580	98 843 287	332	23.4	0	9.1	0	0	97	1
70	6	q16.1-q21	99 143 367	107 975 847	94	31.3	9.1	9.1	9.1	0	31	0
71	6	q21-q24.1	108 0 267	142 541 419	445	18.6	0	9.1	0	0	140	0
72	6	q24.1-q27	142 597 923	170 892 301	368	38.5	0	27.3	0	18.2	121	0
73	7	p22.3-p12.1	54 185	51 342 696	670	32.5	9.1	45.5	0	9.1	235	0
74	7	p12.1-q36.1	51 520 727	148 463 836	1185	37	9.1	36.4	4.6	0	415	3
75	7	q36.1	148 481 134	151 711 831	79	36.5	0	36.4	0	0	33	0
76	7	q36.1-q36.3	151 748 853	155 257 297	39	44.5	9.1	36.4	9.1	0	13	0
77	7	q36.3	155 397 659	158 909 737	41	40.7	0	45.5	0	9.1	19	0
78	8	p23.3-p23.2	191 530	3 889 590	36	54.1	9.1	72.7	0	9.1	7	0
79	8	p23.2-p12	4 494 837	31 158 464	366	50.8	9.1	63.6	4.6	0	165	0
80	8	p12-p11.21	31 488 003	42 704 918	141	15.5	0	63.6	0	0	50	0
81	8	p11.21-q11.1	42 729 970	46 943 014	12	22.9	0	72.7	0	0	5	0
82	8	q11.1-q12.1	47 536 057	56 652 072	70	33.5	0	81.8	0	0	31	0
83	8	q12.1	56 682 642	57 129 002	12	71.7	0	90.9	0	9.1	9	0
84	8	q12.1-q13.2	57 229 343	69 867 282	148	21.7	0	81.8	0	0	44	0
85	8	q13.2-q13.3	70 106 133	70 744 066	8	18.8	0	90.9	0	13.7	6	0
86	8	q13.3	70 890 166	71 024 682	3	10.5	0	72.7	0	0	1	0
87	8	q13.3-q21.11	71 126 134	76 351 498	64	17.5	9.1	72.7	9.1	0	16	0
88	8	q21.11-q22.1	76 402 380	96 269 295	204	33.1	0	90.9	0	18.2	64	0
89	8	q22.1-q22.2	96 846 254	101 164 771	66	28.1	9.1	72.7	9.1	0	26	0
90	8	q22.2-q24.12	101 251 572	121 937 154	225	20.7	0	90.9	0	18.2	77	0
91	8	q24.12-q24.13	122 329 490	124 357 012	23	9.3	0	72.7	0	0	9	0
92	8	q24.13	124 403 872	124 857 149	9	0	0	81.8	0	0	4	0
93	8	q24.13-q24.21	124 997 293	129 147 781	48	10.4	0	90.9	0	13.7	14	0
94	8	q24.21-q24.3	129 505 388	142 270 534	106	20.1	9.1	72.7	9.1	0	44	1
95	8	q24.3	142 367 717	143 742 450	14	52.4	0	72.7	0	0	3	0
96	8	q24.3	143 744 897	146 280 019	85	74.6	9.1	72.7	9.1	0	49	0
97	9	p24.3	214 367	893 558	7	97.6	27.3	0	9.1	0	1	0
98	9	p24.3	983 204	2 088 586	11	74.5	18.2	0	0	0	0	0
99	9	p24.3-p24.1	2 119 502	5 437 548	44	9.5	18.2	9.1	0	9.1	18	0
100	9	p24.1	5 463 902	5 967 385	10	9	18.2	0	0	0	5	0
101	9	p24.1-p23	6 099 101	9 345 120	36	52.8	18.2	9.1	0	9.1	5	0
102	9	p23	9 453 833	13 595 913	33	73.2	18.2	0	0	0	1	0
103	9	p23	13 752 900	13 877 338	2	1.2	18.2	9.1	0	4.6	0	0
104	9	p23-p22.2	14 025 606	17 0 152	39	52.6	27.3	9.1	9.1	0	38	0
105	9	p22.2-p22.1	17 143 289	19 296 157	35	100	18.2	9.1	0	0	10	0
106	9	p22.1	19 324 347	19 550 178	6	100	18.2	18.2	0	9.1	1	0
107	9	p22.1-p21.3	19 597 233	20 310 569	9	100	18.2	9.1	0	0	0	0
108	9	p21.3	20 346 094	21 002 924	10	57	27.3	9.1	0	0	2	0
109	9	p21.3	21 077 574	21 331 240	9	22.6	36.4	9.1	0	0	1	0
110	9	p21.3	21 347 678	21 743 468	8	42	45.5	9.1	0.1	0	1	2
111	9	p21.3	21 805 270	21 968 098	5	83.1	54.5	9.1	0	4.6	3	0
112	9	p21.3	21 978 346	22 008 225	4	100	63.6	0	9.1	0	1	0
113	9	p21.3	22 008 596	22 009 028	2	100	54.5	0	0	0	0	0
114	9	p21.3	22 146 626	23 690 331	8	13.6	45.5	9.1	0.1	4.6	0	0
115	9	p21.3	23 724 814	24 884 047	9	40.5	36.4	9.1	0	0	0	0
116	9	p21.3	25 091 725	25 583 086	4	58.9	27.3	9.1	0	0	0	0
117	9	p21.2-p21.1	25 738 780	32 633 126	61	56.2	18.2	9.1	0	0	6	0
118	9	p21.1-p13.2	32 844 623	36 839 510	108	29.9	9.1	9.1	0	4.6	59	0
119	9	p13.2	36 893 592	37 778 639	20	22.6	9.1	0	0	0	8	0
120	9	p13.2-p11.2	37 781 956	38 768 290	13	62.2	18.2	0	0	0	9	0
121	9	p11.1-q21.11	39 140 222	69 073 065	5	39.4	63.6	0	50.0	0	10	0
122	9	q21.11-q21.2	71 035 346	80 686 497	134	17.8	9.1	9.1	0	9.1	38	0
123	9	q21.2-q21.32	80 880 861	85 857 356	37	36.1	9.1	0	0	0	9	0
124	9	q21.32-q21.33	85 925 423	88 713 377	46	21.6	9.1	9.1	0	9.1	11	0
125	9	q21.33	88 847 218	88 938 882	4	53.9	9.1	0	0	0	1	0
126	9	q21.33-q22.33	89 077 377	100 702 888	178	24.9	9.1	9.1	0	4.6	54	2
127	9	q22.33	100 762 247	100 839 267	3	0	18.2	9.1	4.6	4.6	0	0
128	9	q22.33	100 844 340	100 966 852	5	0	18.2	0	4.6	0	1	0
129	9	q22.33-q31.3	101 052 175	112 078 084	145	19.8	9.1	9.1	0	9.1	40	0
130	9	q31.3	112 151 626	112 528 900	6	51.6	9.1	0	0	0	0	0
131	9	q31.3	112 594 901	112 878 524	6	1.1	9.1	9.1	0	9.1	0	0
132	9	q31.3	112 924 505	113 492 528	10	49.9	9.1	0	0	0	4	0
133	9	q31.3-q33.2	113 562 937	124 862 123	169	24.7	9.1	9.1	0	9.1	65	0
134	9	q33.2	124 918 446	125 063 494	6	2.9	9.1	0	0	0	1	0
135	9	q33.2-q34.3	125 136 991	140 590 976	380	37.1	9.1	9.1	0	9.1	163	1
136	9	q34.3	140 657 467	141 008 914	7	50.7	9.1	0	0	0	2	0
137	10	p15.3-p11.1	148 206	38 054 336	456	28	27.3	0	9.1	0	140	0
138	10	p11.1-q11.22	38 126 835	47 604 876	62	43.4	18.2	0	0	0	20	0
139	10	q11.22-q11.23	48 334 407	50 311 671	26	58.3	27.3	0	9.1	0	10	0
140	10	q11.23-q21.3	50 358 703	66 265 375	145	49.2	18.2	0	0	0	42	0
141	10	q21.3	66 753 598	68 535 270	8	73.6	27.3	0	9.1	0	1	0
142	10	q21.3	68 686 933	69 971 598	22	30.2	18.2	0	0	0	5	0
143	10	q21.3	69 991 540	70 051 814	2	0	18.2	9.1	0	9.1	1	0
144	10	q21.3-q22.1	70 094 900	74 506 680	99	40.9	18.2	0	0	0	40	0
145	10	q22.1-q22.3	74 542 787	80 049 004	89	38	27.3	0	0	0	37	0
146	10	q22.3	80 270 710	81 839 337	16	53.8	36.4	0	9.1	0	5	0
147	10	q22.3-q23.33	81 937 998	95 155 984	155	27.6	27.3	0	0	0	54	0
148	10	q23.33	95 185 893	95 216 687	2	0	18.2	9.1	0	9.1	0	0
149	10	q23.33-q24.1	95 287 995	97 583 032	49	11.3	27.3	0	9.1	0	13	0
150	10	q24.1-q26.3	97 805 360	135 404 522	582	27.2	18.2	0	0	0	183	0
151	11	p15.5	196 966	1 483 678	57	92.6	9.1	27.3	0	9.1	22	0
152	11	p15.5	1 491 097	1 588 270	4	71.5	18.2	18.2	4.6	0	1	0
153	11	p15.5-p15.4	1 634 162	3 381 998	40	63.3	18.2	9.1	4.6	0	14	0
154	11	p15.4	3 402 850	6 639 296	71	62.5	9.1	18.2	0	9.1	22	0
155	11	p15.4	6 659 171	8 075 942	32	12.8	18.2	9.1	9.1	0	6	0
156	11	p15.4	8 105 834	8 951 375	27	53.9	9.1	18.2	0	9.1	3	0
157	11	p15.4	8 962 586	10 476 891	33	39.7	18.2	9.1	9.1	0	19	0
158	11	p15.4-p15.2	10 508 827	15 781 881	87	12.3	9.1	18.2	0	9.1	31	0
159	11	p15.2-p14.3	15 993 305	23 445 066	110	21.3	18.2	9.1	0	0	30	0

Continued on the next page...

			aCGH probes				absolute % of		relative % of		diff. expressed	
	chr	cytobands	start	end	num	CNV %	losses	gains	losses	gains	mRNAs	miRNAs
160	11	p14.3-p14.2	23 710 376	26 742 957	16	47.7	27.3	9.1	9.1	0	0	0
161	11	p14.2-p14.1	26 744 883	28 728 110	31	0.4	18.2	9.1	0	0	10	0
162	11	p14.1	28 910 482	30 741 670	17	17.4	27.3	9.1	9.1	0	2	0
163	11	p14.1-p12	30 951 602	41 944 417	139	41.9	18.2	9.1	0	0	52	0
164	11	p12-p11.2	42 226 159	45 758 621	53	9.8	9.1	9.1	0	0	15	0
165	11	p11.2	45 826 054	49 0 0	85	37.8	0	18.2	0	9.1	33	0
166	11	p11.12	49 230 043	50 682 252	6	92.8	9.1	9.1	9.1	0	0	0
167	11	p11.11-q14.2	55 137 204	88 087 269	752	37.4	0	18.2	0	4.6	288	0
168	11	q14.2-q21	88 240 997	93 885 399	55	46.4	18.2	18.2	18.2	0	11	0
169	11	q21	93 903 054	95 564 607	35	6.8	0	18.2	0	0	24	0
170	11	q21	95 591 751	95 621 376	2	0	36.4	18.2	36.4	0	1	0
171	11	q21-q25	95 644 909	134 446 159	620	26.3	0	18.2	0	0	180	1
172	12	p13.33-p13.2	179 706	10 164 582	244	38.4	18.2	36.4	18.2	0	75	0
173	12	p13.2-q12	10 223 118	39 114 237	366	36.6	0	45.5	0	9.1	119	0
174	12	q12-q23.3	39 223 163	108 153 773	1104	20.4	0	36.4	0	0	410	2
175	12	q23.3-q24.11	108 641 156	109 700 234	31	37.9	0	45.5	0	13.7	11	0
176	12	q24.11-q24.12	109 857 930	112 280 894	69	3.1	18.2	27.3	18.2	0	31	0
177	12	q24.13	112 308 881	112 711 579	12	47.7	0	36.4	0	9.1	5	0
178	12	q24.13-q24.21	112 890 753	114 634 078	40	4.3	18.2	27.3	13.7	0	13	0
179	12	q24.21	114 791 887	114 845 865	2	0	9.1	36.4	0	4.6	3	0
180	12	q24.21-q24.22	115 109 251	117 527 891	17	23	0	36.4	0	4.6	13	0
181	12	q24.22-q24.23	117 619 855	118 104 214	14	11.1	18.2	27.3	18.2	0	3	0
182	12	q24.23-q24.31	118 227 019	122 102 983	90	8.1	0	36.4	0	9.1	32	0
183	12	q24.31	122 156 586	122 370 332	7	13	18.2	27.3	18.2	0	0	0
184	12	q24.31-q24.33	122 389 356	133 767 985	172	43.3	0	36.4	0	9.1	82	0
185	13	q12.11-q12.13	19 703 703	27 260 598	115	56.2	0	18.2	0	0	46	0
186	13	q12.13-q13.1	27 296 407	33 759 862	104	10	0	27.3	0	9.1	44	0
187	13	q13.1-q34	33 859 640	113 562 711	765	25.1	0	18.2	0	4.6	245	4
188	13	q34	113 657 076	113 794 203	5	75.6	0	0	0	0	0	0
189	13	q34	113 813 185	114 792 948	26	54.1	0	9.1	0	9.1	18	0
190	13	q34	114 860 149	115 059 019	7	83.9	0	0	0	0	1	0
191	14	q11.2	20 295 211	21 491 711	38	91.3	9.1	9.1	0	0	12	0
192	14	q11.2	21 499 240	23 541 793	51	64.3	9.1	18.2	0	9.1	27	0
193	14	q11.2-q21.2	23 565 233	46 870 392	300	39.4	9.1	9.1	0	0	91	0
194	14	q21.2-q32.12	46 975 576	94 247 844	753	19.9	27.3	0	18.2	0	248	0
195	14	q32.12-q32.33	94 387 348	107 258 823	235	41.1	9.1	9.1	0	9.1	86	4
196	15	q11.2	20 849 110	24 058 972	22	94.2	0	18.2	0	9.1	5	0
197	15	q11.2-q25.3	24 305 037	87 891 922	1065	36	9.1	9.1	0	0	404	0
198	15	q25.3	87 960 119	88 422 554	9	0.4	18.2	9.1	9.1	0	0	0
199	15	q25.3-q26.2	88 424 230	96 982 259	137	29.2	9.1	9.1	0	0	46	0
200	15	q26.2-q26.3	97 048 169	99 057 623	18	33.4	18.2	9.1	9.1	0	1	0
201	15	q26.3	99 168 589	102 351 194	59	61.5	9.1	18.2	0	9.1	24	0
202	16	p13.3	96 766	97 190	2	100	18.2	0	9.1	0	0	0
203	16	p13.3	105 258	4 013 224	188	82.1	9.1	0	0	0	95	0
204	16	p13.3	4 015 316	4 191 733	6	100	18.2	0	9.1	0	0	0
205	16	p13.3-p13.11	4 240 608	14 944 618	177	35.1	9.1	0	0	0	52	1
206	16	p13.11	15 048 751	15 960 142	26	75.3	9.1	9.1	0	0	5	0
207	16	p13.11	16 031 655	16 148 753	3	100	9.1	18.2	0	9.1	0	0
208	16	p13.11-p12.1	16 180 946	27 556 866	206	52.3	9.1	9.1	0	0	77	0
209	16	p12.1-p11.2	27 629 749	31 227 835	125	78.6	9.1	18.2	0	9.1	71	0
210	16	p11.2	31 260 819	31 542 173	17	5.9	9.1	9.1	0	0	1	0
211	16	p11.2-p11.1	31 693 728	34 202 146	10	97.7	9.1	0	0	0	3	0
212	16	p11.1-q21	34 258 235	58 195 273	251	18.5	27.3	0	4.6	0	77	0
213	16	q21-q24.2	58 230 636	87 420 977	590	29.4	36.4	0	0	0	150	2
214	16	q24.2-q24.3	87 433 214	90 124 278	107	72.7	45.5	0	9.1	0	26	0
215	17	p13.3-p13.1	48 539	7 576 821	288	39	36.4	0	0	0	111	2
216	17	p13.1	7 589 646	8 274 696	39	33.1	45.5	0	4.6	0	15	0
217	17	p13.1	8 283 340	8 508 202	7	5.3	45.5	9.1	4.6	4.6	4	0
218	17	p13.1-p11.2	8 543 914	20 936 654	258	44.1	36.4	9.1	0	4.6	57	0
219	17	p11.2-q11.1	21 034 071	25 311 034	20	96.1	36.4	0	9.1	0	4	0
220	17	q11.1-q11.2	25 626 982	31 344 701	175	21.3	18.2	0	0	0	85	2
221	17	q11.2-q21.1	31 439 049	38 150 391	174	40.1	27.3	0	4.6	0	62	0
222	17	q21.1-q21.31	38 174 028	42 765 451	230	36.5	27.3	9.1	4.6	4.6	86	0
223	17	q21.31	42 792 021	43 039 386	11	52.4	18.2	9.1	0	0	8	0
224	17	q21.31	43 074 718	43 240 165	12	35.5	18.2	18.2	9.1	0	6	0
225	17	q21.31	43 304 352	44 159 861	25	77.9	0	27.3	0	0	14	0
226	17	q21.31	44 231 946	44 345 037	3	100	9.1	36.4	9.1	9.1	4	0
227	17	q21.31-q22	44 787 865	50 235 142	158	41.3	0	27.3	0	0	79	1
228	17	q22	50 309 176	54 913 791	64	24.4	0	18.2	0	0	7	0
229	17	q22-q25.3	54 940 391	80 695 819	690	42.5	0	27.3	0	4.6	240	2
230	17	q25.3	80 707 119	81 029 940	13	100	9.1	27.3	9.1	0	2	0
231	18	p11.32-p11.21	180 229	11 693 0	135	19.4	18.2	9.1	9.1	0	57	0
232	18	p11.21	11 798 492	12 309 677	11	54.1	9.1	9.1	0	0	5	0
233	18	p11.21	12 374 179	13 438 286	18	16.3	9.1	18.2	0	9.1	10	0
234	18	p11.21	13 574 714	13 666 289	3	3.7	18.2	9.1	4.6	0	2	0
235	18	p11.21	13 681 934	14 594 415	11	65.3	18.2	0	4.6	0	7	0
236	18	p11.21-q11.1	14 748 584	18 539 911	5	17.5	9.1	0	0	0	1	0
237	18	q11.1-q12.1	18 650 189	27 681 937	104	13.5	9.1	9.1	0	4.6	36	0
238	18	q12.1	27 828 604	28 170 749	3	72.1	18.2	9.1	9.1	0	0	0
239	18	q12.1-q12.3	28 354 894	41 402 061	145	22.7	9.1	9.1	0	0	33	0
240	18	q12.3-q23	41 474 995	77 982 125	432	29.8	18.2	9.1	9.1	0	113	0
241	19	p13.3-p12	281 0	21 179 841	871	47.9	18.2	9.1	0	0	342	2
242	19	p12-q11	21 242 399	28 272 555	49	51.9	27.3	9.1	13.7	0	14	0
243	19	q11-q12	28 407 342	28 707 649	4	12.7	9.1	9.1	0	0	0	0
244	19	q12-q13.2	28 902 630	43 096 865	463	34.6	18.2	9.1	0	4.6	118	0
245	19	q13.2-q13.31	43 124 033	43 859 667	5	100	27.3	0	9.1	0	7	0
246	19	q13.31-q13.32	43 898 922	47 889 510	175	29.2	18.2	9.1	0	9.1	58	0
247	19	q13.32-q13.33	47 978 395	48 790 416	38	57.4	18.2	0	0	0	8	0
248	19	q13.33-q13.43	48 799 718	59 092 569	491	56.1	18.2	9.1	0	9.1	126	0
249	20	p13	70 580	1 751 212	47	45.6	0	36.4	0	0	22	0
250	20	p13	1 864 447	3 463 329	41	37.8	0	45.5	0	9.1	19	0

Continued on the next page...

			aCGH probes				absolute % of		relative % of		diff. expressed	
	chr	cytobands	start	end	num	CNV %	losses	gains	losses	gains	mRNAs	miRNAs
251	20	p13-p12.3	3 515 894	6 074 749	59	26.6	0	36.4	0	0	24	0
252	20	p12.3-p12.1	6 096 672	16 360 097	106	43.4	9.1	36.4	9.1	0	24	0
253	20	p12.1-p11.22	16 506 753	21 784 342	79	11.9	0	36.4	0	0	28	0
254	20	p11.22-p11.21	21 905 826	24 780 452	40	41	9.1	36.4	9.1	0	3	0
255	20	p11.21-p11.1	24 861 269	25 732 553	26	12.1	0	36.4	0	0	6	0
256	20	p11.1-q11.21	26 075 784	29 467 995	3	8.6	9.1	36.4	4.6	0	0	0
257	20	q11.21	29 888 477	29 972 934	3	0	9.1	45.5	4.6	4.6	0	0
258	20	q11.21-q13.33	29 976 753	60 778 112	617	25.6	0	45.5	0	0	229	0
259	20	q13.33	60 791 724	60 814 359	2	100	0	54.5	0	9.0	0	0
260	20	q13.33	60 835 033	62 893 188	77	99.9	0	45.5	0	0	29	0
261	21	q11.1	10 991 392	11 096 085	3	100	18.2	18.2	18.2	0	0	0
262	21	q11.2-q21.1	14 627 297	19 869 008	65	44.9	0	27.3	0	4.6	17	0
263	21	q21.1	20 0 526	22 977 676	28	87	9.1	27.3	9.1	0	1	0
264	21	q21.1-q22.3	23 065 538	47 599 452	433	23.6	0	27.3	0	0	123	0
265	21	q22.3	47 609 029	47 822 354	10	5.8	0	36.4	0	9.1	10	0
266	21	q22.3	47 875 269	48 067 923	10	42.2	0	27.3	0	0	2	0
267	22	q11.1-q12.1	16 053 473	29 580 803	271	69.2	9.1	0	9.1	0	86	0
268	22	q12.2-q13.1	29 617 783	39 329 093	265	42	0	0	0	0	107	0
269	22	q13.1	39 359 112	39 385 484	3	100	0	18.2	0	18.2	0	0
270	22	q13.1-q13.2	39 419 037	41 221 432	58	23.8	0	0	0	0	19	0
271	22	q13.2-q13.33	41 256 433	51 043 489	227	48.3	0	9.1	0	4.6	91	0
272	22	q13.33	51 065 861	51 178 263	3	100	9.1	9.1	9.1	0	1	0
273	X	p22.33-p22.31	1 314 894	6 385 370	36	67.2	9.1	54.5	0	0	39	0
274	X	p22.31	6 457 403	8 032 119	16	82.8	9.1	63.6	0	9.1	6	0
275	X	p22.31-p22.2	8 266 181	14 039 227	77	21.2	9.1	54.5	4.6	0	16	0
276	X	p22.2-p11.22	14 167 254	53 221 664	494	35	0	54.5	0	0	122	2
277	X	p11.22	53 240 164	53 283 765	2	100	9.1	54.5	9.1	0	0	0
278	X	p11.22-q21.1	53 325 084	79 884 773	293	40.4	0	54.5	0	0	70	0
279	X	q21.1-q21.2	79 975 0	85 198 467	52	15	9.1	54.5	9.1	0	12	0
280	X	q21.2-q21.31	85 282 468	90 374 528	36	31.4	0	54.5	0	0	1	0
281	X	q21.31-q26.2	90 530 805	130 407 536	462	31.1	0	63.6	0	0	112	0
282	X	q26.2-q26.3	130 419 292	137 430 408	98	22.4	0	72.7	0	9.1	35	1
283	X	q26.3-q27.1	137 628 563	138 145 138	9	1.3	0	63.6	0	0	2	0
284	X	q27.1-q28	138 231 171	154 841 454	236	31.6	0	72.7	0	9.1	63	0